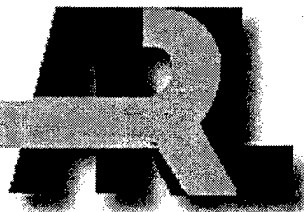


ARMY RESEARCH LABORATORY



Relationship of Protective Mask Seal
Pressure to Fit Factor and Head
Harness Strap Stretch

Kathryn Stemann Cohen

ARL-TR-2070

SEPTEMBER 1999

DTIC QUALITY INSPECTED 4

19991108 047

Approved for public release; distribution is unlimited.

FitPlus® is a registered trademark of TSI, Inc.

Plexiglas® is a registered trademark of Rohm and Haas.

The findings in this report are not to be construed as an official Department of the Army position
unless so designated by other authorized documents.

Citation of manufacturer's or trade names does not constitute an official endorsement or approval of
the use thereof.

Destroy this report when it is no longer needed. Do not return it to the originator.

Army Research Laboratory

Aberdeen Proving Ground, MD 21005-5425

ARL-TR-2070

September 1999

Relationship of Protective Mask Seal Pressure to Fit Factor and Head Harness Strap Stretch

Kathryn Stemann Cohen
Human Research & Engineering Directorate

Approved for public release; distribution is unlimited.

Abstract

Currently, protective mask seals are evaluated indirectly by measuring fit factor (FF), a ratio of the concentration of particles outside versus the concentration of particles inside the mask. This report describes an alternate process for evaluating mask seals by measuring seal pressure distribution. The goal was to develop a relationship between FF and seal pressure for evaluating seal performance, and relationships between FF and strap stretch and between seal pressure and strap stretch for determining proper strap adjustment. Pressure was measured using a thin film flexible sensor placed at 11 locations around the seal of an M40 mask on a headform. Corresponding FF was measured using a protective mask fit tester. Stretch in each of the six head harness straps was measured manually using a caliper and gauge length markers on the strap. Measurements were made for three degrees of strap tightness over a total of 22 trials. Data and model analysis indicated a strong relationship between FF and seal pressure ($R^2 = 0.87$), and weak relationships between FF and strap stretch ($R^2 = 0.2$) and between seal pressures and strap stretch ($R^2 = 0.09-0.27$). Eleven validation trials were conducted to verify predictive capability of the seal pressure and FF relationships. Passing or failing FF was correctly predicted by a single seal pressure in 9 of 11 trials. These findings suggest that seal pressure measurement may be a promising new tool for design and evaluation of protective mask seals. In contrast, strap stretch measurements could not be used to determine proper adjustment of the head harness for achieving a passing FF and adequate seal pressure.

ACKNOWLEDGMENTS

The author would like to thank Professor Stephen Belkoff, Ph.D., University of Maryland at Baltimore (UMAB), for his interest in and willingness to guide and support her research efforts. She would also like to thank David Harrah, Human Research and Engineering Directorate (HRED) of the U.S. Army Research Laboratory (ARL), for his expert guidance in the use and study of protective masks, as well as for an extensive review of her manuscript.

The author would like to thank many others who provided assistance along the way: Ronald Carty, ARL, for his skilled preparation of photos and illustrations; Vince Novak, of UMAB, for his guidance in evaluating behavior of head harness straps; Chris Karwacki, of the Edgewood Research, Development, and Engineering Center (ERDEC¹), in the use of the breathing simulator; Corey Grove, David Caretti, William Fritch, all of ERDEC, and Anand Kasbekar, Ph.D., of Visual Sciences, Inc., for reviewing protocols and supporting this project; the Simulation Systems Branch, HRED, ARL, for constructing test fixtures and repairing equipment; and the ERDEC mask prototyping shop for supplying the equipment and materials necessary for this effort.

¹Beginning October 1998, ERDEC became the Edgewood Chemical Biological Center.

CONTENTS

INTRODUCTION	5
Background	5
The Problem	7
Research Focus	9
Previous Work	10
Purpose	12
Objectives	12
MATERIALS AND METHODS	12
Headform	13
M40 Protective Mask and Head Harness	13
Head Harness Strap Adjustment Conditions	19
Head Harness Strap Stretch	20
Breathing Simulator	22
Fit Factor	22
Seal Pressure	28
Procedure	40
Data Analysis	41
Model Development	41
Validation	43
Required Seal Pressure Profile and Head Harness Strap Adjustments	45
RESULTS	47
Data Analysis	47
Model Development	54
Validation	57
Required Seal Pressure Profile and Head Harness Strap Adjustments	63
DISCUSSION	64
Seal Pressure	64
Pressure Measurement System	67
Fit Factor	68
Head Harness Strap Stretch and Adjustment	69
Future Research Efforts	69
SUMMARY	70
REFERENCES	73

APPENDICES

A. Pilot Evaluation 79
B. Head Harness Evaluation 93
C. Protective Mask Clearing Evaluation 99
D. Pressure Sensor Calibration Evaluation 103
E. Acronyms and Abbreviations 109

DISTRIBUTION LIST 113

REPORT DOCUMENTATION PAGE 115

FIGURES

1. M40 Protective Mask 8
2. Headform 14
3. Schematic of Headform 15
4. Schematic of M40 Protective Mask 16
5. Mask Sealing Surface Cross Section A-A From Figure 4 17
6. Head Harness With Gauge Length Markers 21
7. Waveform Generator 23
8. Breathing Machine 24
9. M41 Protective Mask Fit Validation System 26
10. Pressure Measurement System 30
11. Schematic of a Typical Tekscan Sensor 31
12. Force-Sensing Elements 32
13. Calibration Platform and Weight Loading the Sensor 34
14. Distribution of Load to Sensor Surface 35
15. Accuracy of a Sensor Across the Load Range, Based on Three Calibration Files 37
16. Measurement Locations on the Sealing Surface of the M40 Mask 38
17. Sensor Placed Between Mask and Headform for Measurement 39
18. Seal Pressure Profiles Based on Average Seal Pressures for Adjustment
Conditions 1, 2, and 3 48
19. Average Seal Pressure Profiles and Standard Deviations for Passing (n=14) and
Failing (n=8) FF Trials 49
20. Comparison of Pressure Profiles Corresponding to Average Seal Pressures
From the Distributions of Figures 21 and 22 50
21. Seal Pressure Distribution for Condition 1 51
22. Seal Pressure Distribution for Condition 3 52
23. FF Measured for 21 Trials in Conditions 1, 2, and 3 53
24. FF Versus Ambient Particle Concentration; Pearson Correlation
Coefficient = 0.0015 53
25. Average Strap Stretch and Standard Deviation for Conditions 1 (n=3), 2 (n=9),
and 3 (n=10) 54
26. Scatterplot Matrix of FF and Seal Pressure Values 56
27. FF Measured for 11 Validation Trials in Conditions 1, 2, and 3 58

28. Average Seal Pressure Profiles and Standard Deviations for Validation Trials (Condition 1 (n = 1), Condition 2 (n = 5), and Condition 3 (n = 5))	59
29. Estimated Versus Measured FF for Model Equation (5)	60
30. Estimated Versus Measured FF for Model Equations (6), (7), and (8)	61
31. Pressure Profiles for the 95th Percentile of All Passing Trials (n = 22), the Mean of All Passing Trials, and the Mean of All Failing Trials (n = 11)	63
32. Pressure Profile for Achieving an FF of 7000 Based on 11 Models of FF as a Function of a Single Pressure (n = 32)	64
33. Seal Pressure Along the Sealing Surface of an M17 Protective Mask	66

TABLES

1. Historical Use of Chemical Agents in War	6
2. Anthropometric Measurements and Percentiles for the Headform	15
3. Head Harness Strap Adjustment Conditions	19
4. Respiration Values for Masked and Unmasked Breathing at Varied Activity Levels	25
5. Model of FF as a Function of 11 Seal Pressures	55
6. Squared Multiple Correlation of Each Pressure With All Remaining Pressures .	55
7. Models of FF as a Function of a Single Location Seal Pressure	57
8. Prediction of Passing or Failing by Model of FF as a Function of 11 Seal Pressures	59
9. Prediction of Passing or Failing by Model of FF as a Function of RTS Pressure	62
10. Prediction of Passing or Failing by Model of FF as a Function of LT Pressure .	62
11. Prediction of Passing or Failing by Model of FF as a Function of RFS Pressure	62

RELATIONSHIP OF PROTECTIVE MASK SEAL PRESSURE TO FIT FACTOR AND HEAD HARNESS STRAP STRETCH

INTRODUCTION

Background

U.S. Army soldiers wear protective masks to protect their eyes, faces, and respiratory systems from the damaging effects of chemical and biological agents used by enemies on the battlefield. Protective masks were first developed during World War I (WWI) after a chlorine gas attack on the Allies by the German army in 1915, in which 20,000 unprotected troops were gassed and 5,000 died (Parragh, Szabo, Geck, & Madaras, 1967; Tzihor, 1992; Raines, 1983). At this point in the war, the French and other Allies had no protective gear, whereas the Germans had only primitive protection provided by gauze pads soaked in thiosulfate and held over their mouths and noses to filter air (Parragh et al., 1967). By the end of the war, 125,000 tons of chlorine, phosgene, and mustard agents had been used by both sides, causing 1.3 million casualties and 100,000 deaths (Chandler, 1985; Tzihor, 1992). As a result, protective mask development proceeded rapidly. Late WWI masks, made of close fitting airtight materials (such as rubber or leather saturated with oil) and having replaceable dry filter cans, closely resembled the masks of today (Parragh et al., 1967).

After WWI, many countries engaged in chemical warfare (see Table 1). Today, more than 30 nations, including the third world and those with many active terrorist organizations, possess chemical weapons in their military inventory.

During the Gulf War, Saddam Hussein was reported to have the capability to fire missiles into the U.S. Air Force Base in Incirlick, Turkey (Tzihor, 1992). He was also reported to have the intent to use chemical weapons, so Allied ground forces wore their chemical suits and had their protective masks ready at their hips (Thornton, 1993). No chemical events were reported. After the Gulf War, United Nations (U.N.) inspection teams suspected human testing of chemical and biological weapons when they discovered mass graves near the Iraqi's main chemical and biological warfare laboratories in 1994 (Windrem, 1998). Shortly afterwards, the graves were secretly moved. Saddam Hussein's recent efforts in 1997 and 1998 to interfere with U.N. weapons inspections for chemical and biological agents brought the U.S. once again to the brink of war (Chronology II, 1998; Still Skeptical, 1998). Central Intelligence Agency director George Tenet reported to Congress that Iraq could resume a biological warfare program within weeks and a chemical warfare program within 6 months without weapons inspections (U.S. is Ready, 1998). As troops were sent to the

Persian Gulf, Defense Secretary Cohen ordered 1.5 million service men and women to be inoculated for anthrax, a deadly bacterial disease (1.5 Million, 1997). Les Aspin, the previous chairman of the U.S. House of Representatives, Armed Services Committee, noted (Ellis & Record, 1992) that “Saddam Hussein and his scuds should teach us that we are increasingly likely to face adversaries who are not deterred by the possibility of terrible retaliation.”

Table 1
Historical Use of Chemical Agents in War

Year(s)	Chemical warfare user	Target
1935-1936	Italy	Ethiopia
1932-1943	Japan	China
1963-1967	Egypt	Yemen
1975-1976	North Vietnam	South Vietnam, civilians
1978	North Vietnam	Khymer Rouge
1979	Soviet Union	Afghanistan
1983-1988	Iraq	Iran
1988	Iraq	Kurdish civilians

Data from Tzihor, 1992.

The threat of chemical warfare is not abating; consequently, more than 20 countries have active programs for developing protective masks (Brletich, Tracy, & Dashiell, 1992). The U.S. Army currently has five ongoing mask programs (M40/M42, M43A1, M45, Joint Service General Purpose Mask, and Joint Service Aircrew Mask).

The chemical and biological threat is not limited to military populations. In 1995, containers of the nerve gas sarin were left in several cars of the Tokyo subway system during the morning rush hour (Terrorists Hit, 1995). The leaking gas killed six people and sickened thousands. Authorities treated the incident as a terrorist attack. In 1997, a leaking package was left in the B'nai B'rith mail room in a Washington, DC, office building (Powell & Lengel, 1997). A petri dish containing a gelatin-like substance, labeled with the word “anthrax,” was found inside the package. A two-block area of the city was closed and workers were left barricaded in their offices for more than 8 hours during the biological hazard alert. Two employees and 12 firefighters who had close contact with the package had to undergo decontamination. The

material in the dish was analyzed and found to be harmless. Such terrorist activities against civilian populations have prompted non-military government agencies and first responder units such as fire, police, and medical teams to seek protection in the form of escape hoods and masks (Weiss, 1997; R. A. Weiss, personal communication, February 10, 1998) to be prepared for terrorism in the United States.

Other nations are also preparing civilians for the threat of chemical and biological attack. Concerned about the stockpiles of chemical agents in neighboring hostile Arab countries, the Israelis embarked on a protective mask program to provide protection to all citizens (Adler, 1986). They believed that the most likely target of a chemical attack would be the unprepared and unprotected civilian population.

A protective mask, which is the first line of defense against chemical and biological agents, provides a clean air source by preventing the entrance of contaminants at the peripheral sealing edge of the mask and by filtering incoming air through an attached canister. The protective mask material, typically rubber, forms a seal with the facial skin when correctly fitted on the head and face (see Figure 1). The fit of a mask is adjusted by tightening the straps of the head harness, thus securing the mask on the face. If a mask is not correctly adjusted, sized, or designed for the shapes and sizes of faces in the user population, inadequate seals may be formed on some individuals, allowing dangerous agents to leak inside their masks.

Designing protective masks for civilians presents new sizing and fitting challenges because of the larger population and larger variation of face shapes and sizes. Although soldiers' faces vary in size and shape, the degree of variation is less than in the general population because soldiers are physically fit individuals between the ages of 18 and 50 years (U.S. Total Army Personnel Command, Deputy Chief of Staff for Plans, Force Integration and Analysis, 1993).

The Problem

Current protective mask design and evaluation techniques do not include means to directly evaluate how the sealing surface of the mask performs or to identify probable leakage sites. Mask performance is defined in terms of the protection factor, a ratio of the challenge aerosol concentration in the ambient air outside the mask to the challenge aerosol concentration inside the mask resulting from leakage (Gardner, Laye, & Hughes, 1988). Quantitative fit testing is performed on a given mask to measure this ratio, commonly referred to as the fit factor (FF). Thus, FF is a measure of protection made in a controlled environment while a prescribed test procedure is followed, whereas protection factor is the level of protection a mask provides to a soldier in his or her normal work

environment. Fit factor is an overall performance measure that accounts for all sources of mask leakage, including seal leakage and leakage through a filter or around mask components such as eye lenses. Fit testing plays a major role in the development and evaluation of military protective masks.

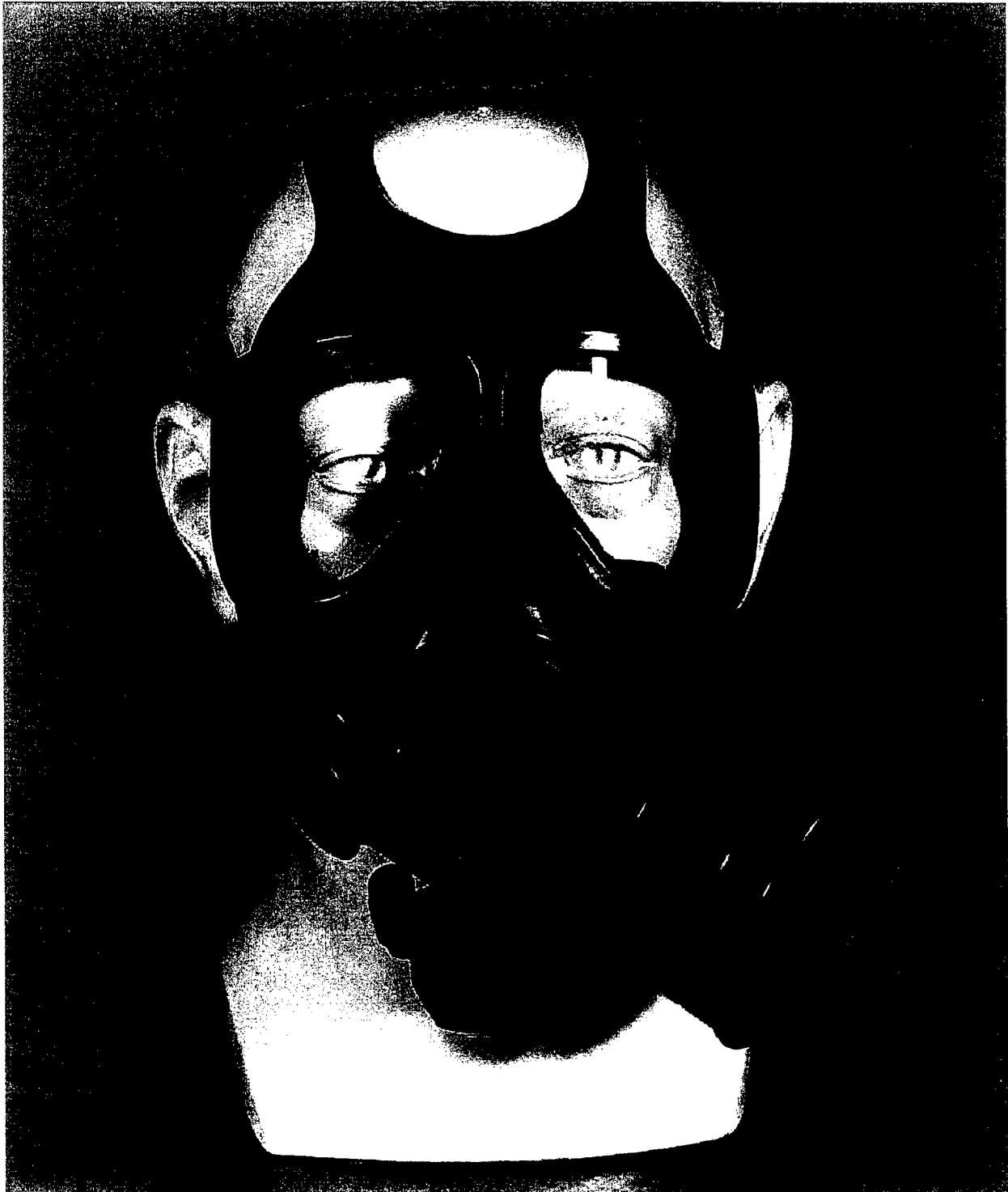


Figure 1. M40 protective mask.

The Army's standard method of quantitatively evaluating masks is to perform FF tests in a chamber that can provide a constant challenge concentration of corn oil aerosol particles (Gardner et al., 1988; Laye, 1987). Air is sampled from the chamber and via probes placed in the mask. Particle concentrations are determined by forward light-scattering photometry. Subjects perform head and facial maneuvers during the fit test to simulate normal movements that might break the seal between the mask and face. The measured FF is checked against the Army established protection requirement or FF criterion that each developmental mask must meet or exceed to be acceptable (Brletich, 1992; Headquarters, U.S. Army Training and Doctrine Command [TRADOC], 1992).

The FF criterion is based upon the anticipated threat to be encountered and the degree of protection that must be provided to a soldier to prevent detrimental effects that would cause him or her to become a casualty. Thus, the protection requirement is usually written in terms of a typical attack scenario, a concentration of a particular agent delivered over an amount of time for which a mask must provide protection. The protection required of the mask is determined from the permissible exposure limit, the concentration of agent delivered over time that a soldier can withstand. From the protection requirement, the FF is derived, usually in terms of two different levels and corresponding probabilities of being met. For example, the Army's M40 protective mask protection requirement is interpreted as an 88% probability of obtaining an FF of at least 1667 and a 75% probability of obtaining an FF of at least 6667 (Brletich, 1992; TRADOC, 1992).

Fit factor is an overall performance measure that does not provide any information about the location of leaks and therefore provides little feedback to the designer as to how to correct the problem. In addition, FF tests are expensive, time consuming, and cannot be performed on early prototype masks. Prototypes are commonly crude versions of the future mask and are usually not of the quality required to pass a chamber FF test. Thus, in the current mask design process, many important decisions are made before designers evaluate the most critical performance requirement—protection.

Research Focus

The primary focus of the present research was to demonstrate that measuring and evaluating the pressure distribution between the mask sealing surface and face provides valuable information about seal integrity. A related goal was to develop relationships between seal pressure and FF in order to determine the required seal pressure to produce a passing FF. Displaying and examining the distribution of pressure along the seal between mask and face will

allow mask designers to understand how the mask sealing surface performs and to identify plausible sites for leakage (regions of relatively low seal pressure or contact area). This type of seal pressure analysis can be performed early in a development program because all that is required is a mask prototype that is capable of forming a seal on a headform or human face. Thus, designers could use an iterative process to make mask design changes and directly evaluate the effects on seal pressure. Early evaluation of seal pressure will produce masks that fit and seal better than their predecessors, saving time and cost of late redesign efforts and ultimately providing an earlier and better product to the soldier in the field.

A secondary focus was to determine relationships between head harness strap stretch (a measure of strap tightness) and either FF or seal pressure. These relationships would provide the foundation for determining the required strap adjustments to form a seal of adequate pressure to produce a passing FF.

Previous Work

Few researchers have attempted to measure seal pressure between a mask and face. Until recently, pressure sensors were ill suited for measuring low pressures between two highly conformable surfaces such as the human face and rubber protective mask. In addition, the sensors that were available altered the fit of the mask when placed between the sealing surface and the face.

Goldberg, Raeke, Jones, and Santschi (1966); Goldberg, Jones, Wang, and Crooks (1967); and Goldberg (1970) measured pressure using air bladders constructed from heat-sealed sheets of plastic film sandwiched between sheets of cardboard to control expansion. The deflated bladder was placed beneath the mask sealing surface and inflated until the cardboard sheets separated. The pressure at which separation occurred was interpreted as the seal pressure acting on the bladder. Goldberg et al. (1966, 1967) and Goldberg (1970) made measurements for two tightness levels of the M17 protective mask on one subject. The technique was problematic, however, because the operator had to control the bladder inflation and judge when minimum separation of the cardboard surfaces occurred. This was especially difficult on curved surfaces, at soft tissue sites, and in regions where the mask sealing surface bridges the skin because of an anatomical indentation. The researchers speculated that a higher pressure than actually exists may have been measured at these sites.

Jelier and Hughes (1994) measured oronasal mask seal pressure using a Talley Oxford pressure-monitoring system. An oronasal mask is similar to a nosecup, covering only the nose and mouth, whereas a full facepiece mask covers the entire face from forehead to chin and

includes an internal nose cup that seals around the mouth and nose. Jelier and Hughes attached four transducer cells made of a polymer-based material (25-mm diameter) to the sealing surface of the oronasal mask. The mask was placed on a human face, and the cells were inflated while the characteristic pressure-volume graph for each cell was monitored and compared to the normal unrestricted graph (as observed when the cell is inflated freely without contacting any surface). At the point of departure from the unrestricted graph, pressure was measured and assumed to be the seal pressure between the mask and face. Jelier and Hughes reported wide variations in measured pressures and bladder inflation problems resulting from measurement on curved surfaces, poor bladder attachment methods, and inadequate seal surface contact with the large cell bladder. They concluded that the results were difficult to interpret and that further studies using smaller transducers were required before mask seal pressure values could be reported.

Lu (1995) measured the pressure change in a pre-inflated air bladder placed between the M40 protective mask head harness pad and back of the head. Lu believed that the head pad pressure was related to the seal pressure but did not prove that relationship. Seal pressure was not measured directly because the inflated bladder, when placed between the mask sealing surface and face, significantly altered the fit of the protective mask. Lu did not present a means for calibrating the pressure bladder. Because the bladder was inflated before placement, Lu's pressure values actually represent pressure changes within the bladder, not absolute values of pressure. Thus, Lu's pressure values can only be interpreted qualitatively within the context of that report. Lu attempted to develop relationships among pressure, protection, comfort, and fit as the head harness pad was either tightened or loosened over a series of trials. Comfort and fit were evaluated subjectively. Lu found no significant relationships between head harness pad pressure and protection, fit, or comfort for the tightening trials and only a few weak relationships between pressure, comfort, and fit for the loosening trials.

In summary, all of the previously used methods provided point measures of pressure that were difficult to interpret. Two of the researchers measured pressure at locations other than the sealing surface of a full facepiece mask. Thus, these studies yielded little information about seal pressure distributions and possible leak paths. In addition, the air-filled bladders were too bulky to place between a mask sealing surface and face without causing leaks or drastically altering the normal interface boundary conditions. Problems were encountered during bladder inflation which led to difficulties in interpreting when the bladder pressure was equivalent to the seal pressure. None of the previous researchers found a significant relationship between measured seal pressure and mask seal performance (FF).

Purpose

The purpose of this study was to determine whether seal pressure distributions can be used to evaluate the performance of protective masks and to determine if seal pressure, tightness of the mask, and FF are interrelated. If significant relationships were found, then an additional purpose of this study was to determine levels of seal pressure and mask strap adjustment needed to produce a good seal with a passing FF.

Objectives

The specific objectives of this research were to

1. Develop a method for measuring and investigating the pressure distribution between a protective mask sealing surface and face for the purpose of evaluating seal integrity and understanding how mask design characteristics influence seal performance.
2. Determine the relationship between
 - a. Seal pressure and FF,
 - b. Head harness strap stretch and FF, and
 - c. Seal pressure and head harness strap stretch.
3. Determine the required seal pressure profile and head harness strap adjustments of the protective mask for achieving a passing FF.

MATERIALS AND METHODS

This section describes the equipment and unique methods that were developed in order to satisfy the goals of this project. Standard equipment was employed using new techniques to simulate a breathing human for mask fit testing: headform, protective mask, breathing simulator, and fit tester. Strap stretch was developed as a measure of strap tightness. New pressure-sensing technology was used to measure seal pressure; thus, procedures for calibration and measurement had to be developed as a part of this effort. Procedures for completing a test trial, analyzing the data, developing models to meet the objectives, and validating the models are described. Then, approaches for determining seal pressure profiles and head harness strap adjustments required for achieving a passing FF are presented.

Headform

A headform with rubber skin and a wooden core was used to simulate a human head (see Figure 2). The wooden core of the headform has a hollow cavity with openings at the nose and back of the neck to allow the headform to be connected to a breather pump to simulate human breathing (see Figure 3).

A headform was used to simulate a human head for three reasons. First, a pilot study indicated that the current design of the low pressure sensors precluded using them on human subjects. Human facial perspiration entered the sensor and shorted the electrical connections, destroying the sensor. Second, the headform serves as a consistent baseline for which data about multiple protective masks can be collected and compared. Third, the use of the headform eliminated the variable of anthropometry in this early evaluation.

The subject headform has been used extensively by Army mask designers at the Chemical and Biological Defense Command (CBDCOM¹) and is considered a standard for performance testing of masks. Anthropometric measures and percentiles of the headform are provided in Table 2.

M40 Protective Mask and Head Harness

The M40 protective mask (see Figure 1) was chosen for evaluation because it is the standard Army field mask and because FF data already existed for this mask (Brletich, 1992; Fritch, 1996). The M40 is a full facepiece mask that is made in three sizes. The M40 was designed to provide an FF of at least 1667 for 88% of the Army population when correctly fitted (Brletich, 1992; TRADOC, 1992). An FF of 1667 provides a level of protection that ensures that for every 1667 particles in the air outside the mask, only one such particle will leak inside the mask.

The M40 consists of a silicone rubber facepiece (see Figure 4) with an attached peripheral surface for forming a seal with the human face (Headquarters, Department of the Army [HQDA], 1988). The sealing surface has two distinct regions that can apply pressure to the face. The outer region is firmly connected to the faceblank or outer shell of the mask, whereas the inner or inturned region is a curved flap of material extending from the outer region (see Figure 5). A side-mounted replaceable canister filters contaminants from inhaled air. The canister screws hand tight into a ring on the facepiece assembly. A one-way outlet valve allows for exhalation and prevents unfiltered air from entering the mask. The mask valves operate under the influence of natural pressures created during respiration. Inhalation creates a negative pressure which opens

¹This organization changed name after the research was finished in October 1998 to the Soldier and Biological Chemical Command.



Figure 2. Headform.

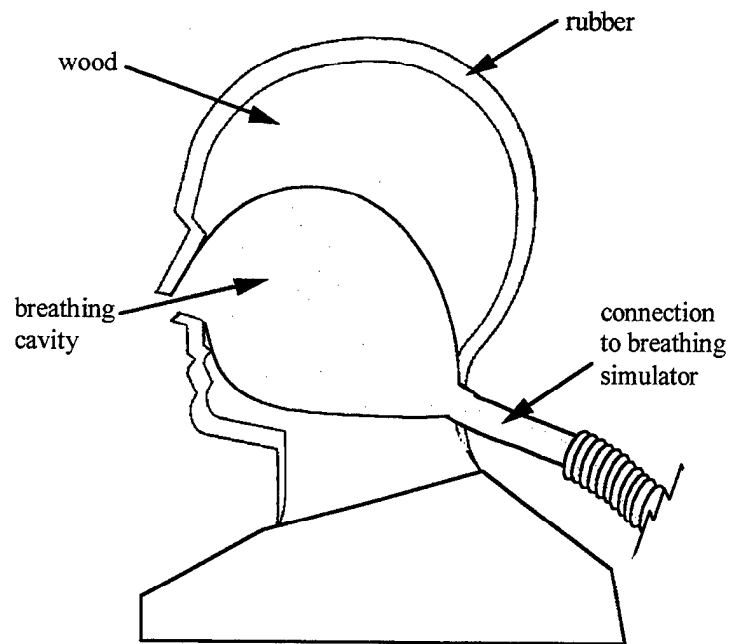


Figure 3. Schematic of headform.

Table 2

Anthropometric Measurements and Percentiles for the Headform

Measurement	Length (cm)	Percentile (male)
Interpupillary breadth	6.95	90th
Bizygomatic breadth	13.6	25th
Menton-sellion length	12.1	50th
Subnasale-sellion length	5.5	90th
Bitrignon crinion arc	31.0	10th
Bitrignon frontal arc	29.7	30th
Bitrignon chin arc	32.6	55th
Bitrignon submandibular arc	31.5	80th
Head circumference	56.0	35th

Note. Anthropometric measurement definitions and techniques from Gordon et al. (1989).

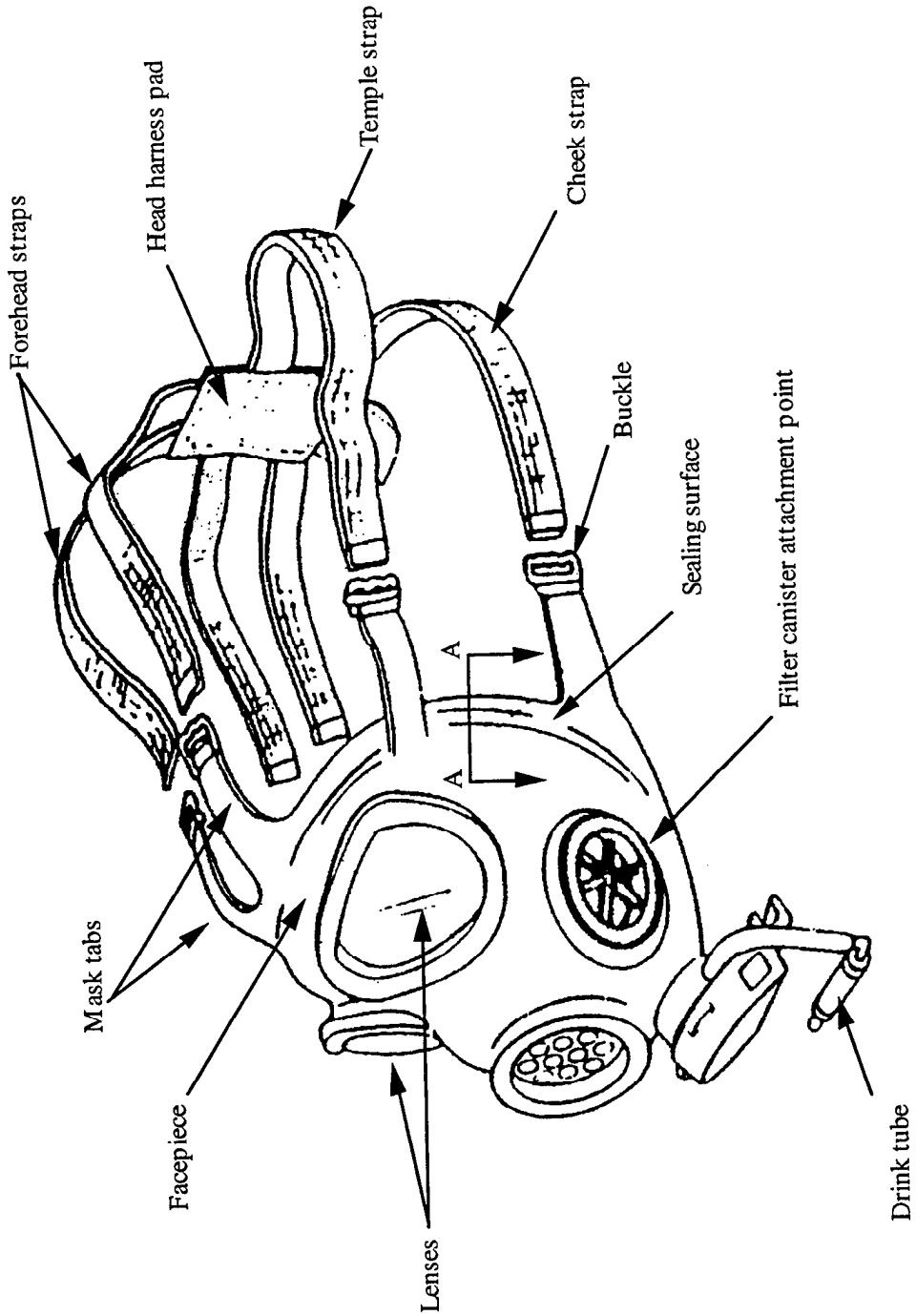


Figure 4. Schematic of M40 protective mask (HQDA, 1988).

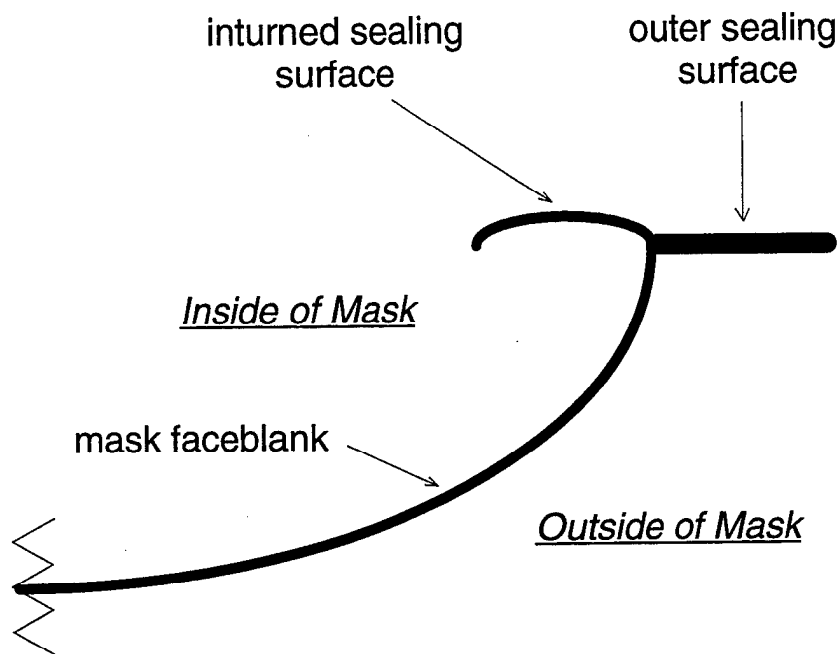


Figure 5. Mask sealing surface cross section A-A from Figure 4.

the inlet valve and draws air through the filter canister. Negative pressure also closes the outlet valve, preventing leaks. Exhalation creates positive pressure, which closes the inlet valve and opens the outlet valve, allowing air to flow out of the mask. A drink tube provides an opening to the inside of the mask and was used during this evaluation as an access port through which internal mask air was sampled.

An elastic head harness attaches to the mask facepiece tabs to secure the mask to the head and face. The six straps of the harness (forehead, temple, and cheek) are fed through the buckles molded into the tabs of the mask, allowing local individual adjustment of each strap to achieve a good seal. A head pad joins the six straps at the back of the head, and strap end clips prevent the loose strap ends from fraying.

A single M40 mask was used for the entire evaluation because of a limited supply of masks available at the Edgewood Research, Development, and Engineering Center (ERDEC²). Using a single M40 mask was considered appropriate for the present evaluation because the

²Beginning October 1998, ERDEC became the Edgewood Chemical Biological Center.

objective was to develop a method of measuring and evaluating seal pressure, not to prove that relationships between seal pressure and FF are the same for all masks.

Before being sent to soldiers in the field, each mask is quality assurance (QA) tested for leakage through the filter and around mask hardware components such as eye lenses and voice-mitters. The M40 mask used in the present evaluation was QA tested at ERDEC.

Head harnesses have a limited life because the straps lose elasticity as a function of time and use (HQDA, 1988). Therefore, a new head harness was used for each trial to eliminate the effects of permanent deformation that might transfer from trial to trial if the same head harness were used throughout the entire evaluation.

The best fit for the headform was achieved with a medium M40 mask because the eyes were centered in the lenses and the mask sealing surface was in full contact with the face but did not contact the ears or the hairline. For this evaluation, the mask was fitted on the headform for each test trial in the manner described in the operator's manual (HQDA, 1988) and reviewed briefly here. The head harness was attached to the mask, its straps were loosened, and then it was reversed and pulled down over the front of the mask. The headform chin was seated in the chin pocket of the mask, and the rest of the mask was rotated up to contact the headform at the cheeks, temples, and forehead. The headform eyes were checked to verify that they were centered horizontally in the mask lenses, and the nosecup was checked to be sure it was open and sealed against both sides of the face and nose of the headform. Then the head harness tab was grasped and the head harness was pulled up and over the top and back of the headform, ensuring that the headform ears were between the temple and cheek straps. Then the straps were pulled through the buckles to remove any slack in the straps and to prevent the mask from slipping on the headform, but they were not pulled enough to tighten the mask and form a seal.

Guides were used to verify that the mask was in the same initial position on the headform at the beginning of each trial. Two staples, forming a notch in the back of the headform, were used as a guide for aligning the head harness pad to ensure that it was consistently located at the back of the head. Distances from the peripheral edge of the mask to headform features such as ears, hairline, and neck were measured and checked against the intended initial position measurements. The initial position measurements were 2 mm from hairline to mask edge, 29 mm from ear to mask edge, with the edge of the mask just touching the neck at the chin. The mask was moved on the headform if necessary and rechecked. After the mask was verified to be in the initial position on the headform, the harness straps were further adjusted by pulling more strap material through the

buckles to achieve one of the specified strap adjustment conditions as designated by the test protocol for that trial.

Head Harness Strap Adjustment Conditions

Head harness strap adjustment was used as a control variable in the present experiment. Three strap adjustment conditions were investigated during this study and were specified by the length of strap that was pulled through the buckle (see Table 3). The strap tightness increases from Condition 1 to 3. A standard flexible plastic ruler with metric units was used to measure strap lengths (± 0.5 mm) during adjustment of head harness straps. The length of strap was measured from the metal strap end clip to the mask buckle.

The strap adjustment conditions were determined during pilot investigations and were selected to allow the mask FF to go from failing to passing as strap tightness increased from Condition 1 to 3. In an earlier investigation, many adjustment conditions were explored (see Appendix A), but in the current investigation, trials were conducted around the point of passing FF, 1667. A passing FF was normally achieved in adjustment Condition 3 and sometimes in Condition 2; therefore, more trials were conducted in Conditions 2 and 3 than in Condition 1, in which FFs were usually well below the criterion of 1667.

Table 3

Head Harness Strap Adjustment Conditions

Condition	Number of trials	Length of strap pulled through buckle (mm)		
		Forehead	Temple	Cheek
1	3	51.0	91.0	91.0
2	9	56.0	96.0	96.0
3	10	61.0	101.0	101.0

There are two of each (right and left) forehead, temple, and cheek straps. Right and left straps were adjusted identically.

Head Harness Strap Stretch

Strap stretch was chosen as a measure of head harness strap tightness because it was simple to measure and was thought to be related to strap tension and FF. If strap stretch was strongly related to FF, it could easily be measured in the field to ensure that masks were fitted and worn correctly.

Strap tension was explored briefly as an alternate measure of strap tightness, but additional investment would have been required to procure and explore the feasibility of using a sensor such as a buckle transducer which has been used to measure tension in tendons and ligaments (Salmons, 1969; Komi, 1990). An early attempt to develop calibration curves for determining tension in a head harness strap from the measured strap stretch (see Appendix B) revealed wide variations in strap behavior that precluded reliable tension predictions by this approach. Thus, strap stretch was chosen as the independent variable instead of strap tension.

Strap stretch is defined as

$$\text{Strap Stretch} = \frac{\text{Stretched Strap Gauge Length}}{\text{Unstretched Strap Gauge Length}} \quad (1)$$

A Fowler Ultra-Cal II digital caliper (accuracy ± 0.03 mm) was used to measure gauge length in the head harness straps for calculating strap stretch. The gauge length was marked by small stitches sewn on each strap, along its length, approximately 10 mm apart (see Figure 6). The stitches were sewn perpendicular to the direction of stretch; thus, they did not change the behavior of the strap. The location and distance between gauge length markers was chosen for easy access to the markers to allow measurements to be made and to prevent loss of a marker when strap material was pulled through the buckles.

The unstretched strap gauge length was measured on new head harnesses before testing. After stitches were sewn on the head harness straps to designate gauge length, the gauge length was measured using digital calipers while the harness was lying flat on a table. After the harness was attached to the mask, put on the headform, and tightened according to the test scenario, the stretched gauge length was measured. The stretched gauge length was measured a second time (at the end of the trial) to determine if it had changed as a result of lifting the mask sealing surface to place and remove pressure sensors during the trial. Each measure of strap gauge length (unstretched, first stretched, and second stretched) was made three times, and the average of each was used to calculate the strap stretch. A new head harness was used for each trial.

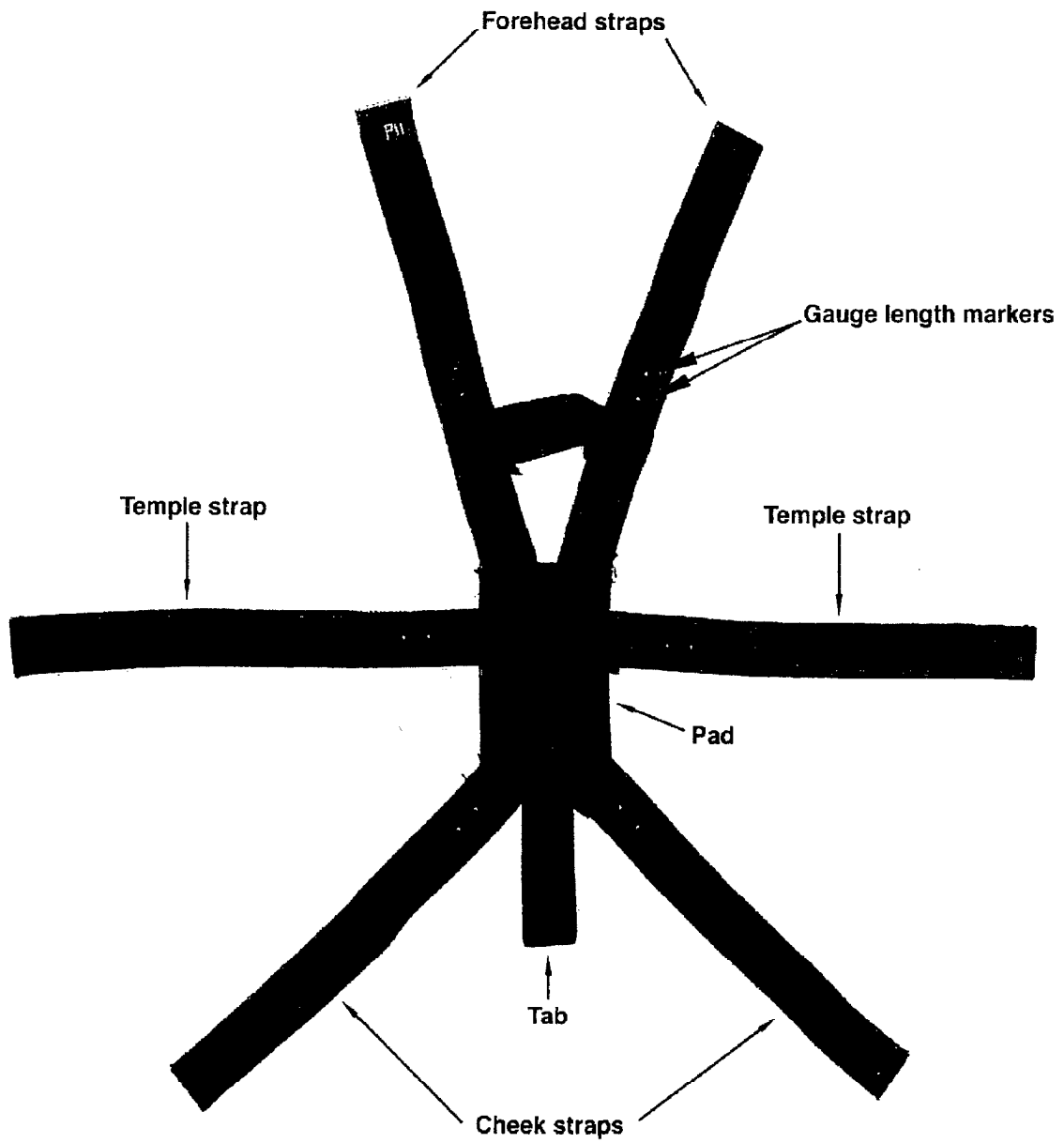


Figure 6. Head harness with gauge length markers.

Breathing Simulator

A breathing simulator was connected to the headform to simulate human breathing during the evaluation. Breathing must be simulated in order to clear the inside of the mask of particles by drawing in clean air through the mask filter and expelling particle-laden air through the mask outlet valve. Over time, respiration clears the mask, leaving fewer particles inside than outside, and resulting protection factors can be measured.

The breathing simulator (see Figures 7 and 8) was developed by Reimers Engineering, Inc. (1984) under contract to CBDCOM for performance testing of protective masks. The simulator was designed to reproduce a wide range of respiration rates, waveforms, and volumes. The simulator consists of a control box containing a waveform generator and a breathing machine. The waveform generator controls the breathing machine which pumps a volume of air to and from the headform to simulate breathing. The waveform generator provides control of four respiration variables: breathing rate, exhalation-to-inhalation time ratio, tidal volume, and breathing waveform.

For this evaluation, the following values were used: 20 breaths per minute, 1-to-1 exhalation-to-inhalation time ratio, 1.5-liter tidal volume, and a sinusoidal waveform. These values allowed the mask volume to clear in 10 minutes, a reasonable amount of time for the test scenario (see Appendix C). Similar respiration values have been reported in the literature (see Table 4) and were used as a guide in selecting the respiration values for this evaluation.

Fit Factor

M41 Protective Mask Fit Validation System

The Protective Mask Fit Validation System (PMFVS) was used to measure the FF of the M40 protective mask on the headform (HQDA, 1993). The PMFVS consists of the protective mask fit tester, high-efficiency particulate air (HEPA) filter, sample and ambient tubing assemblies, alcohol cartridge, M40 drink tube sampling adapters, and FitPlus[®] fit test software (see Figure 9). The fit tester was designed to measure FF, a ratio of the concentration of particles outside versus inside the mask (TSI [not an acronym], Inc., 1991). Particles inside the mask were assumed to be present as a result of seal leakage because particles cannot pass through a QA-tested mask filter canister or around QA-tested mask hardware components. The system measures microscopic particles that exist naturally in air; generated aerosols, such as corn oil or salt, can be used but are not required.

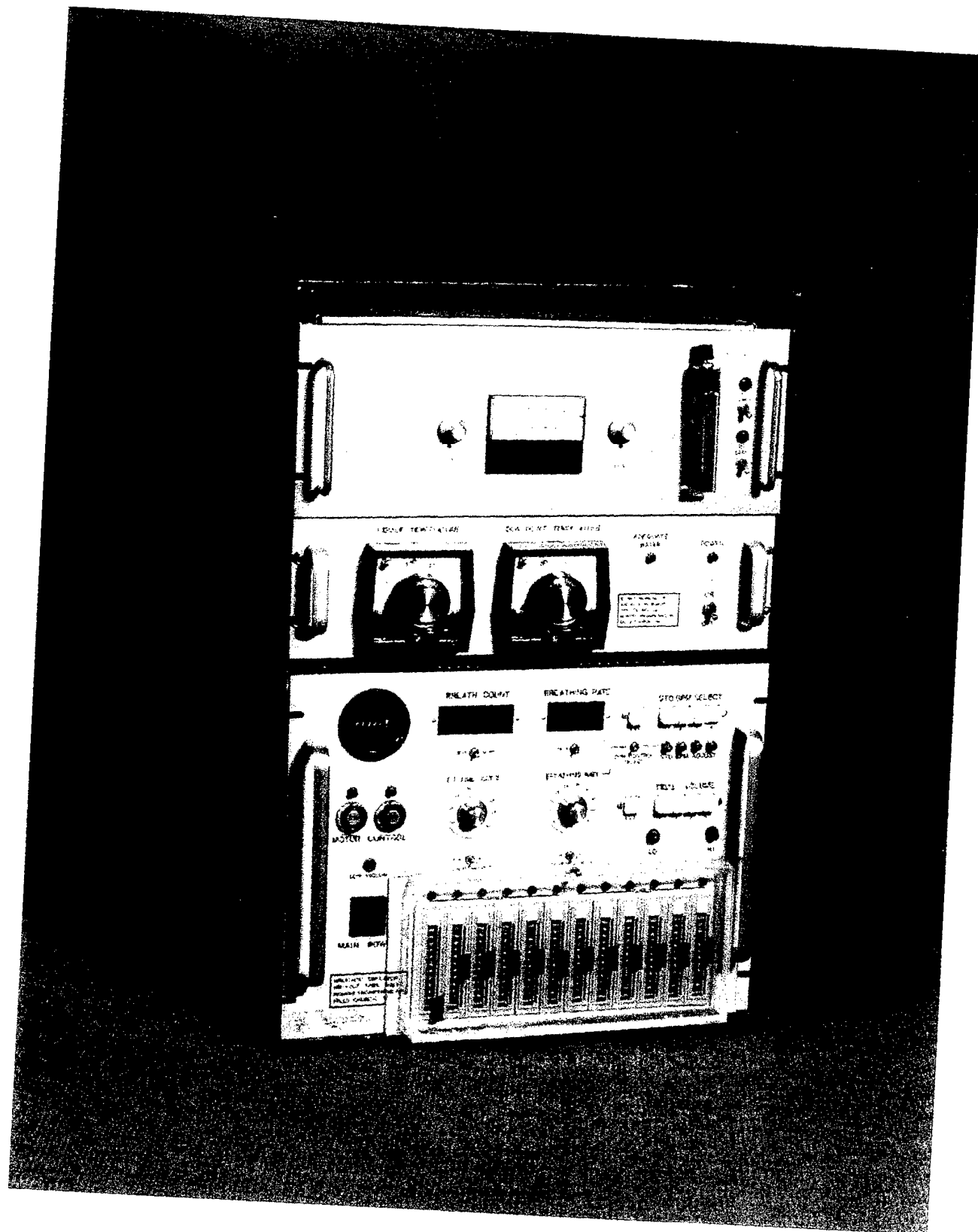


Figure 7. Waveform generator.

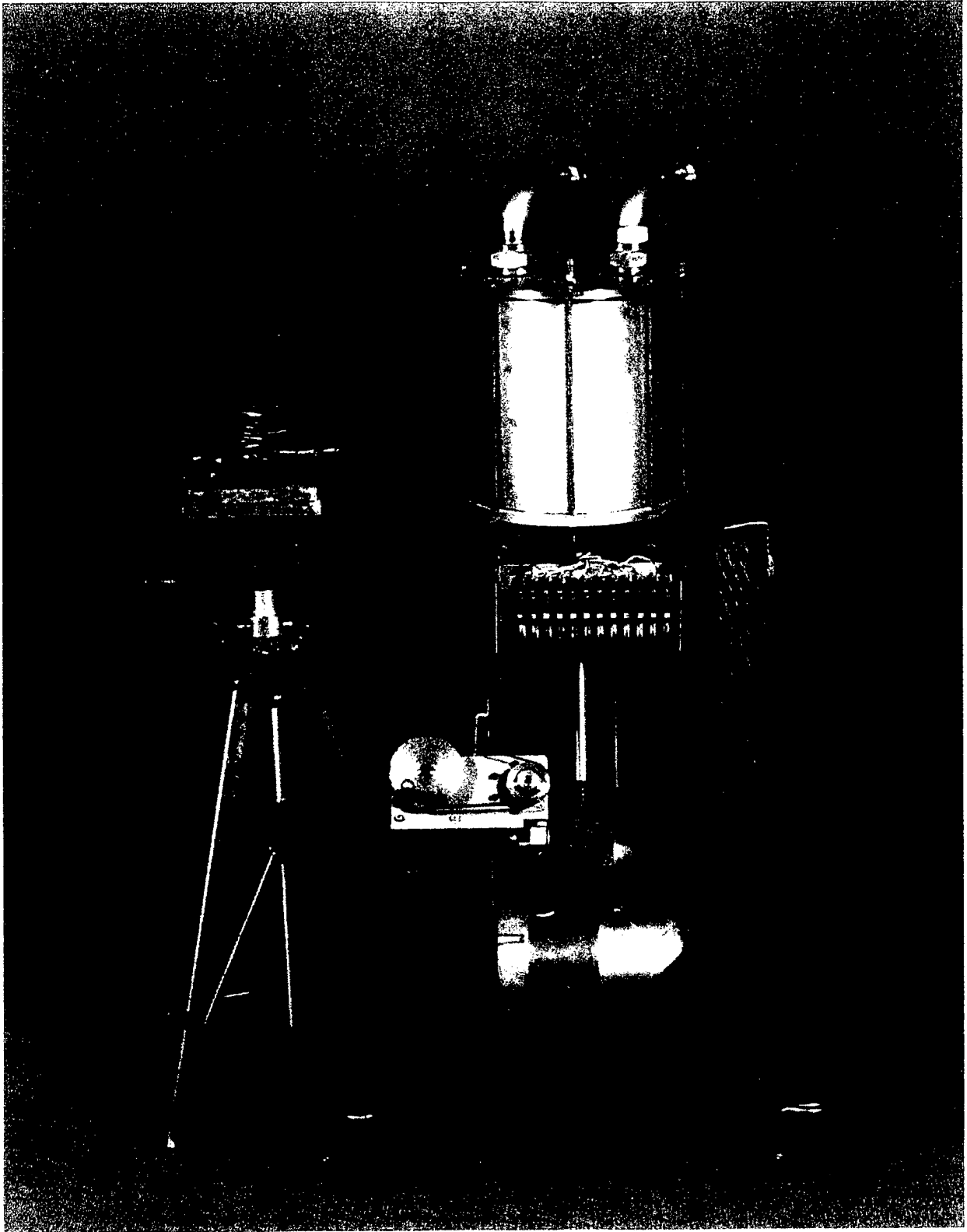


Figure 8. Breathing machine.

Table 4

Respiration Values for Masked and Unmasked Breathing at Varied Activity Levels

Mask	Exercise level	Respiration rate (min ⁻¹)	Tidal volume (l)	E:I ^a time ratio	Waveform	Source
M17	rest	12.0	0.48	1:1	sinusoidal	Johnson, 1976
M17	light	24.0	0.65	1:1	rectangular	Johnson, 1976
Sim1 ^b	rest	14.8	0.61			Silverman, Lee, Plotkin, Sawyers, & Yancey, 1951
Sim1 ^b	moderate	20.7	1.3			Silverman et al., 1951
None	moderate	22.7	1.3			Silverman et al., 1951
None	moderate	25.0	1.3			Craig & Cain, 1955
None	moderate	21.4	1.1	1.38:1		Harber, SooHoo, & Lew, 1988
Sim2 ^b	moderate	20.8	1.3	1:1		Harber et al., 1988

^aE:I = exhalation-to-inhalation time ratio. Missing values were not reported by the investigator.

^bSim1 and Sim2 are simulated resistance values that approximate those of full facepiece masks.

Fit factors measured using the PMFVS have been compared with those measured using the standard Army method of forward light-scattering photometry (FLSP) in generated aerosol chambers. Researchers found the two methods to be equivalent. Gardner et al. (1988) reported a correlation of 0.996 between FFs measured using a device similar to the PMFVS and those measured using FLSP. Laye (1987) reported a 96% correspondence in pass-fail results over 100 trials that compared the PMFVS to the FLSP. Meunier and Constantine (1990) reported a much lower correlation of 0.59 but stated that this result was probably attributable to the process used in the experiment rather than to performance of the PMFVS. These researchers concluded that the PMFVS and FLSP techniques were comparable in their ability to assess mask FFs. In addition, Gardner et al. stated that because the PMFVS functions as a single particle counter at very low concentrations, it can detect concentrations below the sensitivity of the FLSP and thus has the potential to measure the higher FFs that are required of current military masks. Therefore, the PMFVS was used in the current evaluation because it provided a capability similar to that of the FLSP and generated aerosol chamber system, yet was not as expensive to use or time consuming to set up. Also, the PMFVS was readily available and easily used in a small laboratory.

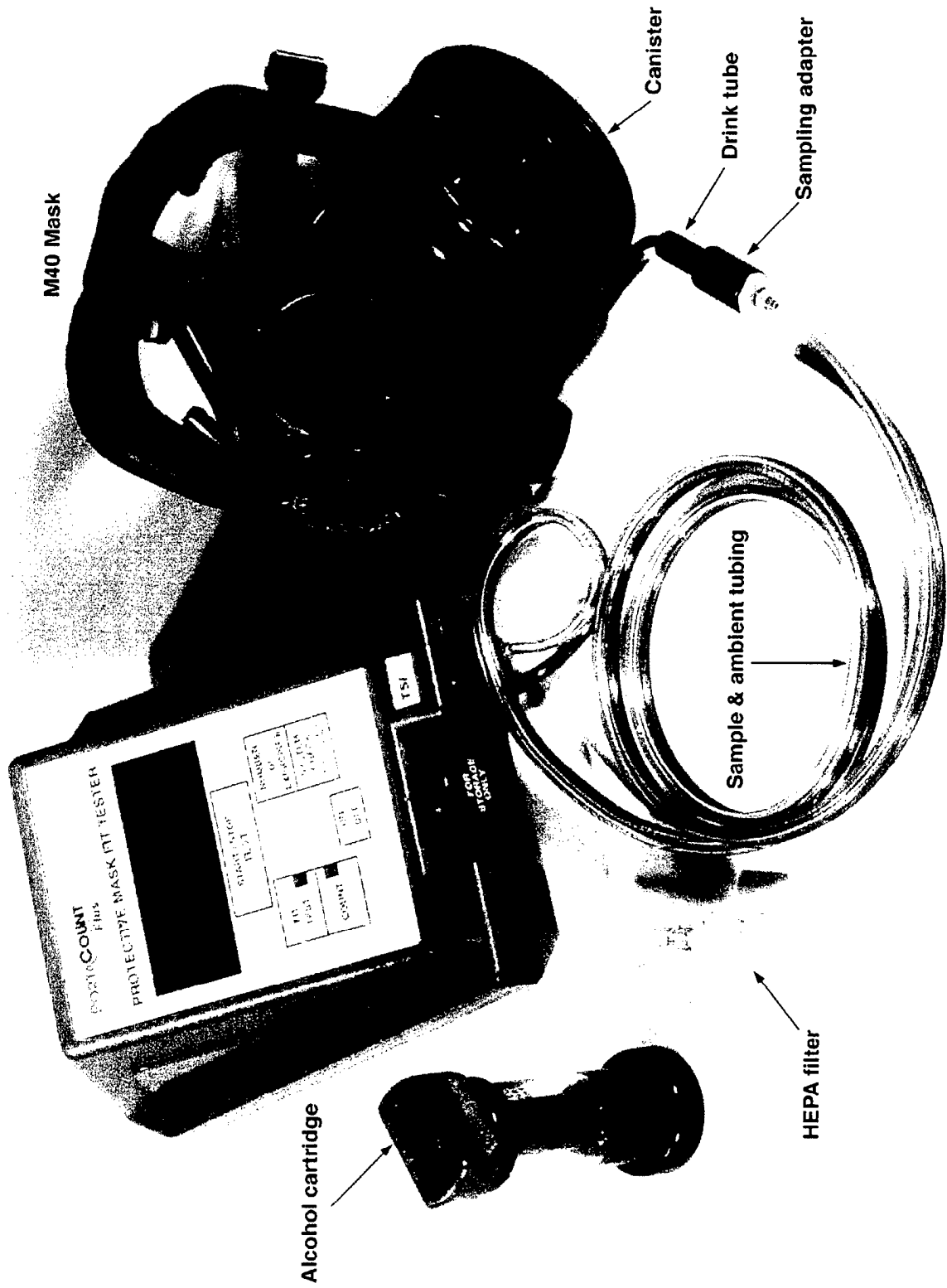


Figure 9. M41 Protective Mask Fit Validation System.

The fit tester functions as a particle counter and calculates concentration based on the particle count, flow rate, and time period:

$$\text{Particle Concentration} = \frac{N}{P \bullet 1.67 \text{ cm}^3/\text{sec}}, \quad (2)$$

in which N is the number of particles counted in a time period, P , at a flow rate of $1.67 \text{ cm}^3/\text{sec}$. The fit tester can measure particle concentrations from 0.01 to 500,000 particles/cm³.

Fit Testing

For fit testing, the sample and ambient tubing assemblies are connected to the fit tester inlet ports, and the opposite end of the sample tube is attached to the drink tube of the protective mask via a drink tube adapter. The free end of the ambient tube draws air samples from the ambient air, whereas the sample tube draws samples of air from inside the mask. The fit tester automatically controls the air sampling by switching a valve and alternately sampling from inside and outside the mask at user-defined intervals. The air samples are passed through the inlet ports and the fit tester calculates the concentration of each sample.

A fit test consists of a series of subtests during which both ambient and mask air samples are taken and intermediate FFs are computed. Head and facial movements or exercises are performed during each of the subtests to simulate normal activities that might break the seal between the mask and face. Each subtest consists of a beginning ambient sample, followed by a mask sample, and completed by an additional ambient sample. The intermediate FF is calculated by the fit tester as follows:

$$\text{Intermediate FF} = \frac{C_B + C_A}{2 \bullet C_M}, \quad (3)$$

in which FF is the fit factor, C_B is the ambient particle concentration taken before the mask sample, C_A is the ambient particle concentration taken after the mask sample, and C_M is the particle concentration in the mask. The average ambient concentration is used to account for any shifts in particle concentration over the duration of the test.

Then, an overall FF is computed from the intermediate FFs as follows:

$$\text{Overall FF} = \frac{n}{\frac{1}{FF_1} + \frac{1}{FF_2} + \frac{1}{FF_3} + \dots + \frac{1}{FF_{n-1}} + \frac{1}{FF_n}} \quad (4)$$

in which n is the number of subtests and FF_n is the fit factor for the n th subtest (TSI, Inc., 1991). The overall FF is a weighted average that emphasizes low intermediate FFs and the resulting amount of airborne hazard that a mask wearer would inhale. For Army fit testing, five to six subtests are normally used, with 20-second mask samples and 5-second ambient samples. The fit tester can measure FFs from 1 to greater than 10,000 and has an accuracy of $\pm 10\%$ of the reading.

For this evaluation, fit testing was performed on a headform with a breathing simulator; therefore, various procedures had to be modified or added. The headform was fit tested with a series of six subtests with the same sampling intervals used for human testing. Soldiers normally clear their masks immediately after they don them by exhaling forcefully to evacuate the air space within the mask and then inhaling to refill it with clean air drawn through the filter. A procedure was developed to clear the mask on the headform before the mask was fit tested. A pilot study revealed that the pumping action of the breathing simulator eventually cleared the internal air space of the mask on the headform. Steady state particle concentrations were reached within 10 minutes of attachment of the filter canister to the mask facepiece while the mask was on the headform with the breathing simulator turned on (see Appendix C). After the mask was cleared, the fit test was performed and the overall FFs were saved using the FitPlus[®] software program.

Preventive maintenance and performance verification checks were performed daily in accordance with the operator's manual to ensure that the mask fit tester was functioning correctly. Fit testing was performed on days when the ambient particle concentration was above 3000 particles/cm³ as recommended in the operator's manual (TSI, Inc., 1991). When ambient particle concentrations are low, the number of particles that leak into the mask may not be sufficient to produce an accurate measurement, and resulting FFs may be overestimated. On days when the ambient particle concentration was below 3000 particles/cm³, no test trials were conducted.

Seal Pressure

Pressure Measurement System

A Tekscan pressure measurement system was used to measure seal pressure (Tekscan, Inc., 1992, 1993). The system consists of thin film flexible pressure sensors, a scanning handle connector, International Business Machines (IBM)-compatible PC parallel port connection

box, and pressure display and analysis software (see Figure 10). These components were used in conjunction with an IBM-compatible PC to display and record real-time seal pressure distributions for subsequent analysis.

Sensor Technology and Software

The sensor consists of a sensing area, arm, and connection end (see Figure 11). The entire sensor is formed from two overlaid sheets of polyester film held together with adhesive to form a very thin (0.15 mm) and flexible sensor. The sensing area is a grid of multiple sensing elements. The grid is formed by screen printing conductive rows on the inner surface of one sheet and columns on the inner surface of the facing sheet of film. A pressure-sensitive semi-conducting layer, commonly called resistive ink, is sandwiched between the conductive grids at the points of intersection to form individual force sensing elements (see Figure 12). The sensing elements change electrical resistance in response to force applied normal to the sensor surface. The conductive traces for each row and column pass along the length of the sensor from the sensing area, through the arm, to the connection pads in the end. The connection end of the sensor is placed inside the scanning handle where the sensor connection pads align with and contact a series of pins. The sensor is locked in place by a latch on the outside of the scanning handle.

The scanning handle is connected to the computer and software via the parallel port interface box. The handle scans the row and column connection pads, and the software records the resistance and converts it to a force measured at each intersection or sensing element. Pre-recorded calibration files are used to make the conversion. Sequential scanning of the sensing elements allows the computer to record force, location, and timing of contacts on the surface of the sensor. The software calculates the pressure from the recorded force and area of each sensing element.

For this evaluation, 4.5- by 2-cm low pressure sensors were used with the Tekscan Industrial Sensing System, Adjustable Gain (ISCAN-AG) v3.820 software. The sensors have a grid of 24 by 11, or a total of 264 sensing elements. These sensors were selected because they were “off the shelf” and their size allowed them to be easily placed between the mask sealing surface and headform face to measure seal pressure and record distribution features.

Sensitivity

The v3.820 software version has an adjustable gain or sensitivity adjustment feature that allows adjustment of the electronic gain of the scanning handle for the range of loads that will be applied. For example, a 30-pound-per-square-inch (psi) sensor could be adjusted to measure pressures in the range of 0 to 5 psi.

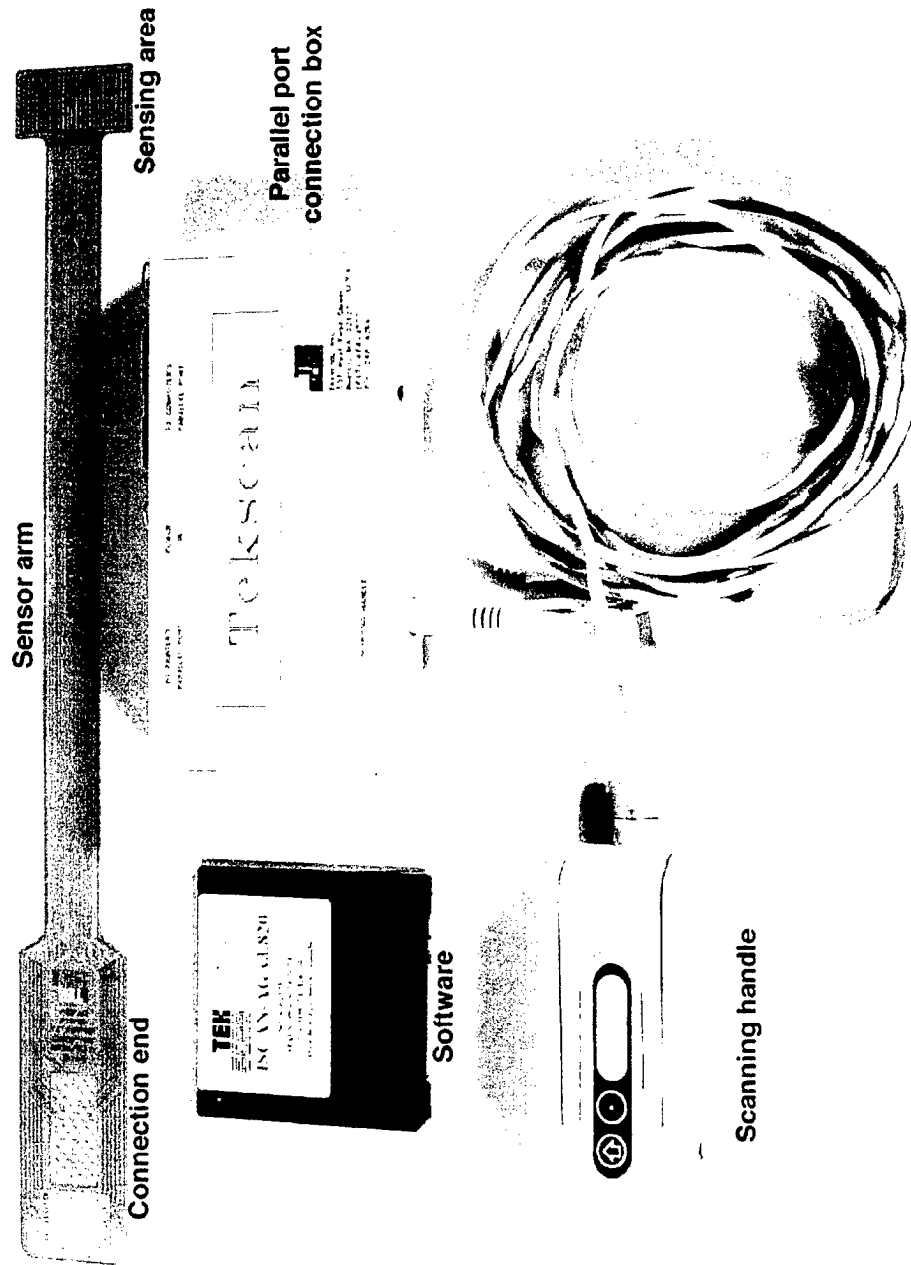


Figure 10. Pressure measurement system.

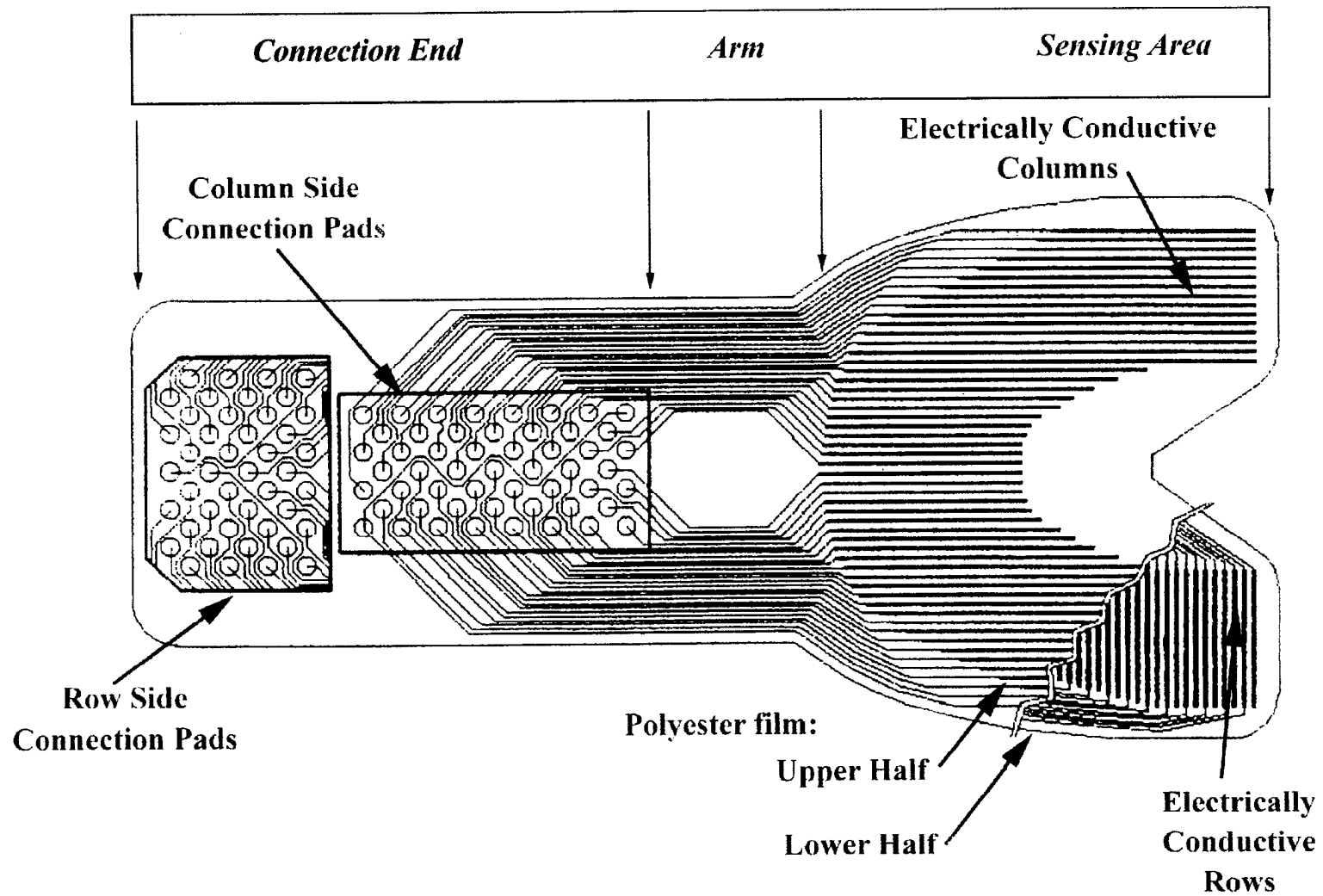


Figure 11. Schematic of a typical Tekscan sensor (Tekscan, Inc., 1992).

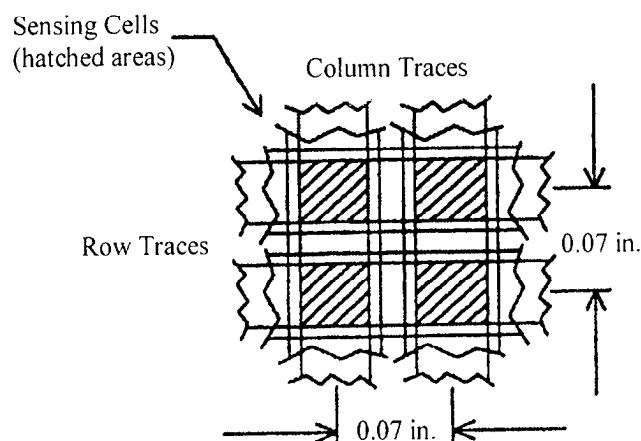


Figure 12. Force-sensing elements (Tekscan, Inc., 1992).

The sensitivity must be adjusted for each sensor just before calibration. As recommended by the manufacturer, a known weight well above the upper range of the loads to be applied during the experiment is placed on the sensor for 15 seconds, and the automatic software sensitivity adjustment is performed. The weight is selected above the upper range of force to be applied in order to prevent saturation of the sensing elements during the evaluation. Saturation of sensing elements causes overall pressures to be underestimated. During sensitivity adjustment, the software measures the contact force at each sensing element and assigns each force level one of 13 colors that the software can display, with red being the highest force and blue being the lowest. This allows the software to display a range of colors for the range of force that will be measured. For this evaluation, sensitivity was adjusted using a weight of 2000 grams (g), which is well above the upper range of force (1000 g) to be expected at the mask and face scal, based on pilot studies (see Appendix A).

Calibration

Calibration was performed for each sensor after sensitivity adjustment. Calibration assigns specific values and units of force to both the color-coded pressure display and the sensor output by comparing sensor output to a reference value or calibration weight.

Calibration is performed by placing a known weight upon the sensor for a period of time determined by experimental application (time required to perform measurements) and sensor settling time (see Appendix D) and then specifying the weight and units in the software calibration procedure. Forces closest in value to the calibration weight are measured most accurately. Calibration and sensitivity files for a particular sensor were saved and reloaded before measurements were made using that sensor.

Several materials were required to calibrate the sensors. A small piece of Plexiglas® glued to a load-distributing piece of foam the same size as the sensor served as a platform for the calibrated brass weights (1 to 5000 g, Ohaus Scale Corporation, Union, New Jersey). The sensor was placed on a sheet of silicone rubber, the same material and approximate thickness (2.9 mm) as the mask faceblank. Then, the platform was placed on the sensor. A series of circular targets was drawn on the platform as a guide for consistent placement of the cylindrical brass weights. This setup was required for even distribution of loads on the sensor surface as well as to approximate the experimental loading conditions (see Figures 13 and 14).

During calibration, a weight was placed on the sensor and the calibration was performed 15 seconds later, after the sensor reached a steady state value (see Appendix D). The 15-second period was chosen to allow enough time to place the sensor between the mask sealing surface and headform face when actual measurements were made during testing. Thus, both calibration and test measurements were performed 15 seconds after the sensor was loaded.

Special Procedures

Pilot investigations of sensor performance (see Appendix D), as well as reports from other users (Baumann, Krabbe, & Farkas, 1992; McPoil, Cornwall, & Yamada, 1995; Quesada, Rash, & Jarboe, 1996), revealed that Tekscan sensors experience changes in performance over time and because of repeated use and temperature changes. With this in mind, a conservative approach for use of the sensors was adopted.

Calibration was performed daily, immediately before and at the same ambient temperature as testing. Calibration was completed in about 1 hour, and testing was performed and completed in the following hour. Calibration and test measurements were made 15 seconds after sensor loading to ensure consistent settling and drift of values. Because sensor performance changes with time and use, each sensor was used in as few trials as possible. A limited supply of sensors precluded the use of a new sensor for each trial. The maximum number of trials completed using a single sensor was three. Adequate performance and calibration, as described in the following paragraph, was verified before any sensor was used for testing.

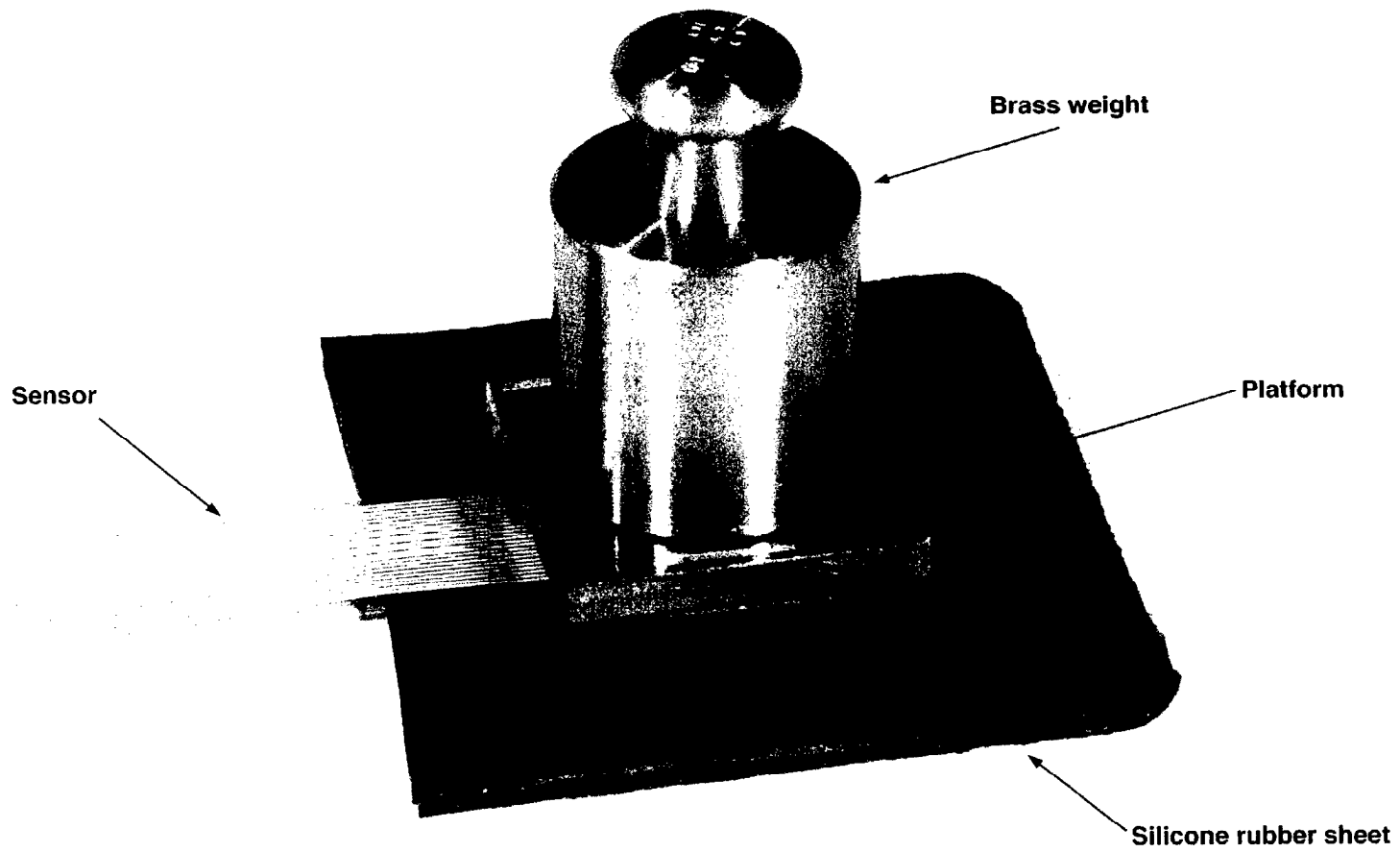


Figure 13. Calibration platform and weight loading the sensor.

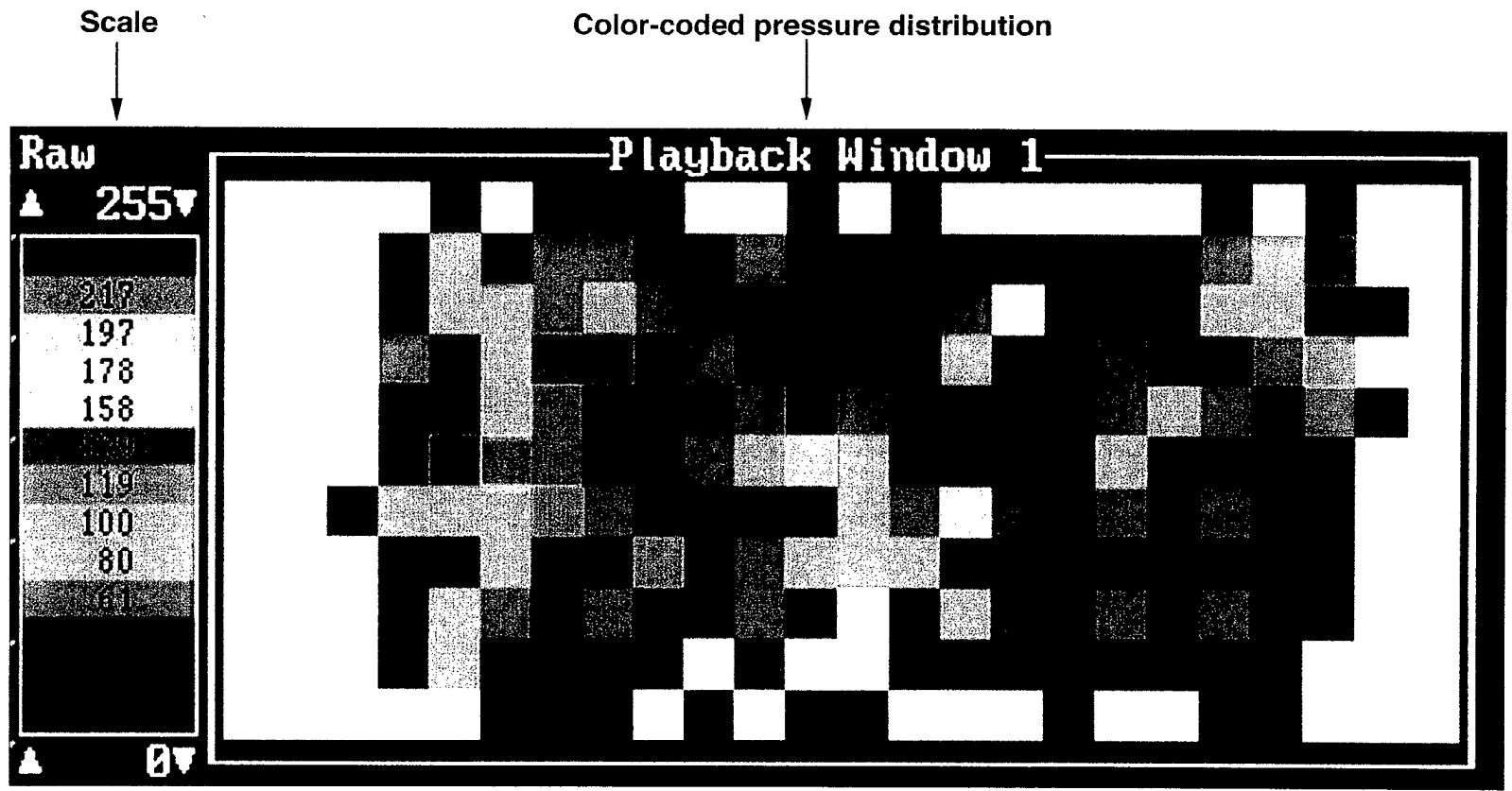


Figure 14. Distribution of load to sensor surface, Tekscan map.

Based on pilot evaluations (see Appendix A), a wide range of forces was anticipated for the present evaluation (50 to 1000 g), so a modified calibration approach was adopted to ensure higher accuracy at low force values (< 250 g). Calibration was performed multiple times at several different loads across the range, because a single calibration did not provide accurate measurements ($\pm 10\%$ of the actual load placed on the sensor) across the entire range of forces (50 to 1000 g). Therefore, a sensor might have as many as four calibration files to cover the entire range. Accordingly, each of the calibration files had a limited range over which accurate pressure measurements could be made. The usable range of a calibration file was defined as the upper and lower limit force values at which the desired accuracy could be achieved ($\pm 10\%$ of the actual load placed on the sensor). Outside this range, the accuracy was less than $\pm 10\%$ of the applied load. The usable range was determined by checking load measurement accuracy at several incremental values higher and lower than the load used to calibrate the sensor. Before each measurement was made, the calibration file with a usable range covering the anticipated load was opened. After the measurement was made, the value was verified to be within the usable range of the current calibration file. If it was not, the measurement was repeated using a different calibration file. Measurements were accepted for record when they fell within the usable range of the calibration file that was used to make the measurement. The overall accuracy of a typical sensor across the entire load range was based on several calibration files (see Figure 15).

Early pilot evaluations revealed that sensors were difficult to calibrate at low force levels because loads did not distribute evenly across the sensing elements. A small residual volume of air between the two sealed polyester sheets that form the sensor created a pillowing effect. Weights less than 300 g were observed to oscillate slightly when placed upon the sensor. Weights greater than 300 g were heavy enough to cause the air to evacuate the sensor and pass into an air channel created in the arm of the sensor. Because loads less than 300 g were expected in the seal measurements, three small slits were cut in the polyester sheets of the sensor to allow air to escape at low loads. The slits were located at the junction of the sensing area and the arm where the air channel begins. These slits allowed the air to evacuate; however, during a pilot study using humans, the slits allowed sweat from human faces to leak into the sensor and cause damage. Consequently, this study had to be conducted on a headform.

Measurements

After daily calibration of the sensor, seal pressure was measured. Eleven locations were selected for measurement (see Figure 16) to provide pressure distributions along as much of the sealing surface of the mask as possible. Measurements were not made in the area of the chin because the nearly 90° angle formed where the head meets the neck on the headform made it impossible to

place a sensor without severely bending or damaging the sensor lead. The 11 measurement locations were the left cheek strap (LCS), right cheek strap (RCS), left cheek (LC), right cheek (RC), left temple strap (LTS), right temple strap (RTS), left temple (LT), right temple (RT), left forehead strap (LFS), right forehead strap (RFS), and forehead (F). The exact placement of the sensor at each location was determined during pilot investigations and corresponds to the placement at which distinct and predominant seal pressure contact was observed.

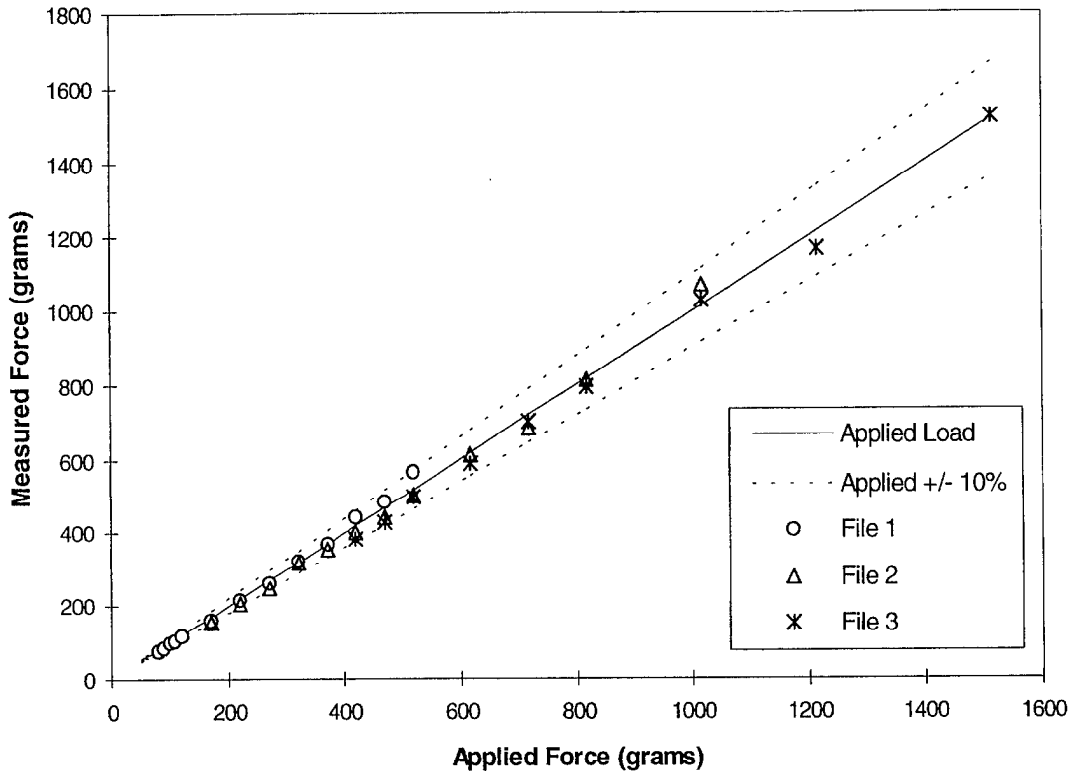


Figure 15. Accuracy of a sensor across the load range, based on three calibration files.

Measurements were made by carefully lifting the mask sealing surface on the headform, placing the sensor, gently replacing the sealing surface, and making a 10-second software recording of the pressure distribution at one frame per second (see Figure 17). About 5 seconds elapsed from sensor loading to the beginning of the recording because the sensor connection end had to be placed and latched in the handle and the software recording had to be started. The pressure distribution values at 10 seconds were used for analysis because they were actually the values at 15 seconds after load, which corresponded with the calibration procedure. Each measurement was made twice and sensors were removed and replaced between measurements. The average of the two measures was reported for data analysis and model development.

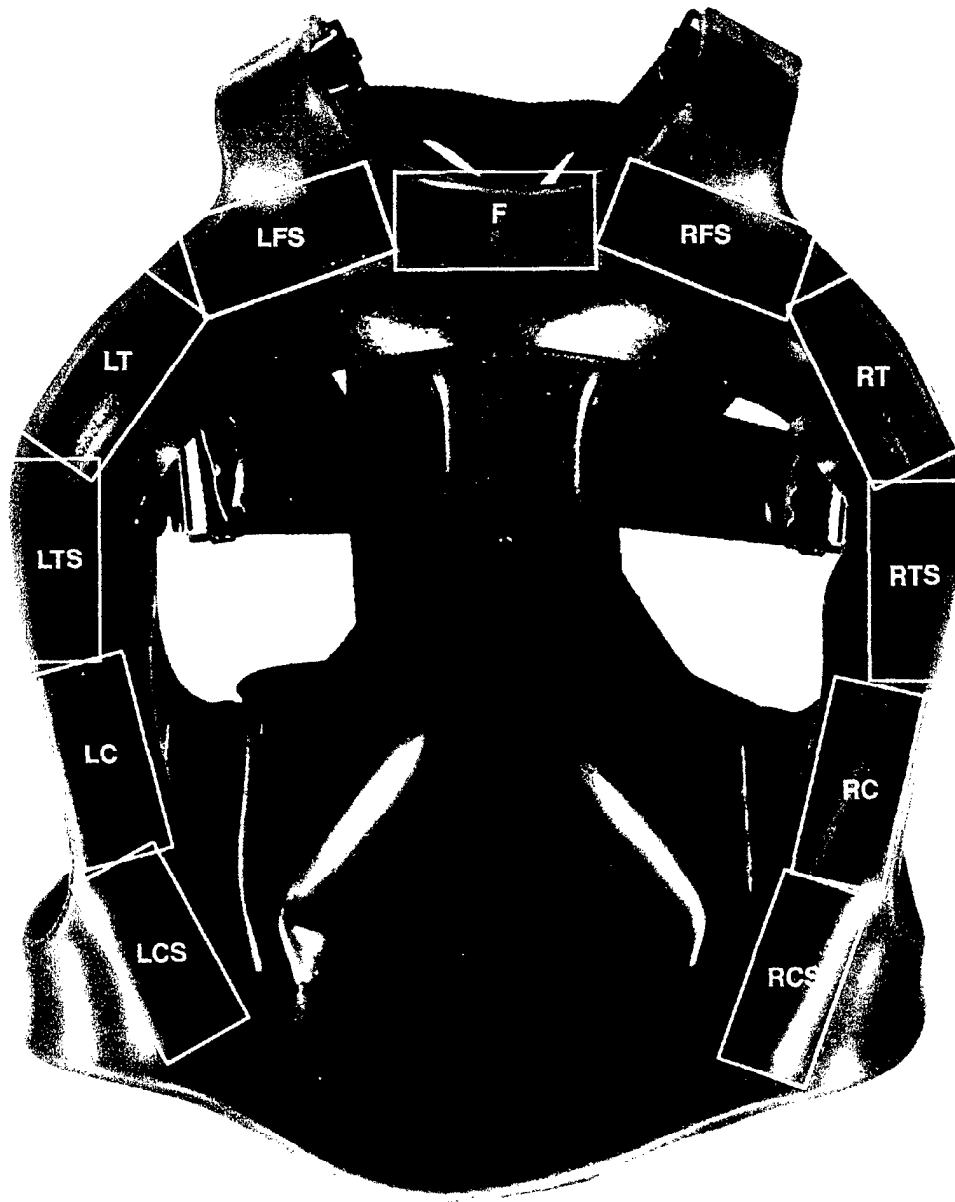


Figure 16. Measurement locations on the sealing surface of the M40 mask.

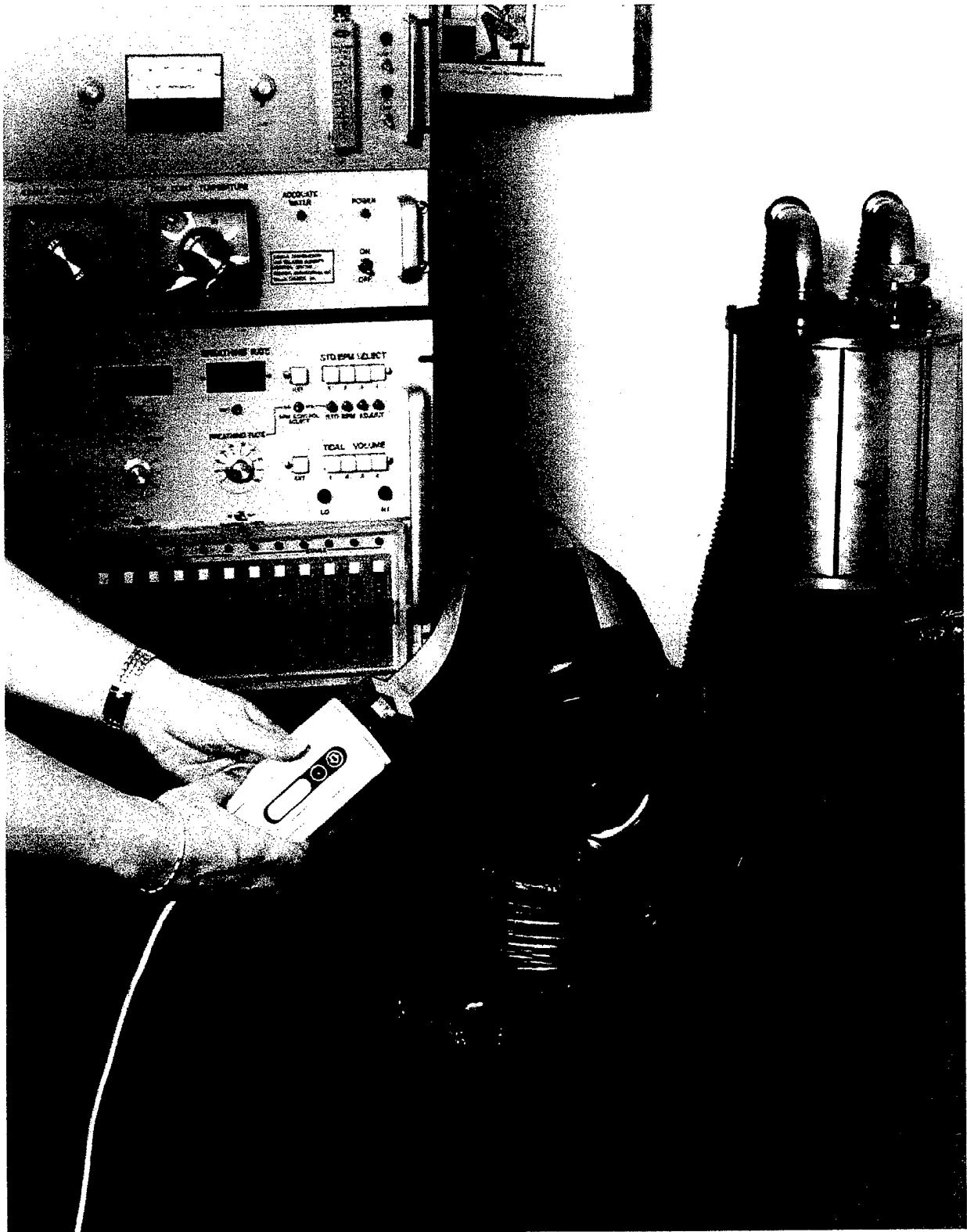


Figure 17. Sensor placed between mask and headform for measurement.

Procedure

A full day of experimentation was required to complete each trial. Twenty-two trials were performed for the three conditions presented in Table 3. For the present evaluation, the mask with a new head harness was placed on the headform for each trial, measurements were made, and the mask was removed at the end of the trial. The head harness strap adjustment condition was randomly selected for each trial. In an earlier investigation, the mask was left on the headform between trials and the straps were increasingly tightened over a series of day-long trials (see Appendix A). The current procedure was adopted to eliminate any carry-over effect created by leaving the mask on the headform, to more closely reflect fit testing in the field, and to verify results from the earlier evaluation.

Before a trial was started, the ambient particle concentration was measured using the fit tester and verified to be greater than 3,000 particles/cm³. The unstretched head harness strap gauge length in each of the six straps was measured and recorded. The strap adjustment condition (see Table 3) was randomly selected. The harness was attached to the mask and the mask was fitted on the headform. The head harness straps were tightened according to the adjustment condition selected for that trial. The mask was allowed to rest on the headform for 2 hours, which was convenient for the evaluation scenario and allowed sufficient time for harness viscoelastic effects to settle (see Appendix B). Stretched head harness strap gauge length in each of six straps was measured and recorded.

Then the FF was measured. Performance verification checks were performed on the mask fit tester. The fit tester sample line was attached to the mask drink tube. The breathing simulator was started. The filter canister was removed from the mask to allow the mask to reach equilibrium with the ambient particle conditions. Mask particle concentrations were monitored using the fit tester until steady state conditions were reached and then the filter canister was reattached. The mask was allowed to clear for 10 minutes and then the fit test was started. After the FF was recorded, the breathing simulator and fit tester were turned off and the sample line was disconnected from the drink tube.

Next, the seal pressure measurements were made. The sensitivity of the sensor was adjusted and then the sensor was calibrated. Seal pressure measurements were made at each of the 11 locations around the mask sealing surface. The appropriate calibration file was loaded before each measurement was made. To complete the trial, the stretched head harness strap gauge length was measured a second time and then the mask was removed from the headform.

Data Analysis

Seal Pressure

To meet the first objective, “*develop a method for measuring and investigating the pressure distribution between a protective mask sealing surface and face for the purpose of evaluating seal integrity and understanding how mask design characteristics influence seal performance,*” general trends in the pressure distributions at the 11 locations were observed. Pressure profiles, consisting of average seal pressures measured at each of the 11 locations along the seal from left to right cheek straps, were plotted for each of the three conditions of Table 3, and trends were compared. In addition, pressure profiles for passing FF trials were compared to pressure profiles for failing FF trials. Then, examples of color-coded pressure distributions at each of the 11 locations were compared for Conditions 1 and 3.

Fit Factor

Fit factor data were plotted by adjustment condition in order to observe trends as the mask was tightened on the headform. The Pearson correlation coefficient between FF and the average ambient particle concentration during the fit test was calculated in order to determine whether fluctuating ambient particle concentrations would influence the FF measurements.

Head Harness Strap Stretch

The stretched gauge length was measured twice, before and after pressure measurements, to determine whether lifting the peripheral mask sealing surface to place and remove sensors altered the calculated strap stretch. Thus, there were two measures of strap stretch for each of the six straps for each trial. The first and second stretch measures for each strap under each condition were compared using Student’s t-tests to determine if significant ($p < 0.05$) differences existed between the two. If the two measures were significantly different, separate relationships between each of the first and second set of stretch measures and FF or seal pressure were developed (see *FF and Head Harness Strap Stretch*, p. 42, and *Seal Pressure and Head Harness Strap Stretch*, p. 43). Average strap stretch for each strap was plotted by condition in order to observe trends as the mask was tightened on the headform.

Model Development

FF and Seal Pressure

To meet the second objective, “*determine the relationship between seal pressure*

and FF ,” multiple regression analysis was used to formulate the following single function linear relationship:

$$FF = A + \alpha_1 P_1 + \alpha_2 P_2 + \dots + \alpha_{11} P_{11} \quad (5)$$

in which FF is the fit factor, P_m are the average seal pressure measurements at each of the 11 locations, α_m are the regression coefficients, and A is the regression constant. If the model yielded a squared multiple correlation $R^2 \geq 0.5$ and was significant at $p < 0.05$, it was analyzed as follows; otherwise, no further analysis was performed.

The independent variable set, P_m , was checked for multicollinearity by determining correlations between the independent variables (scatterplot matrix) and by determining the squared multiple correlation (R^2) of each pressure with the remaining pressures in the independent variable set. Squared multiple correlations (R^2) close to 1 indicate a high degree of multicollinearity and a strong possibility that the associated variable is a linear combination of one or more of the other variables (Pedhazur, 1982). A high degree of multicollinearity leads to imprecise estimation of regression coefficients that have large confidence intervals (Pedhazur, 1982). Other consequences of high multicollinearity include negative regression coefficients when the associated variable is expected to have a positive effect in the model (Pedhazur, 1982).

If multicollinearity was high, indicating redundancy in the independent variable set, the following models based on single location seal pressures were developed:

$$FF = D_1 + \gamma_1 P_{S1}, \quad (6)$$

$$FF = D_2 + \gamma_2 P_{S2}, \quad (7)$$

$$FF = D_3 + \gamma_3 P_{S3}, \quad (8)$$

in which FF is the fit factor, P_{Sm} are selected single location average seal pressures, γ_m are the regression coefficients, and D_m are the regression constants. The three pressures having the highest correlation with FF were selected from the set of 11 seal pressures to serve as the P_{Sm} independent variables for the models (6), (7), and (8).

FF and Head Harness Strap Stretch

To meet the second objective, “*determine the relationship between head harness strap stretch and FF* ,” multiple regression analysis was used to formulate the following single function linear relationship

$$FF = B + \delta_1 S_1 + \delta_2 S_2 + \dots + \delta_6 S_6, \quad (9)$$

in which FF is the fit factor, S_n are the strap stretch measurements, δ_n are the regression coefficients, and B is the regression constant. If the two measures of strap stretch were significantly different (see *Head Harness Strap Stretch*, p. 41), two models based on Equation (9) were developed. One was based on the first set of strap stretch measurements and the other was based on the second set of strap stretch measurements. If the models yielded squared multiple correlations $R^2 \geq 0.5$ and were significant at $p < 0.05$, they were analyzed in a manner analogous to that described for the FF and seal pressure model (see *FF and Seal Pressure*, p. 41); otherwise, no further analysis was performed.

Seal Pressure and Head Harness Strap Stretch

To meet the second objective, “determine the relationship between seal pressure and head harness strap stretch,” multiple regression analysis was used to formulate the following single function linear relationships:

$$\begin{aligned} P_1 &= C_1 + \eta_{11} S_1 + \eta_{12} S_2 + \dots + \eta_{16} S_6 \\ P_2 &= C_2 + \eta_{21} S_1 + \eta_{22} S_2 + \dots + \eta_{26} S_6 \\ &\vdots \\ P_{11} &= C_{11} + \eta_{11,1} S_1 + \eta_{11,2} S_2 + \dots + \eta_{11,6} S_6 \end{aligned}, \quad (10)$$

in which P_m are the average seal pressure measurements at each of the 11 locations, S_n are the strap stretch measurements, η_{mn} are the regression coefficients, and C_p are the regression constants. If the two measures of strap stretch were significantly different (see *Head Harness Strap Stretch*, p. 41), two sets of models (10) were developed. One set of models was based on the first set of strap stretch measurements and the other set was based on the second set of strap stretch measurements. If the models yielded squared multiple correlations $R^2 \geq 0.5$ and were significant at $p < 0.05$, they were analyzed in a manner analogous to that described for the FF and seal pressure model (see *FF and Seal Pressure*, p. 41); otherwise, no further analysis was performed.

Validation

Eleven validation trials were conducted following the same protocol (see *Procedure*, p. 40) used for the 22 trials to formulate the models. One trial was performed in strap adjustment Condition 1, and five trials were performed in strap adjustment Conditions 2 and 3 (see Table 3). The measured pressure and strap stretch data from the validation trials were used as independent

variables in the model Equations (5) through (10) to predict the dependent variables, FF or seal pressure. The predicted FF or seal pressure was then compared to the measured FF or seal pressure to determine validity of each model.

FF and Seal Pressure

FF and 11 Seal Pressures

Model (5) was validated if $R^2 \geq 0.5$ and $p < 0.05$. Average validation pressure values at the 11 seal locations were used as the P_1, P_2, \dots, P_{11} independent variable values in model Equation (5) to calculate FF estimates. These FF estimates were then compared to the FFs that were measured during the validation trials to determine the capability of the models to predict both FF numerical values and passing or failing FF ($>$ or $<$ 1667).

Two criteria were used to determine the predictive capability of the models. The sum of absolute differences between estimated and measured FF was used to assess the ability of the model to predict numerical values. Then the number of corresponding passing or failing FFs between estimated and measured FFs was used to assess the ability of the model to predict passing or failing FFs.

First, FF estimates versus FF measures were plotted and compared graphically with a theoretical line representing perfect prediction. Then the sum of absolute differences between estimated and measured FF was calculated:

$$\text{Sum of absolute differences} = \sum |FF_{meas} - FF_{est}|, \quad (11)$$

in which FF_{meas} is the measured FF, and FF_{est} is the estimated FF. The sum of absolute differences gives an indication of the ability of the model to predict FF numerical values, based on the validation trial pressures. The sum of absolute differences also indicates how close the FF estimates (points) are to the theoretical line representing perfect prediction. The smaller the sum is, the better the prediction is.

Second, measured and estimated FF numerical values were converted to categorical values of pass (P) or fail (F). Then, the number of matching Ps and Fs between estimated and measured FFs across the 11 validation trials was reported as an indication of the ability to predict passing or failing FF.

FF and a Single Seal Pressure

Models (6), (7), and (8) were validated if $R^2 \geq 0.4$ and $p < 0.05$. The lower criterion of $R^2 \geq 0.4$ was adopted for models (6), (7), and (8) because each was based on a single independent variable (pressure) and thus could account for a smaller amount of variance in the dependent variable (FF) and still be considered an important result.

Average validation seal pressures for the three locations having the highest correlation with FF were used in turn as the P_{Sm} independent variable values in the model Equations (6), (7), and (8) to calculate FF estimates. These FF estimates were then compared to the FFs that were measured during the validation trials to determine the capability of the models to predict both FF numerical values and passing or failing FF. FF estimates versus FF measures were plotted and compared graphically with a theoretical line representing perfect prediction. Then the sum of absolute differences between estimated and measured FF (Equation (11)) was calculated. Measured and estimated FF numerical values were converted to categorical values of pass (P) or fail (F). The number of matching Ps and Fs between estimated and measured FFs across the 11 validation trials was reported as an indication of the ability to predict passing or failing FF.

FF and Head Harness Strap Stretch

Model (9) was validated if $R^2 \geq 0.5$ and $p < 0.05$. The predictive capability of the model was then determined in a manner analogous to that described for the FF and seal pressure model (see *FF and 11 Seal Pressures*, p. 44).

Seal Pressure and Head Harness Strap Stretch

Models (10) were validated if $R^2 \geq 0.5$ and $p < 0.05$. The predictive capability of the models was then determined in a manner analogous to that described for the FF and seal pressure model (see *FF and 11 Seal Pressures*, p. 44).

Required Seal Pressure Profile and Head Harness Strap Adjustments

Required Seal Pressure Profile

If significant relationships were found between FF and seal pressure ($R^2 \geq 0.5$ for (5), or $R^2 \geq 0.4$ for (6), (7), (8), and $p < 0.05$), then required pressure profiles were developed to meet the third objective, “*determine the required seal pressure profile...of the protective mask for achieving a passing FF.*” A required pressure profile was determined from the model and validation data combined (33 trials). The pressure profile consists of 11 average seal pressure

values at the measurement locations along the seal from left to right cheek straps. Two pressure profiles were compared graphically.

The first profile was formed from the 95th percentile pressure values at each of the 11 locations, based on the distribution of pressure data from all trials that had a passing FF. The profile was determined by selecting the subset of passing FF trials from the original set of 33 trials. For each of the 11 locations, the 95th percentile was calculated from the distribution of pressure values. These 95th percentile values were assembled to form the pressure profile.

For the second profile, pressure values were determined from equations of FF as a function of a single seal pressure, with FF set equal to 7000. Fit factor was selected as 7000 to reflect the upper and more stringent level of protection (6667) required for the M40 protective mask (Brletich, 1992; TRADOC, 1992). First, 11 models were developed through regression analysis of FF, with each of the 11 pressures taken in turn as the independent variable:

$$\begin{aligned}
 FF &= J_1 + \omega_1 P_1 \\
 FF &= J_2 + \omega_2 P_2 \\
 &\vdots \\
 FF &= J_{11} + \omega_{11} P_{11}
 \end{aligned}
 \tag{12}$$

in which FF is the fit factor, P_m are the average seal pressures at each of the 11 locations, ω_m are the regression coefficients, and J_m are the regression constants. The entire set of data (33 trials) was used to formulate these models. Then, each of the 11 models was rearranged to calculate the required pressure from a desired FF of 7000:

$$\begin{aligned}
 P_1 &= \frac{FF - J_1}{\omega_1} = \frac{7000 - J_1}{\omega_1} \\
 P_2 &= \frac{7000 - J_2}{\omega_2} \\
 &\vdots \\
 P_{11} &= \frac{7000 - J_{11}}{\omega_{11}}
 \end{aligned}
 \tag{13}$$

Required Head Harness Strap Adjustments

If significant relationships were found between FF and head harness strap stretch ($R^2 \geq 0.5$ for (9) and $p < 0.05$), then required strap adjustments in terms of strap stretch were developed to meet the third objective, “*determine the required...head harness strap adjustments*”

of the protective mask for achieving a passing *FF*.” Required strap adjustments were determined from the model and validation data combined (33 trials) in a manner analogous to that used for the required pressure profile (Equations (12) and (13)).

If relationships between *FF* and head harness strap stretch were not significant, an alternate approach was followed. Strap adjustments in terms of the length of strap pulled through the buckle were determined from the relationship between *FF* and strap adjustment, based on the model and validation data combined (33 trials). Strap adjustments were determined from equations of *FF* as a function of a single strap adjustment, with *FF* set equal to 7000. Fit factor was selected as 7000 to reflect the upper and more stringent level of protection (6667) required for the M40 protective mask (Brletich, 1992; TRADOC, 1992).

First, two models were developed through regression analysis of *FF*, with two strap adjustments taken in turn as the independent variable:

$$\begin{aligned} FF &= K_1 + \psi_1 SA_L \\ FF &= K_2 + \psi_2 SA_U \end{aligned} \quad (14)$$

in which *FF* is the fit factor, *SA_L* is the lower strap adjustment (LCS, RCS, LTS, RTS), *SA_U* is the upper strap adjustment (LFS, RFS), ψ_m are the regression coefficients, and K_m are the regression constants. Only two models are required because strap adjustments are the same for left and right sides, as well as for temple and cheek straps. Then, each of the models was rearranged to calculate the required strap adjustment from a desired *FF* of 7000:

$$\begin{aligned} SA_L &= \frac{FF - K_1}{\psi_1} = \frac{7000 - K_1}{\psi_1} \\ SA_U &= \frac{7000 - K_2}{\psi_2} \end{aligned} \quad (15)$$

RESULTS

Data Analysis

Seal Pressure

Similar pressure profiles were observed in all three conditions (see Figure 18). At all measurement locations, the pressure increased as tightness increased (from Condition 1 to 3). The greatest increases were observed in the forehead and temple regions (LTS, RTS, LT, RT, LFS, RFS, F), which had an average increase of 21 g/cm² from Condition 1 to 3. In each profile, pressures in the temple and forehead regions (LTS, RTS, LT, RT, LFS, RFS, F) were higher than in the cheek

region (LCS, RCS, LC, RC). In the forehead and temple regions, pressures between the straps (LT, RT, F) were higher than adjacent pressures beneath the straps (LTS, RTS, LFS, RFS) for Conditions 1 and 2. This effect was diminished in Condition 3, in which the profile was smoother. Seal pressure profiles for passing and failing FF trials (see Figure 19) exhibited similar trends. The largest differences in pressure between passing and failing trials were observed in the temple and forehead regions (LTS, RTS, LT, RT, LFS, RFS, F), which had an average difference of 23 g/cm².

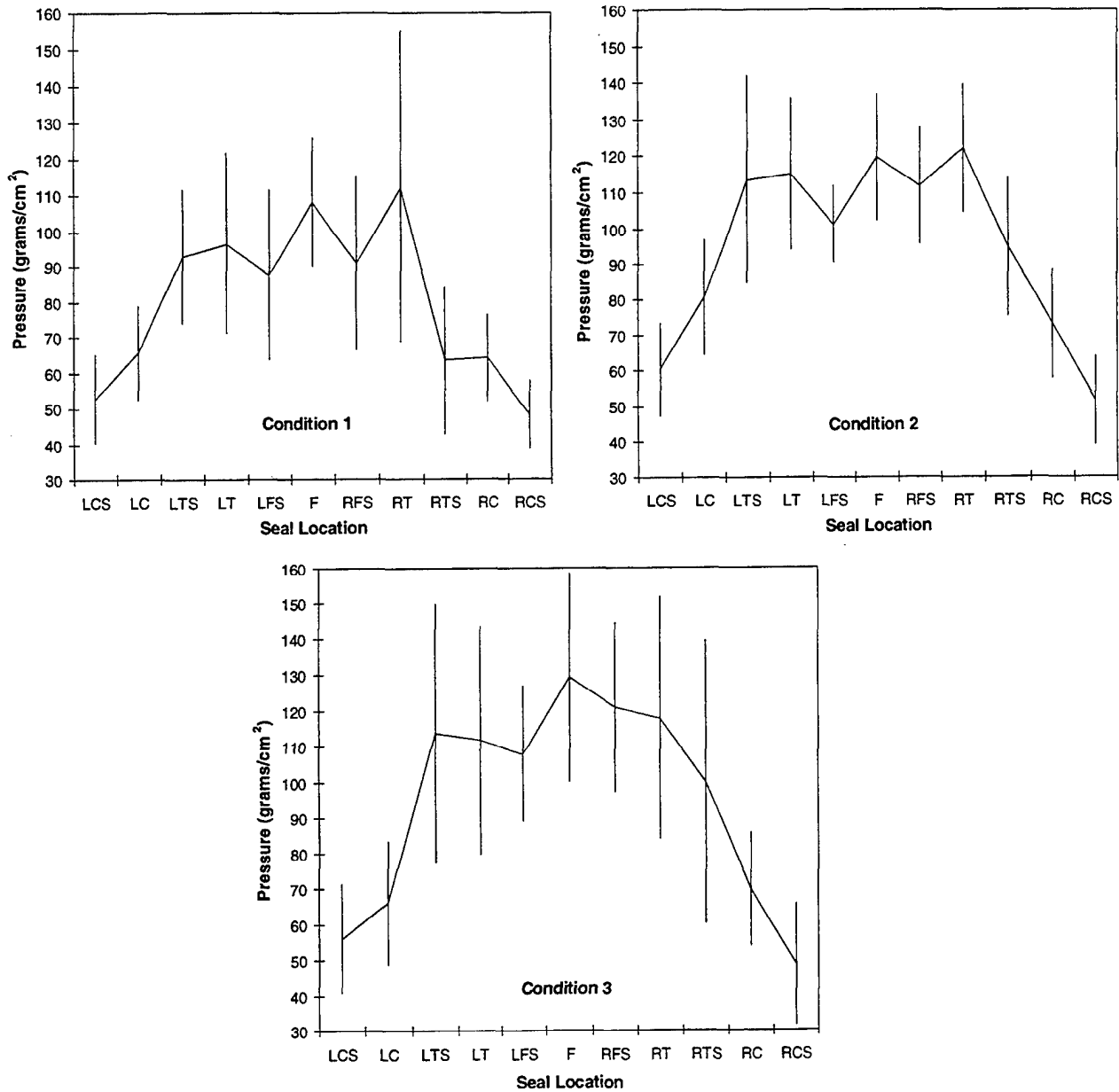


Figure 18. Seal pressure profiles based on average seal pressures for adjustment Conditions 1, 2, and 3. (Vertical bars indicate standard deviation. Seal locations are as defined in Figure 16.)

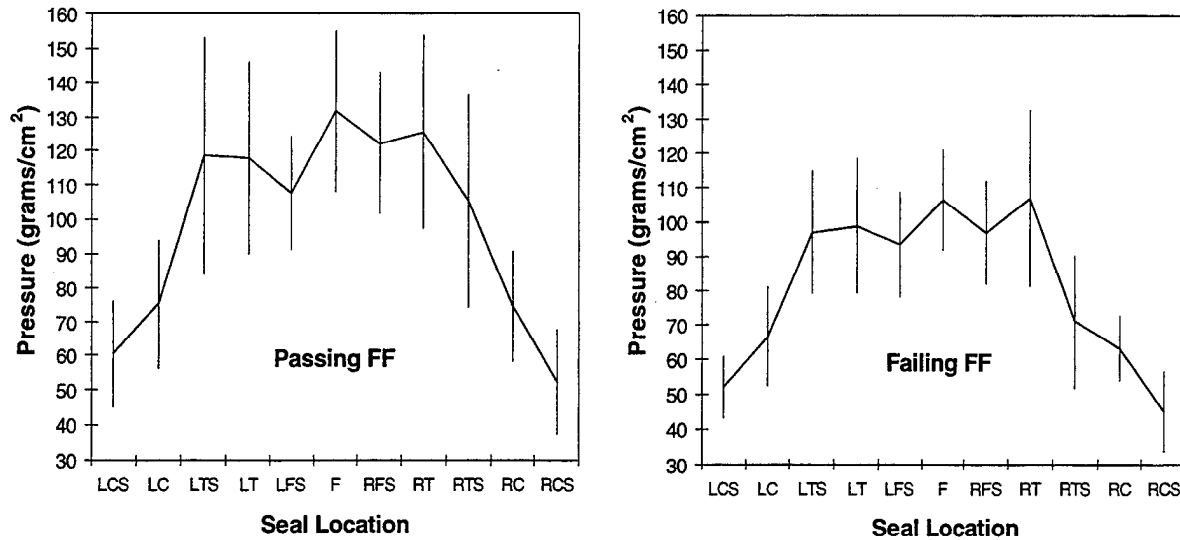


Figure 19. Average seal pressure profiles and standard deviations for passing (n=14) and failing (n=8) FF trials. (FF >1667 is passing.)

Color changes in pressure distributions from Condition 1 to 3 indicated that pressure increased as tightness increased (see Figures 20 through 22). Consistent with the trends observed in Figures 18 and 19, pressure increases, indicated by color changes (see Figures 21 and 22), were greater in the forehead and temple regions (LTS, RTS, LT, RT, LFS, RFS, F) than in the cheek region (LCS, RCS, LC, RC). Areas without color are below the threshold of force that the sensor can measure.

A distinct line of contact crossing the sensor was observed in all but the cheek strap distributions (LCS, RCS) of Conditions 1 and 3 (see Figures 21 and 22). This line of contact was formed by the inturned sealing surface (see Figure 5) exerting pressure on the face of the headform. The inturned sealing surface is curved and raised with respect to the outer sealing surface and was designed to press against the face. In the cheek strap region, the inturned sealing surface flattens, and thus there was no distinct line of pressure in the cheek strap distributions. In the forehead region, the entire sealing surface is nearly flat, but there is a distinct ridge between the inner and outer sealing surfaces. Accordingly, more contact and a line of higher pressure, displayed as bright blue with some yellows and greens, was observed in the forehead distributions. Therefore, the features of the inturned sealing surface correspond with the lines of pressure observed in the output.

Fit Factor

As tightness increased, a larger number of trials achieved passing FFs (see Figure 23): none of three trials in Condition 1, five of nine trials in Condition 2, and nine of ten trials in Condition 3.

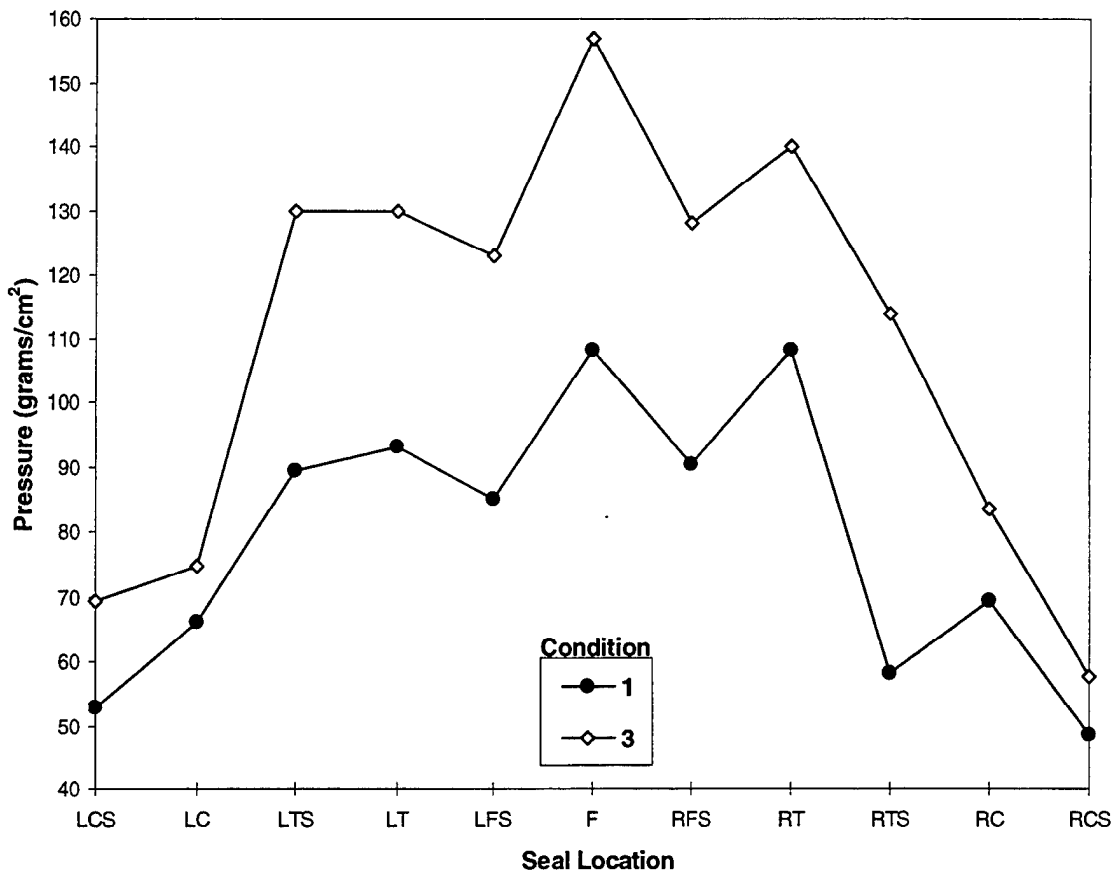


Figure 20. Comparison of pressure profiles corresponding to average seal pressures from the distributions of Figures 21 and 22.

An unexplained outlier in Condition 2 (FF = 66,000) was eliminated from further analysis because it did not appear to be a representative data point and would seriously distort the results (Pedhazur, 1982).

Ambient particle concentrations varied daily but were unrelated to measured FF (see Figure 24). The Pearson correlation coefficient between ambient particle concentration and FF was 0.0015.

Head Harness Strap Stretch

The second measurement of stretch was significantly larger than the first for the left cheek strap in Conditions 2 ($p = 0.039$) and 3 ($p = 0.001$). The second measurement of stretch was significantly larger than the first for the left ($p = 0.046$) and right temple straps ($p = 0.002$) in Condition 3. Therefore, the strap stretch for the middle and lower straps increased as a result of lifting the sealing surface in the tighter conditions. Because of the differences, separate relationships between each of the first and second set of stretch measures and FF or seal pressure were developed (see *FF and Head Harness Strap Stretch*, p. 42, and *Seal Pressure and Head Harness Strap Stretch*, p. 43).

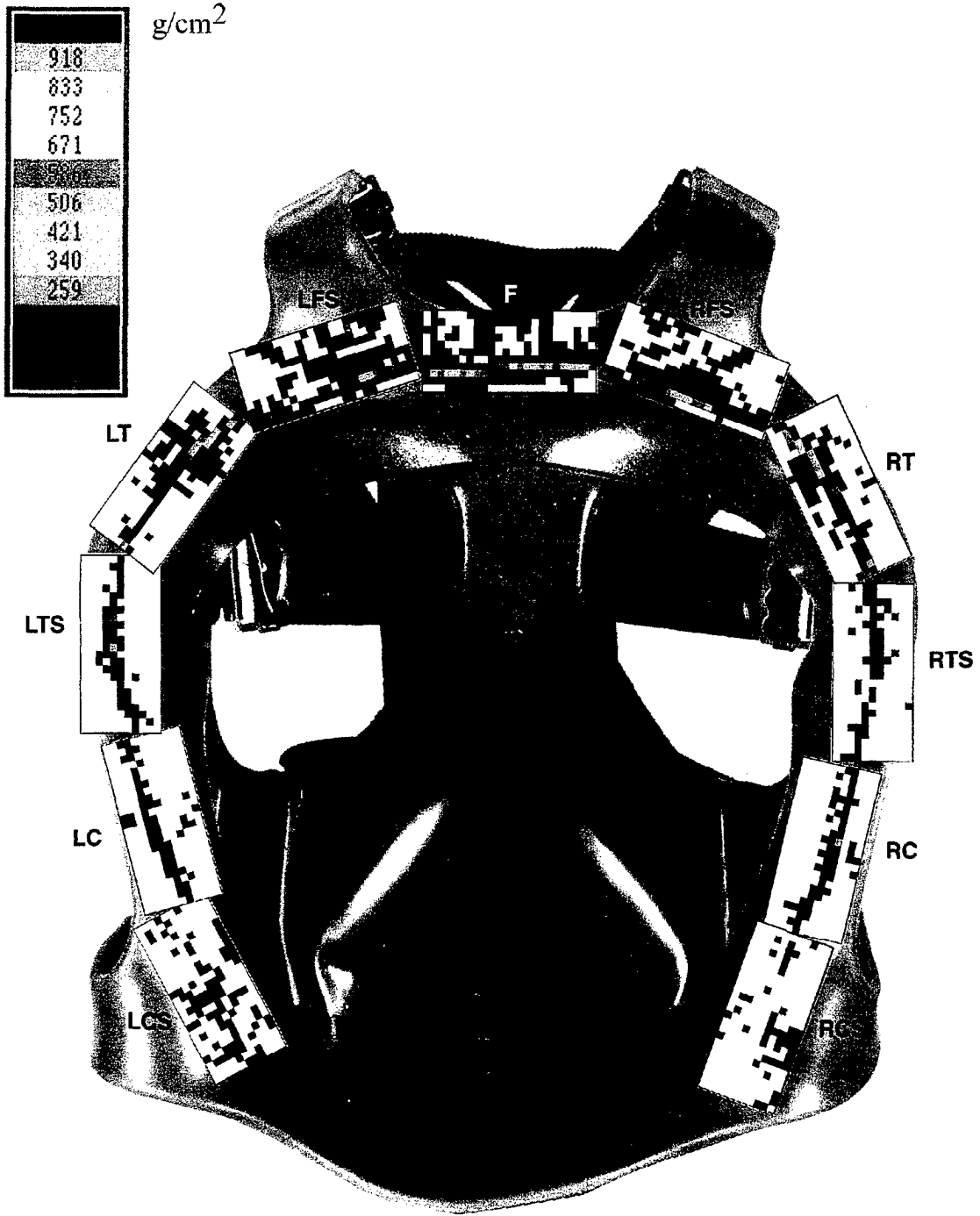


Figure 21. Seal pressure distribution for Condition 1.

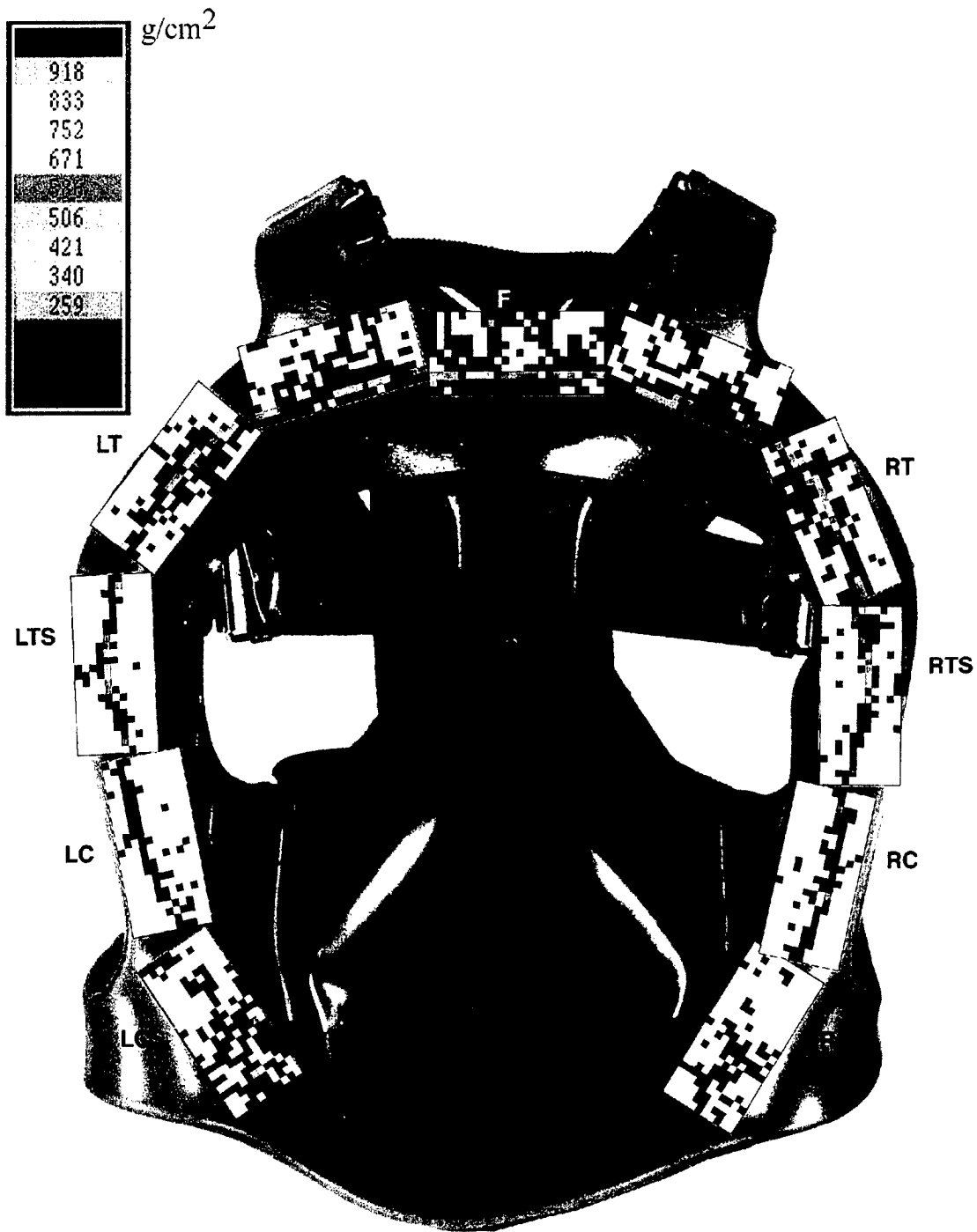


Figure 22. Seal pressure distribution for Condition 3.

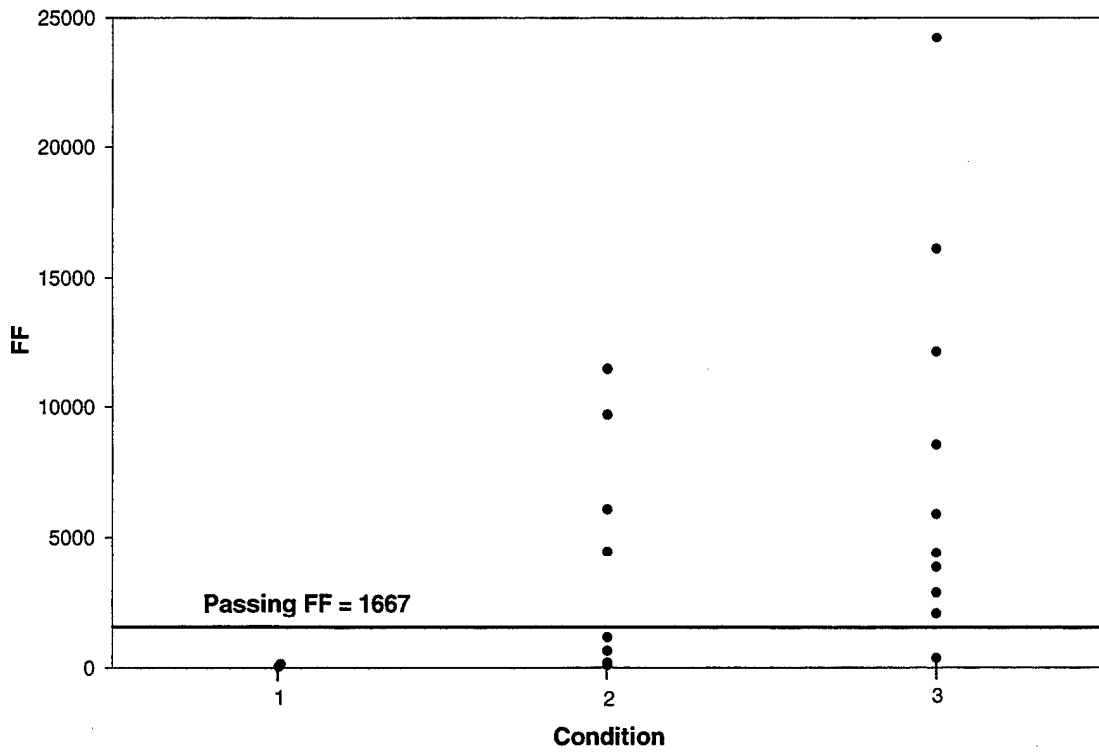


Figure 23. FF measured for 21 trials in Conditions 1, 2, and 3.

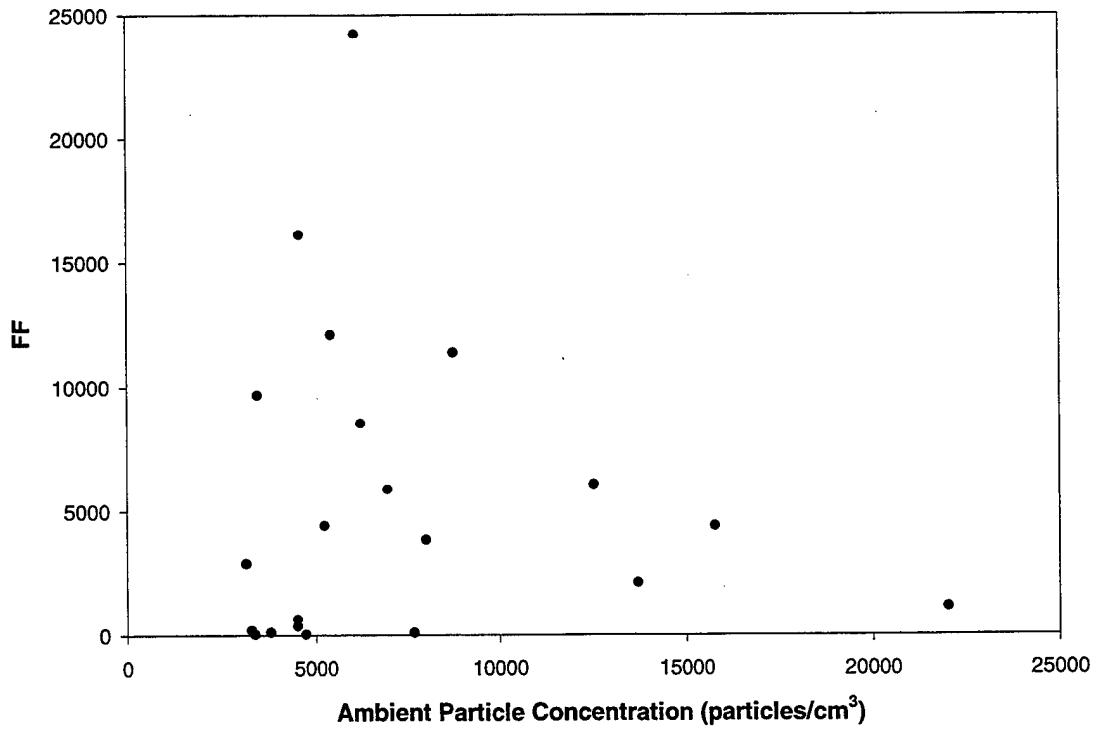


Figure 24. FF versus ambient particle concentration; Pearson correlation coefficient = 0.0015.

Strap stretch increased consistently in all straps as the mask was tightened on the headform (see Figure 25). Strap stretch is nearly symmetric for left and right straps.

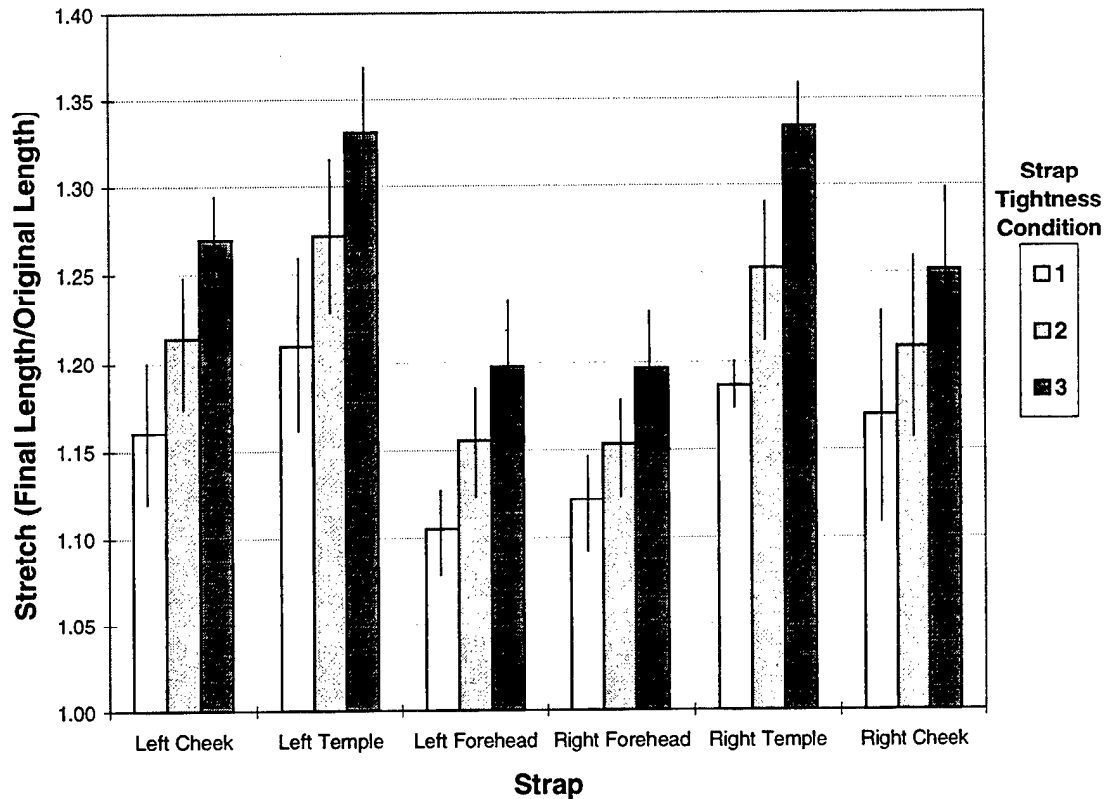


Figure 25. Average strap stretch and standard deviation for Conditions 1 (n=3), 2 (n=9), and 3 (n=10). (Values represent first strap stretch measurement.)

Model Development

FF and Seal Pressure

Multiple regression analysis revealed a strong and significant relationship between FF and seal pressure (see Table 5). The squared multiple correlation (R^2) of 0.87 indicated that 87% of the variation observed in FF was explained by the pressure variables in the model. However, there was evidence of a high degree of multicollinearity in the independent variable set. The independent variables (pressures) were highly intercorrelated (see Figure 26), and the squared multiple correlations of each pressure with the remaining pressures (see Table 6) were close to 1. In addition, eight of the regression coefficients were negative (see Table 5), whereas all pressure

variables had a positive correlation with FF (see Figure 26). Thus, the set of pressures appeared to be redundant, and the resulting model would provide poor estimates of FF.

Table 5
Model of FF as a Function of 11 Seal Pressures

Model (5): $FF = A + \alpha_1 P_1 + \alpha_2 P_2 + \dots + \alpha_{11} P_{11}$ $R^2 = 0.87$ $p = 0.008$

Variable	Coefficient		Standardized coefficient
	Constant, A	9186.7	0.0
LCS (P_1)	α_1	-103.4	-0.228
LC (P_2)	α_2	-292.3	-0.763
LTS (P_3)	α_3	-151.7	-0.756
LT (P_4)	α_4	315.5	1.349
LFS (P_5)	α_5	-166.7	-0.464
F (P_6)	α_6	-32.0	-0.121
RFS (P_7)	α_7	-102.2	-0.365
RT (P_8)	α_8	-38.8	-0.174
RTS (P_9)	α_9	353.1	1.805
RC (P_{10})	α_{10}	138.3	0.315
RCS (P_{11})	α_{11}	-12.6	-0.028

R^2 is the squared multiple correlation; p is the probability that the observed result happened by chance.

Table 6
Squared Multiple Correlation of Each Pressure With All Remaining Pressures

Pressure	R^2	Pressure	R^2
LCS	0.98	RCS	0.95
LC	0.95	RC	0.98
LTS	0.97	RTS	0.93
LT	0.98	RT	0.88
LFS	0.94	RFS	0.92
F	0.96		

Values of R^2 close to 1 indicate linear dependence between variables.

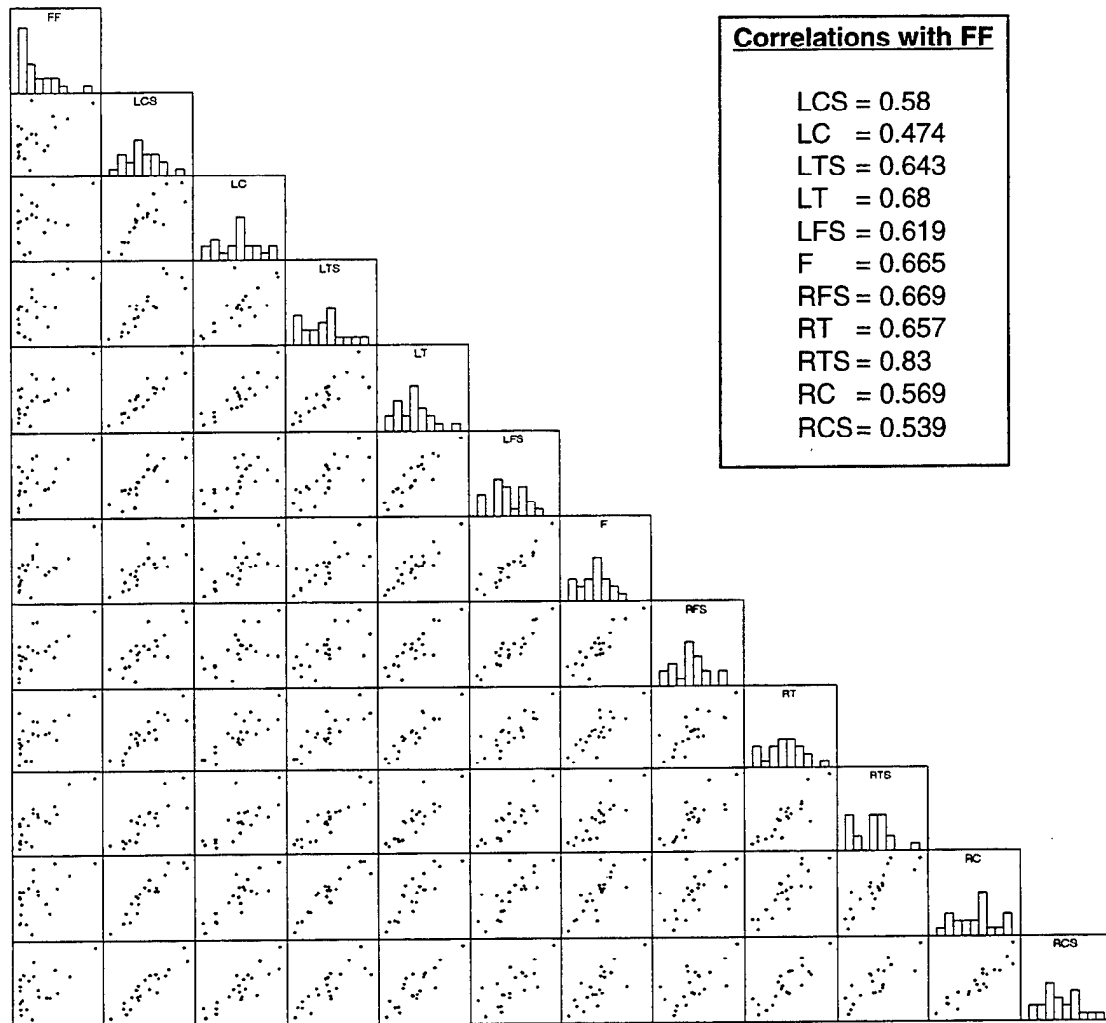


Figure 26. Scatterplot matrix of FF and seal pressure values. (Pearson correlations between seal pressures range from 0.567 [LC and RFS] to 0.93 [LCS and RC].)

Because of redundancy in the set of pressure variables, the three models, (6), (7), and (8), based on single location seal pressures were developed (see Table 7). The RTS, LT, and RFS pressures were most highly correlated with FF (see Figure 26) and were therefore selected as the P_{Sm} pressures. Although the squared multiple correlations (R^2) for models (6), (7), and (8) were not as high as the R^2 for the previous model (5), each model, based on a single pressure, yielded a significant result and explained at least half of the 87% variance in FF that was explained by the model based on all 11 pressures.

Table 7

Models of FF as a Function of a Single Location Seal Pressure

Model: $FF = D_m + \gamma_m P_{Sm}$

Model	Pressure	Constant	Coefficient	R ²	p
(6)	RTS	-9591.8	162.4	0.69	0.000
(7)	LT	-12207.1	158.9	0.46	0.001
(8)	RFS	-15761.9	187.0	0.45	0.001

D_m are the regression constants, γ_m are the regression coefficients, and P_{Sm} are the seal pressures.

FF and Head Harness Strap Stretch

Multiple regression analysis revealed weak, nonsignificant relationships (9) between FF and the first strap stretch measurements ($R^2 = 0.2$, $p = 0.772$) as well as FF and the second strap stretch measurements ($R^2 = 0.25$, $p = 0.604$). Thus, no further analysis was performed.

Seal Pressure and Head Harness Strap Stretch

Multiple regression analysis revealed weak, nonsignificant relationships (10) between each of the 11 pressures and the first strap stretch measurements ($R^2 = 0.09$ to 0.27 , $p = 0.56$ to 0.959), as well as between the pressures and the second strap stretch measurements ($R^2 = 0.03$ to 0.4 , $p = 0.205$ to 0.998). Thus, no further analysis was performed.

Validation

Fit factor (see Figure 27) and seal pressure data (see Figure 28) were collected for 11 validation trials. As tightness increased, a larger number of trials achieved passing FFs: none of one trial in Condition 1, four of five trials in Condition 2, and four of five trials in Condition 3. Seal pressure profiles exhibited trends similar to those observed in the previous data set used for modeling (see Figure 18).

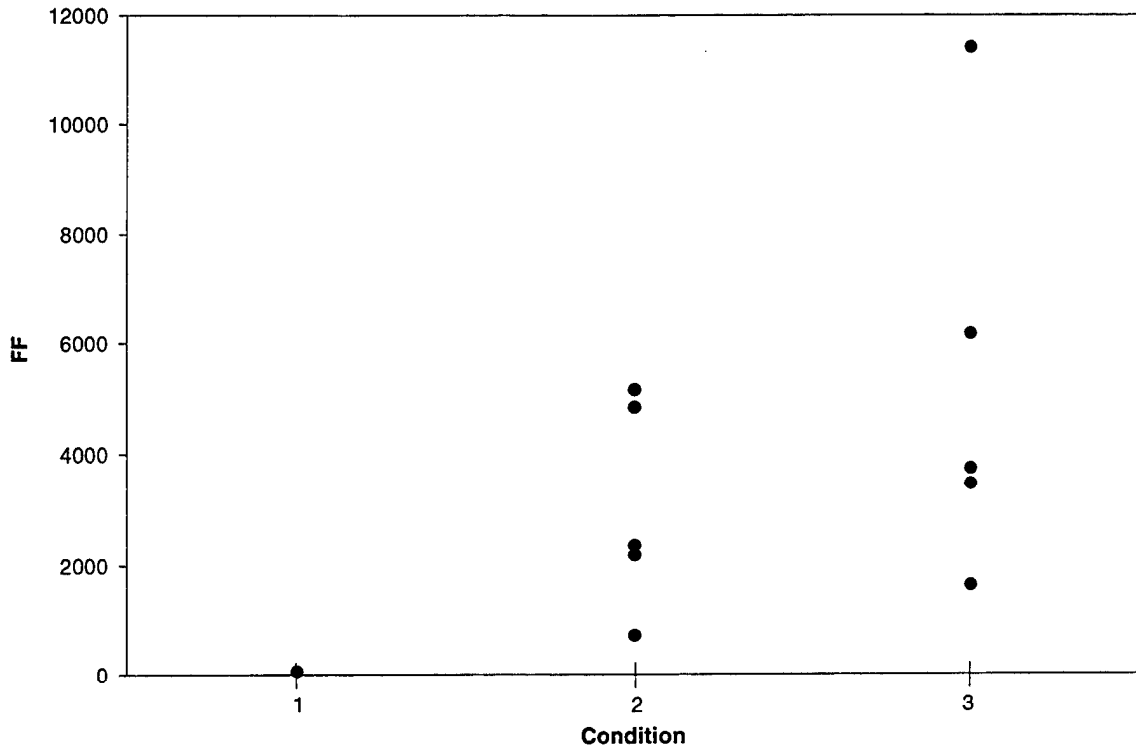


Figure 27. FF measured for 11 validation trials in Conditions 1, 2, and 3.

FF and Seal Pressure

FF and 11 Seal Pressures

FF estimates were compared to the FFs that were measured during the validation trials (see Figure 29). Nine of the estimates were larger and two were smaller than the FF measurements. As expected, high levels of multicollinearity contributed to the poor estimation of FF. Six of the estimates of FF were extremely large and one of the estimates was negative. Accordingly, the sum of absolute differences for validation of model Equation (5) was quite large (91,152).

Although the model poorly predicted the measured FF numerical values, it may adequately predict whether the mask will pass or fail a FF test. Measured and estimated FF numerical values were converted to categorical values of pass or fail (see Table 8). The model of FF as a function of all 11 seal pressures correctly predicted 7 of 11 FFs. It did not correctly predict any of the failing trials, most likely because the majority of FF estimates were high.

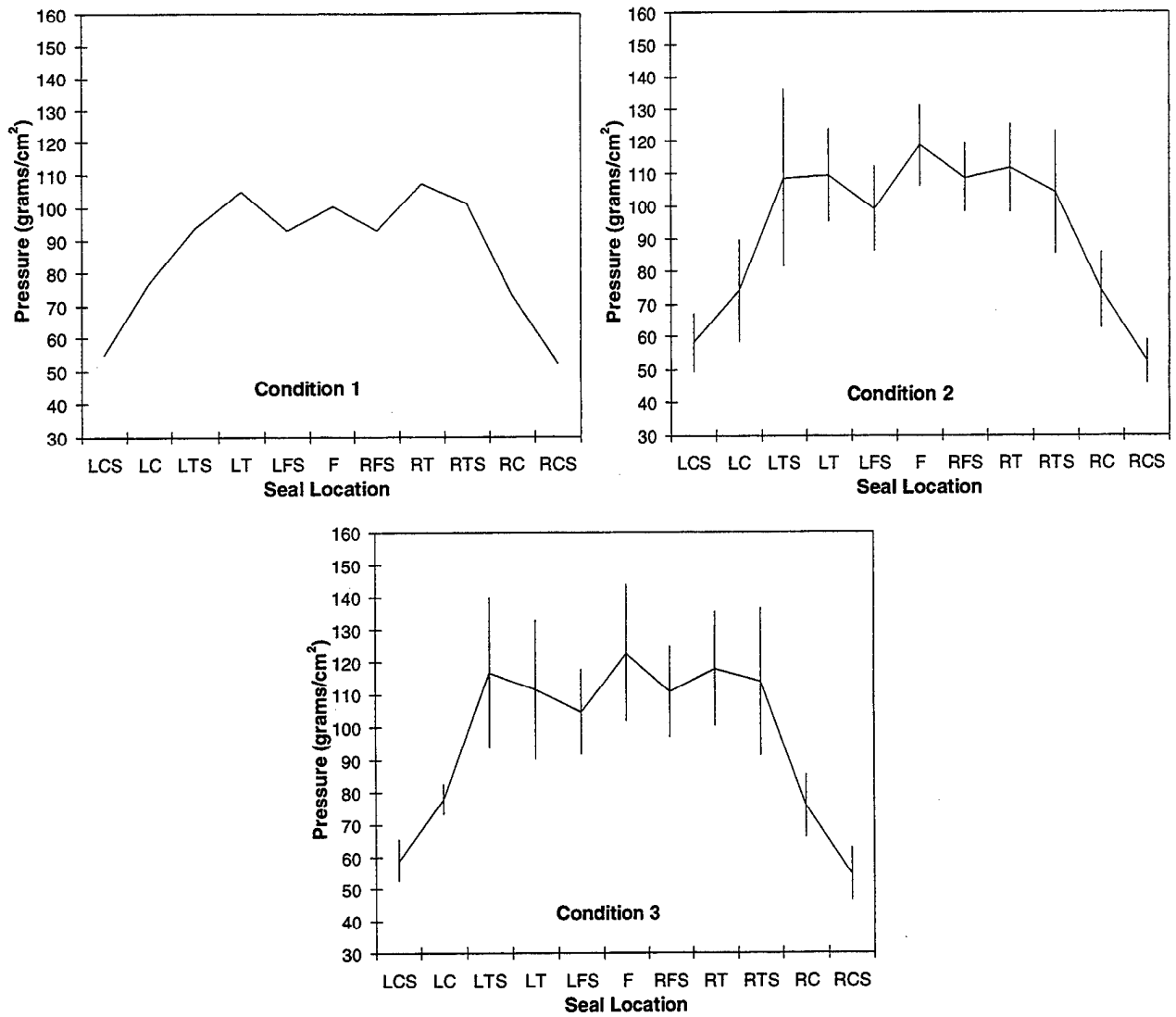


Figure 28. Average seal pressure profiles and standard deviations for validation trials (Condition 1 [n = 1], Condition 2 [n = 5], and Condition 3 [n = 5]).

Table 8

Prediction of Passing or Failing by Model of FF as a Function of 11 Seal Pressures

Validation trial	1	2	3	4	5	6	7	8	9	10	11
Measured FF	P	P	F	P	P	P	P	P	P	F	F
Estimated FF	P	P	P	P	F	P	P	P	P	P	P
Correct prediction	✓	✓		✓		✓	✓	✓	✓		

Model Equation (5). P is passing; F is failing, based on a criterion of 1667.

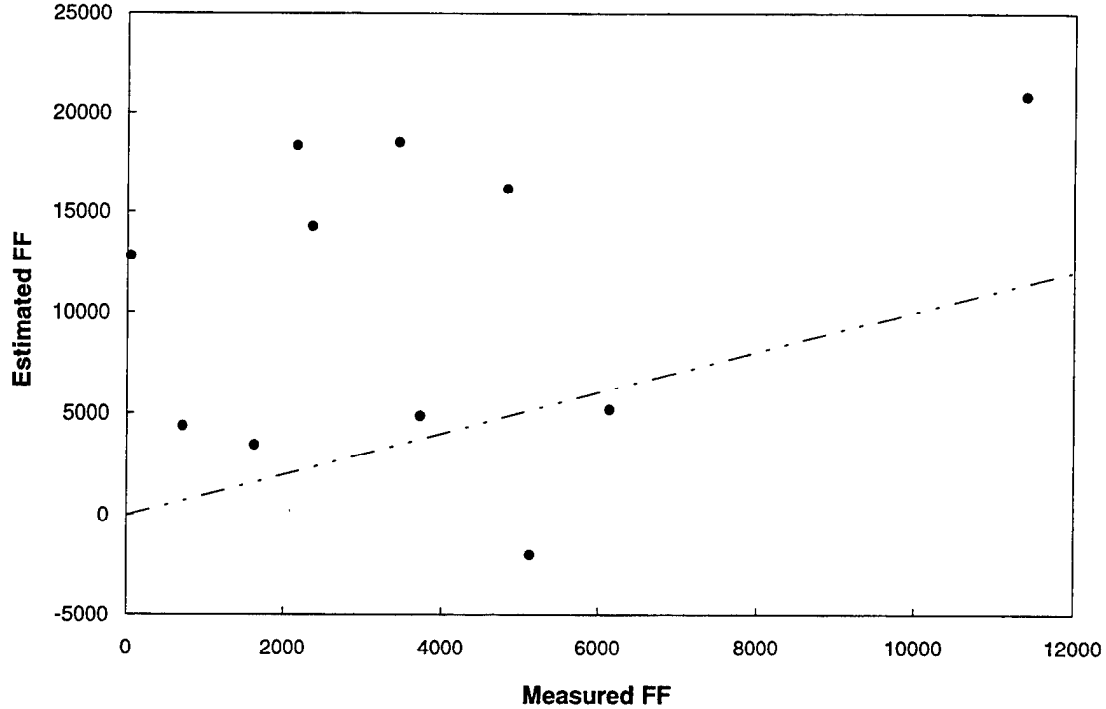


Figure 29. Estimated versus measured FF for model equation (5). (The dashed line represents perfect prediction.)

FF and a Single Seal Pressure

FF estimates were compared to the FFs that were measured during the validation trials (see Figure 30). The models based on a single pressure provided much better prediction of FF values than did the model based on all pressures (see Figure 29). For the FF and RTS model (see A of Figure 30), all 11 estimates were larger than the FF measurements. For the FF and LT model (see B of Figure 30), eight estimates were larger and three were smaller than the FF measurements. For the FF and RFS model (see C of Figure 30), seven estimates were larger and four were smaller than the FF measurements. In addition, the points were clustered closer to the dashed line in plots B and C than in plot A. This is consistent with the calculated sum of absolute differences for the three models: 46,460 (A); 22,980 (B); and 20,678 (C). Recalling that the sum of absolute differences for the model of FF and 11 seal pressures (5) was 91,152 demonstrates again that models of FF based on a single pressure provided better estimates of FF values.

In order to assess the pass-fail predictive capability of the three models, measured and estimated FF numerical values were converted to categorical values of pass and fail (see Tables 9 through 11). The model of FF as a function of RTS pressure (6) correctly predicted

8 of 11 FFs. The model did not correctly predict any of the failing trials because all FF estimates were high. The models of FF as a function of LT (7) or RFS (8) pressure each correctly predicted 9 of 11 FFs. Each model correctly predicted one failing trial.

FF and Head Harness Strap Stretch

Model (9) did not meet the requirements for R^2 and p and thus was not validated.

Seal Pressure and Head Harness Strap Stretch

Models (10) did not meet the requirements for R^2 and p and thus were not validated.

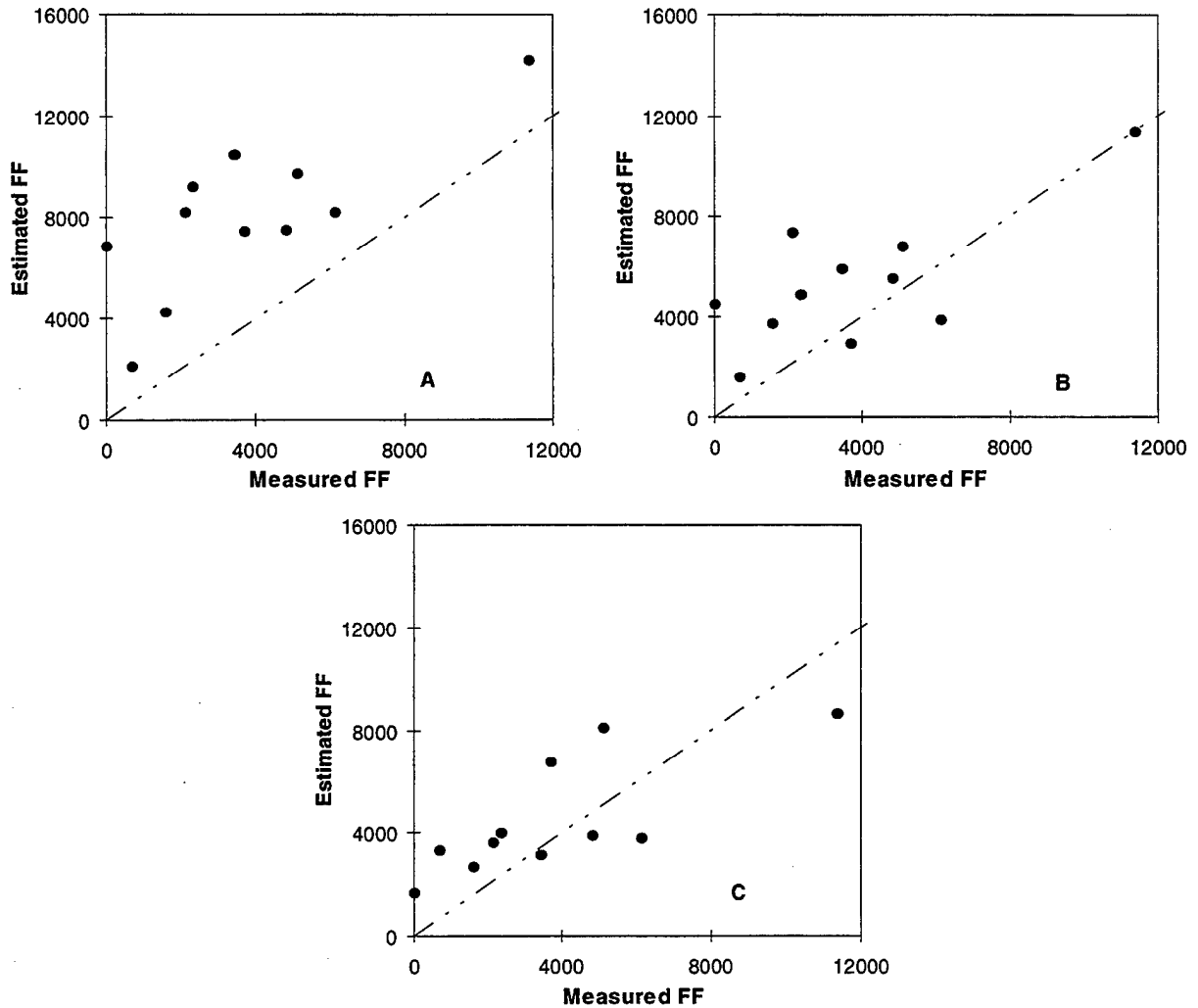


Figure 30. Estimated versus measured FF for model equations (6), (7), and (8). (Plot A is FF as a function of RTS. Plot B is FF as a function of LT. Plot C is FF as a function of RFS. The dashed line represents perfect prediction.)

Table 9

Prediction of Passing or Failing by Model of FF as a Function of RTS Pressure

Validation trial	1	2	3	4	5	6	7	8	9	10	11
Measured FF	P	P	F	P	P	P	P	P	P	F	F
Estimated FF	P	P	P	P	P	P	P	P	P	P	P
Correct prediction	✓	✓		✓	✓	✓	✓	✓	✓		

Model Equation (6). P is passing; F is failing based on a criterion of 1667.

Table 10

Prediction of Passing or Failing by Model of FF as a Function of LT Pressure

Validation trial	1	2	3	4	5	6	7	8	9	10	11
Measured FF	P	P	F	P	P	P	P	P	P	F	F
Estimated FF	P	P	P	P	P	P	P	P	P	F	P
Correct prediction	✓	✓		✓	✓	✓	✓	✓	✓	✓	

Model Equation (7). P is passing; F is failing based on a criterion of 1667.

Table 11

Prediction of Passing or Failing by Model of FF as a Function of RFS Pressure

Validation trial	1	2	3	4	5	6	7	8	9	10	11
Measured FF	P	P	F	P	P	P	P	P	P	F	F
Estimated FF	P	P	P	P	P	P	P	P	P	P	F
Correct prediction	✓	✓		✓	✓	✓	✓	✓	✓		✓

Model Equation (8). P is passing; F is failing based on a criterion of 1667.

Required Seal Pressure Profile and Head Harness Strap Adjustments

Required Seal Pressure Profile

The 95th percentile passing pressure profile is shown in comparison with the mean profile for the passing and failing trials (see Figure 31). These 11 pressure values form one required pressure profile for achieving a passing FF on the headform. The other required pressure profile, based on modeling of FF and single seal pressures at each of the 11 locations, is shown in comparison to the profiles of Figure 31 (see Figure 32).

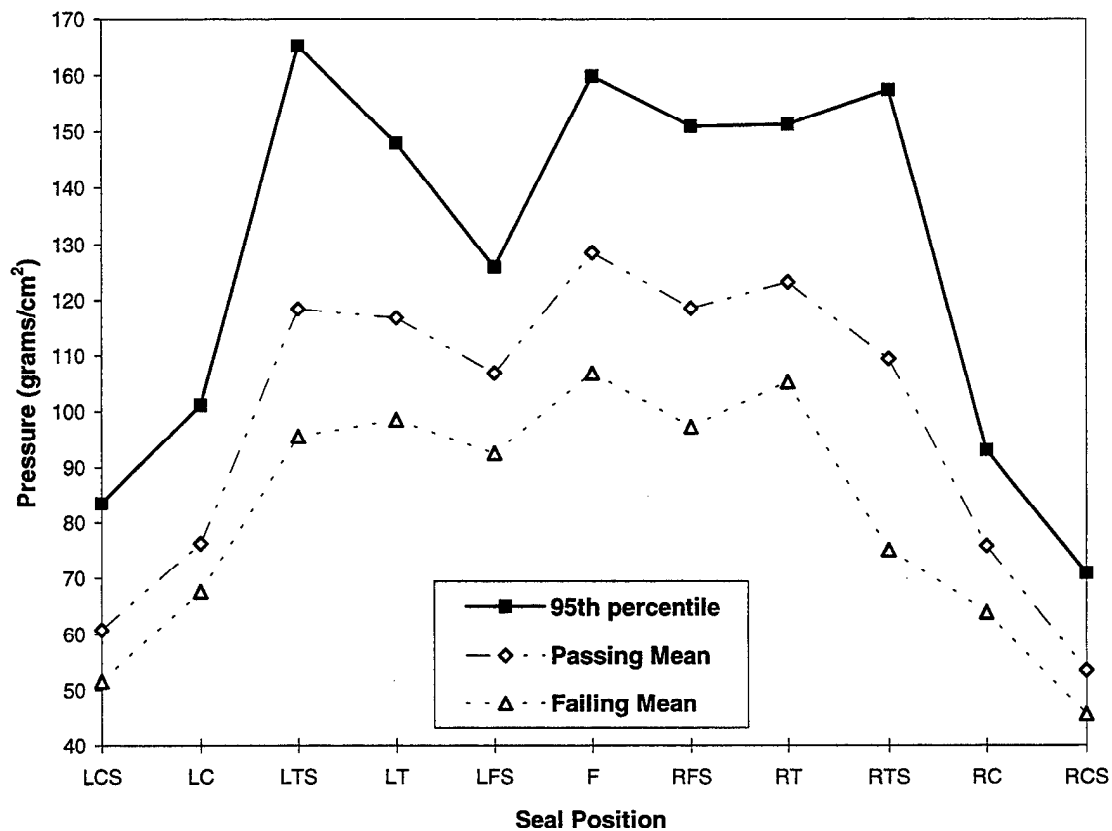


Figure 31. Pressure profiles for the 95th percentile of all passing trials ($n = 22$), the mean of all passing trials, and the mean of all failing trials ($n = 11$).

The second required pressure profile based on modeling (Equations (12) and (13)) exhibits a pattern similar to that of the mean of the passing trials and the mean of the failing trials (see Figure 32), whereas the profile based on the 95th percentile of the passing trials exhibits some irregularities because of values at the extremes in the pressure data set. In addition, the 95th percentile profile pressures are large and may not represent realistic and comfortable fittings of the mask seal. The pressure profile based on modeling is therefore more realistic and a better requirement for achieving a passing FF with the M40 protective mask on a headform.

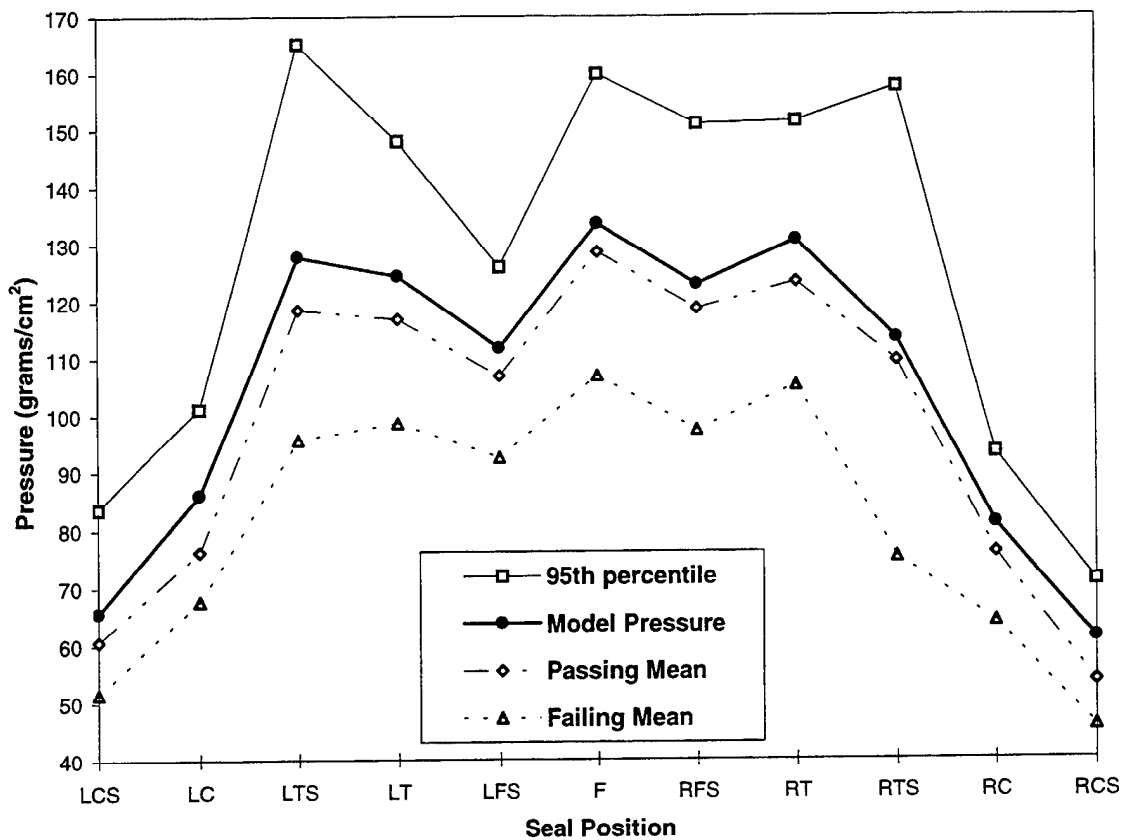


Figure 32. Pressure profile for achieving a FF of 7000 based on 11 models of FF as a function of a single pressure (n = 32). (Other profiles are as in Figure 31.)

Required Head Harness Strap Adjustments

Because the relationship between FF and head harness strap stretch was not significant (see *FF and Head Harness Strap Stretch*, p. 61), the alternate approach was followed (Equations (14) and (15)). The two models of FF and strap adjustment (14) yielded weak but significant relationships ($R^2 = 0.199$, $p = 0.01$ for each). Based on these models, the required strap adjustment (15) calculated for the forehead straps was 61 mm and for the lower straps (LCS, RCS, LTS, RTS), it was 101 mm. These required strap adjustments are exactly those of Condition 3. This result was expected because 13 of 15 trials in Condition 3 had passing FFs.

DISCUSSION

Seal Pressure

One of the most important results of this study was the development of a method to investigate and measure the seal pressure distribution between a protective mask sealing surface and face. Seal integrity and mask design characteristics that influence seal performance can easily

be evaluated by examining seal pressure distributions and profiles (Objective 1). The average seal pressures in the forehead, forehead strap, and temple regions are higher than in the temple strap, cheek, and cheek strap regions, which is consistent with the geometry of the mask and face interaction. In the forehead region, the mask sealing surface exerts largely a force normal to the surface of the headform. This is because the forehead straps, and thus the forces acting on them, are almost perpendicular to the sealing surface in this region. Therefore, more contact and higher pressures were observed. In the cheek region, the forces acting on the temple straps and cheek straps are almost parallel to the mask sealing surface; thus, one would expect largely a shear force in the temple strap and cheek regions. The pressure sensor measures only normal force. In the cheek and temple strap regions, there are distinct lines of pressure but no large areas of contact as in the forehead region. This distinct line of pressure is formed by the curved flap of the inturned sealing surface. Thus, the inturned sealing surface functions by producing a normal force in these regions.

Trends similar to those found in the present study can be observed in the pressure profile data collected by Goldberg et al. (1966), who measured pressure changes along the mask sealing surface of the M17 mask on a human face (see Figure 33). The data represent a pressure change observed in a pre-inflated uncalibrated air bladder; thus, absolute pressure values from the Goldberg et al. study cannot be compared to those from the present study. However, the overall trends from the two evaluations are consistent: larger pressures were observed in the forehead and temple regions than in the cheek region.

In the present evaluation, modeling and validation data were collected by performing test trials on a single sample of the M40 protective mask fitted on a headform. Thus, the results of modeling and validation demonstrate the efficacy of measuring seal pressure to evaluate protective mask seal performance. In the future, generalized models will be developed to account for differences between masks, as well as differences in facial anthropometry.

In the present evaluation, the relationship between FF and seal pressure was determined (Objective 2). The differences in FF were largely explained by the changes in pressure ($R^2 = 0.87$). This means that protective masks can and should be evaluated by examining seal pressure characteristics. FFs were predicted reasonably well from a single seal pressure measurement. This is because the seal pressure response to tightening was consistent at most locations and all straps were uniformly tightened. Therefore, it may only be necessary to examine pressure in a few locations when evaluating mask designs. This will greatly simplify the designer's task and allow for quick and early assessments of seal performance.

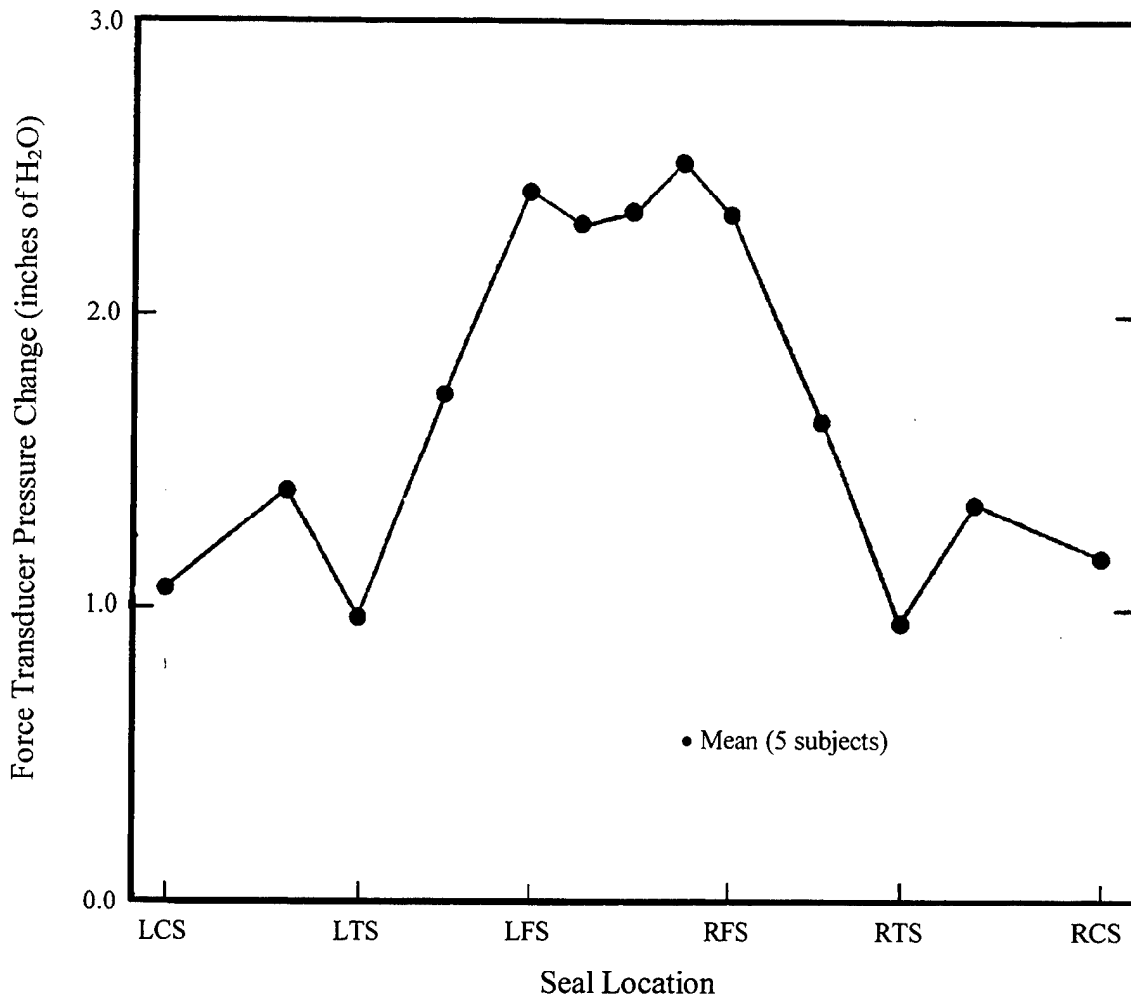


Figure 33. Seal pressure along the sealing surface of an M17 protective mask (adapted from Goldberg et al., 1966).

The models, however, did not predict failing FFs as well as they did passing FFs. This is probably because fewer trials were conducted in Condition 1 ($n = 3$) than in either Condition 2 ($n = 9$) or Condition 3 ($n = 10$), and because 14 trials had passing FFs. A previous effort, which included an even number of trials in each of the three conditions, produced a model that poorly predicted all FFs (see Appendix A). The large and abrupt changes in FF across tightening conditions make the variable difficult to predict using a single model. However, when a model based on a single seal pressure (models (6), (7), and (8)) predicted failure, the measured FF was failing. Thus, if estimates from models (6), (7), and (8) are examined together and failing estimates on any single model are interpreted as overriding corresponding passing estimates from other models in the group, prediction of failing can be improved. For example, validation trials 10 and 11 (FFs of 706 and 50, respectively) were estimated as having a failing FF by at least one of the

models (see Tables 9 through 11). Validation Trial 3 (FF = 1630) was estimated as passing by all three models. Therefore, when considering estimates based on all models, prediction is accurate for 10 of 11 trials. In addition, Trial 3 is clearly a borderline case with an FF very close to the passing criterion of 1667. In the worst case, these models of FF based on seal pressure may predict a passing FF for masks that are close to meeting the requirement, but they will probably estimate failing FFs for masks that do not provide adequate seals. Masks that are close to meeting the FF requirement will be much easier to improve in later phases of development (after FF testing) than masks that are unable to form protective seals. Thus, the models can serve as a tool to be used in early mask design to evaluate seal pressure and predict the corresponding protection.

A more conservative approach for evaluating masks, based on the required pressure profile for achieving a passing FF, may be necessary until more robust models can be developed. The required pressure profile developed during this evaluation can be used as a set of criteria to be met in the design of sealing surfaces for developmental masks (Objective 3). Such a comparison would enable designers to identify regions where the pressure was low and to concentrate redesign efforts on increasing pressure in those regions.

Pressure Measurement System

To alleviate problems experienced in past investigations, seal pressure distributions were measured using a thin film flexible matrix-type pressure sensor that did not alter the geometric configuration of the mask sealing surface on the face when the sensor was in place. The Tekscan pressure measurement system was the only one on the market with a sensor that had these characteristics. The Tekscan system is an adequate tool for evaluating seal pressure characteristics as long as it is used within the scope of its limitations. Specifically, care must be taken to perform calibration and make pressure measurements under the same conditions and within a short period of time (2 to 3 hours). There were both advantages and disadvantages with using this system.

One of the distinct advantages of using the Tekscan pressure measurement system was the ability to actually observe pressure distributions created between the mask and face. This evaluation represents the first effort to collect pressure distribution data in the mask development field. All previous efforts resulted in point measures of seal pressure. The ability to see the pressure distributions created by a feature such as the inturned sealing surface demonstrates how valuable this tool will be to the mask designer. The inturned sealing surface was originally designed to enhance the seal, but until now, there was no direct evidence that it did so. Using this pressure measurement tool, one can compare different designs of mask sealing surfaces and the resulting pressure distributions.

Another distinct advantage is the ability to observe the pressure distribution in real time. Seal pressure dynamics such as those attributed to movement (talking, coughing, sneezing, or running) or adjustment of head harness straps can be observed as they happen or recorded for future examination. Thus, the pressure measurement tool can be used interactively in the mask design process.

In addition, pressure measurements can be used to evaluate the performance of masks very early in the design process, long before FF measurements can be made. This will increase the probability of success of mask prototypes that reach FF testing because design problems attributable to mask sealing can be resolved earlier by evaluating seal pressure distributions. Mask prototypes that fail FF testing because of sealing problems are costly and time consuming to fix because along with redesign of the prototype, expensive tooling (mask molds) must be redesigned, produced, and purchased. Tooling is a major expenditure in mask development programs. Thus, the seal pressure evaluation tool is truly a labor- and cost-saving technology.

The primary disadvantage with using this system was the tedious and frequent calibration of sensors that was required. More durable and stable sensors, as well as a standardized calibration procedure, are needed to enhance the use of the system. In addition, improved sensor performance at low pressures is required so that sealed sensors can be used on human faces. There is also a need for variations in shapes and sizes of sensors to better accommodate measurements in the chin as well as to allow measurement of both intumed and outer sealing surfaces simultaneously. The current sensor is not wide enough to cover the entire sealing surface.

Fit Factor

FF data were highly variable across and within conditions, although an increase in the number of passing trials was observed as strap tightness increased. The large variability, especially as FFs increased, was expected because the fit tester functions as a particle counter at low concentrations. With ambient concentrations above 5,000 particles/cm³ and mask concentrations on the order of 5 particles/cm³, a difference of a single particle inside the mask has a large effect on the resulting FF. The observed variations were not related to fluctuations in the ambient particle concentration; therefore, the PMFVS functioned well in an uncontrolled environment. The PMFVS is an adequate tool for evaluating masks on headforms.

Head Harness Strap Stretch and Adjustment

Head harness strap stretch was not strongly related to either FF or seal pressure and thus is not an adequate measure of strap tightness (Objective 2). There are several probable reasons why strap stretch was not a strong predictor. First and probably most important is that the individual head harnesses exhibited differences in stress-strain behavior (see Appendix B). Second, friction between the rubber headform and elastic harness material probably caused stretch to vary along the length of the strap that was contacting the headform. Thus, the measurement of stretch at one point probably was not representative of stretch at other points along the strap.

A relationship between FF and head harness strap adjustment was developed (Objective 3). From this relationship, it was determined that strap adjustment to Condition 3 would yield a passing FF on the headform used in the present evaluation. This was true for 13 of 15 trials. However, a required head harness strap adjustment in terms of the length of strap pulled through the buckle would be of limited or no use for any other mask, head harness, or headform. If any of the geometries were changed, the relationship between strap adjustment and FF would probably diminish. In future evaluations, it will be necessary to develop a means to measure tension in the mask tab ends that connect to the harness. Then the experiment can be controlled by tightening harness straps until a specified level of tension is developed in the straps, thereby eliminating harness variability from the evaluation. Accordingly, protocols for tightening the mask to achieve a passing FF could be developed and based on strap tension.

Future Research Efforts

The promising results presented in this report demonstrate that seal pressure measurement is a technique worth evaluating further. After steps for improving seal pressure measurements are made (see *Pressure Measurement System*, p. 28), the present evaluation needs to be replicated using the M40 and other masks on human faces. In conjunction with this, a means of measuring tension in the mask tabs is required. Then one can begin to more closely evaluate the actual seal pressure distributions. Areas without contact or with very low pressure may actually be the paths of seal leakage. An investigation of techniques for evaluating pressure distributions, as opposed to pressure averages, should be performed to see if there are alternate methods for evaluating the data. Related to these issues are two variables, seal contact area and number of seal gaps, which were briefly investigated in a previous effort (see Appendix A). These variables should be re-evaluated after improved seal pressure measurement techniques are devised.

Related to both seal contact and pressure is mask seal comfort. In the past, overall mask comfort has been evaluated subjectively and included aspects of comfort such as breathing resistance, thermal load, facial sweating, seal and head harness pressure, nose cup and chin cup pressure, and feelings of anxiety (Harrah & Caretti, 1997; Piccione & Moyer, 1997; Harrah, 1994; Harrah, 1996; Lu, 1995; Mitchell et al., 1986; Barnes et al., 1983; Decker & Piccione, 1982; Burgess, Hinds, & Snook, 1970; Snook, Hinds, & Burgess, 1966). This new capability to evaluate pressure distributions can be used to determine the relationship between seal pressure and seal comfort, and then required seal pressure profiles to meet both protection and seal comfort criteria can be established.

In this evaluation, lifting the mask sealing surface to place and remove sensors changed the strap stretch measurement. Lifting the mask may have also changed the seal pressure, but that change could not be quantified using the current evaluation procedure. Ideally, a headform with embedded sensors or a head and face sock with embedded sensors for measuring on humans is needed so that the mask sealing surface never has to be lifted to make measurements. In addition, a headform with embedded sensors could be used to validate the required seal pressure profile determined in the present effort (see *Required Seal Pressure Profile*, p. 63). The Human Research and Engineering Directorate of the U.S. Army Research Laboratory has proposed to develop a headform with embedded sensors for future evaluations.

Finally, alternate modeling approaches must be investigated. Computer technology has advanced rapidly, and the development of mechanical models of protective masks and faces on computers is now feasible. Techniques such as computer-aided design and finite element analysis can be used to design masks and evaluate seal performance using computers before prototypes are developed. Laser scanning and other imaging technologies such as magnetic resonance imaging can be used to collect facial data such as size, shape, and tissue thickness for representation in computer models. Materials testing of the mask and facial tissues must be performed in order to simulate the behavior of the seal between mask and face in the computer model. The seal pressure measurement techniques developed as a part of the current research can be used to validate computer models of seal pressure between masks and faces.

SUMMARY

This report presented a method for measuring seal pressure, which can be used to evaluate performance of protective masks. Several important technical advances were made during this evaluation:

- The use of a thin film flexible pressure sensor, placed between the sealing surface of the mask and face without altering the normal geometric relationship, solved many of the problems that previous investigators experienced.

- Seal pressure was strongly related to FF, the current method of evaluating mask seal performance. The significance of this result is that seal pressure measurements can be made on early crude prototypes, whereas FF testing cannot. Seal pressure distributions are a direct representation of the mechanical means (i.e., contact and pressure) by which protection is provided.

- Based on the relationship between seal pressure and FF, levels of pressure necessary to produce a good seal with a passing FF were determined. These pressure values can be used by the mask designer as criteria for developing new masks.

- Pressure measurement technology enhances development of the mask by allowing designers to concentrate redesign efforts on improving the seal pressure distribution.

In addition to a fit factor criterion, the Army and industry could develop seal pressure criteria, based upon these results. This study adds to the current knowledge of protective mask performance and provides new information to mask designers as well as information that can feed into the development of computerized models for prediction of mask protection, fit, and comfort. The Army is already embarking on efforts to develop such models (Kasbekar & Heater, 1996; Piccione & Moyer, 1997; Shams, Zhao, Fullerton, Rangarajan, & Cohen, 1997), but much of the empirical data such as seal pressure and head harness strap tightness have not been collected, and the relationship of seal comfort to pressure and FF has not yet been defined. Consequently, this research represented a critical first step in the development of technology to achieve these long-term research goals.

REFERENCES

- Adler, J. (1986). The protection and treatment of civilian populations against chemical warfare. Proceedings of the Second International Symposium on Protection Against Chemical Warfare Agents, Tel-Aviv, Israel, 389-393.
- Barnes, J.A., Bruno, R.S., Hanlon, W.E., Harrah, D.M., Hickey, C.A., Merkey, R.P., Randall, R.B., & Shoemaker, C.M. (1983). XM30 Engineering Design Test-Government (human factors) (TM 5-83). Aberdeen Proving Ground, MD: U.S. Army Human Engineering Laboratory.
- Baumann, W., Krabbe, B., & Farkas, R. (1992). The application of in-shoe pressure distribution measurements in the controlled therapy of diabetes patients. VDI Berichte, 940, 413-419.
- Brletich, R. (1992). Corn oil leakage test for the DT II of the XM40/US-10 protective masks (CBIAC-SS-309). Aberdeen Proving Ground, MD: U.S. Army Chemical Research, Development and Engineering Center.
- Brletich, N.R., Tracy, M.F., & Dashiell, T.R. (1992). Worldwide NBC mask handbook. Edgewood, MD: Chemical Warfare/Chemical and Biological Defense Information and Analysis Center.
- Burgess, W.A., Hinds, W.C., & Snook, S.H. (1970). Performance and acceptance of respirator facial seals. Ergonomics, 13 (4), 455-464.
- Chandler, K. D. (1985). A lesson learned too well? U.S. philosophy regarding CBW (chemical or biological weapons) warfare World War I to the present (CB-004843). Maxwell AFB, AL: Air Command and Staff College.
- Chronology II: Latest events, gulf tension escalates again. (1998, November 17). ABC News (contributors: Reuters and the Associated Press). Available: http://archive.abcnews.com/sections/world/DailyNews/iraq_timeline2.html
- Cohen, K.S. (1995). Research protocol: Development of a technique for measuring protective mask seal pressure and an analysis of the relationship of protective mask seal pressure and strap strain with protection factor. Aberdeen Proving Ground, MD: U.S. Army Research Laboratory.
- Craig, F.N., & Cain, S.M. (1955). Inhalation while donning the gas mask (MLRR384). Edgewood, MD: Army Chemical Center, Chemical Corps Medical Labs.
- Decker, R.C., & Piccione, D. (1982). Development Test II: Prototype Qualification Test – Government (POT-G) of XM33 protective mask, hood, and combat spectacles (CB-005887). Ft. Rucker, AL: U.S. Army Aviation Development Test Activity.

- Ellis, M.W., & Record, J. (1992). Theater ballistic missile defense and U.S. contingency operations. Parameters, XXII, 1, 12.
- Fritch, W.M. (1996). Preplanned Product Improvement (P3I) testing for the M40 series mask (ERDEC-TR-274). Aberdeen Proving Ground, MD: Edgewood Research, Development & Engineering Center.
- Gardner, P.D., Laye, R.G., & Hughes, F.P. (1988). Evaluation of a new automated condensation nucleus counter-based system for quantitative fit testing of respirators (CRDEC-TR-88046). Aberdeen Proving Ground, MD: Chemical Research, Development & Engineering Center.
- Goldberg, M.N. (1970). Individual respiratory protection against chemical and biological agents. Final report, Sections I & II. Unpublished manuscript. Edgewood Arsenal, MD: Defense Development and Engineering Laboratories, Physical Protection Laboratory.
- Goldberg, M.N., Jones, R.E., Wang, Y., & Crooks, T.P. (1967). Individual respiratory protection against chemical and biological agents. Eleventh quarterly progress report (AD No. 823653L). Edgewood Arsenal, MD: Defense Development and Engineering Laboratories, Physical Protection Laboratory.
- Goldberg, M.N., Raeke, J.W., Jones, R.E., & Santschi, W.R. (1966). Individual respiratory protection against chemical and biological agents. Sixth quarterly progress report (CB-042964). Edgewood Arsenal, MD: Defense Development and Engineering Laboratories, Physical Protection Laboratory.
- Gordon, C.C., Churchill, T., Clauser, C E., Bradtmiller, B., McConville, J.T., Tebbetts, I., & Walker, R.A. (1989). 1988 Anthropometric survey of U.S. Army personnel: Methods and summary statistics (Natick/TR-89/044). Natick, MA: U.S. Army Natick Research, Development, and Engineering Center.
- Harber, P., SooHoo, K., & Lew, M. (1988). Effects of industrial respirators on respiratory timing and psychophysiological load sensitivity. Journal of Occupational Medicine, 30, 3, 256-262.
- Harrah, D.M. (1994). Evaluation of prototype nose cups for the M40 protective mask (ARL-MR-150). Aberdeen Proving Ground, MD: U.S. Army Research Laboratory.
- Harrah, D M. (1996). Soldier ratings of the effect of breathing resistance on task performance (ARL-TN-69). Aberdeen Proving Ground, MD: U.S. Army Research Laboratory.
- Harrah, D.M., & Caretti, D.M. (1997). Protective mask modeling study: Performance with the M16A2 rifle (ARL-MR-372). Aberdeen Proving Ground, MD: U.S. Army Research Laboratory.
- Headquarters, Department of the Army (1988). Operator's manual for chemical-biological mask: Field, M40 (TM 3-4240-300-10-1). Washington, DC: Author.

- Headquarters, Department of the Army (1993). Operator's manual for Protective Mask Fit Validation System: M41 (draft). Washington, DC: Author.
- Headquarters, U.S. Army Training and Doctrine Command (April 1992). Joint Service Operational Requirement for the protective mask (M40). Revised edition. Fort Monroe, VA: Author.
- Jelier, P., & Hughes, S. (1994). Mechanical and anthropometric characteristics of soft tissue layers in the head and maxillofacial region, using combined mechanical and ultrasound techniques. Unpublished manuscript, University of Surrey, Guildford, UK.
- Johnson, A.T. (1976). The energetics of mask wear. American Industrial Hygiene Association Journal, 76, 479-488.
- Kasbekar, A.D., & Heater, K.J. (1996). A dynamic model for design optimization of protective masks. Unpublished manuscript. Aberdeen Proving Ground, MD: U.S. Army Research Laboratory.
- Komi, P.V. (1990). Relevance of *in vivo* force measurements to human biomechanics. Journal of Biomechanics, 23, Suppl. 1, 23-34.
- Laye, R. (1987). Evaluation of a miniaturized condensation nucleus counter for measurement of respirator fit factor. Journal of the International Society for Respiratory Protection, 5, 3, 1-8.
- Lu, C. (1995). Biomechanical comfort modeling of the M40 military gas mask. Unpublished manuscript. Aberdeen Proving Ground, MD: U.S. Army Research Laboratory.
- McPoil, T.G., Cornwall, M.W., & Yamada, W. (1995). A comparison of two in-shoe plantar pressure measurement systems. The Lower Extremity, 2, No. 2, 95-103.
- Meunier, P.P., & Constantine, L.R. (1990). Evaluation of a miniature condensation nucleus counter for quantitative fit testing (TN 90-23). Ottawa, Canada: Defence Research Establishment.
- Mitchell, G., Knox, F., Edwards, R., Schrimsher, R., Siering, G., Stone, L., & Taylor, P. (1986). Microclimate cooling and the aircrew chemical defense ensemble (USAARL-86-12). Ft. Rucker, AL: U.S. Army Aeromedical Research Laboratory.
- 1.5 Million in armed forces to be inoculated for anthrax (1997, December 16). Baltimore Sun, p. 4A.
- Parragh, Szabo, Geck, & Madaras (1967). Chemical and biological warfare agents (*A vegyi es biologiai fegyver*) (edited translation, FTD-HT-66-481). Wright-Patterson AFB, OH: Foreign Technology Division.

- Pedhazur, E.J. (1982). Multiple regression in behavioral research (2nd ed.). Orlando, FL: Harcourt Brace Jovanovich.
- Piccione, D., & Moyer, E.T. (1997) Modeling the interface between a respirator and the human face (CB-101437). Alexandria, VA: DCS Corporation.
- Powell, M., & Lengel, A. (1997, April 25). Chemical alert traps workers in buildings: Discovery of leaking package at B'nai B'rith turns into eight-hour ordeal in D.C. The Washington Post, p. A01.
- Quesada, P.M., Rash, G.S., & Jarboe, N. (1996). Assessment of Pedar and Fscan revisited. 5th Emed Scientific Meeting, Penn State University.
- Raines, E.F. (1983). The U.S. 5th division and gas warfare, 1918 (CB-007808). Washington, DC: Army Center of Military History.
- Reimers Engineering, Inc. (1984). Operating and maintenance manual for breathing simulator, Type I, Serial No. 007. Falls Church, VA: Author.
- Salmons, S. (1969). The 8th International Conference on Medical and Biological Engineering—meeting report. Biomedical Engineering, 4, 467-474.
- Shams, T., Zhao, Y., Fullerton, J., Rangarajan, N., & Cohen, K. (1997). Interaction between computer models of face and mask. Proceedings of the Thirty-Fifth Annual Symposium of the Safe Association, 196-208.
- Silverman, L., Lee, G., Plotkin, T., Sawyers, L.A., & Yancey, A.R. (1951). Air flow measurements on human subjects with and without respiratory resistance at several work rates. Archives of Industrial Hygiene & Occupational Medicine, 3, 461-478.
- Snook, S.H., Hinds, W.C., & Burgess, W.A. (1966). Respirator comfort: Subjective response to force applied to the face. American Industrial Hygiene Association Journal, 93-97.
- Still Skeptical that Diplomacy Will Resolve Crisis: Albright Secures Cooperation (1998, February 3). ABC News (contributors: Reuters and the Associated Press). Available: <http://www.abcnews.com/sections/world/DailyNews/iraq0202.html>
- Tekscan, Inc. (1992). Corporate capabilities. Boston, MA: Author.
- Tekscan, Inc. (1993). Sensor presentation software user's manual. Boston, MA: Author.
- Terrorists Hit Tokyo Subway System: Nerve Gas Spews Through Train Cars; at Least 6 Killed, Thousands Stricken. (1995, March 20). Baltimore Evening Sun, p. 1A.
- Thornton, J. (1993). Iraqi chemical preparedness in the Gulf War, Part 1. The ASA Newsletter 37, 1, 14-15.

- TSI, Inc. (1991). PORTACOUNT Plus Model 8020, operation and service manual. St. Paul, MN: Author.
- Tzihor, A. (1992). Chemical warfare, past and future (CB-019633). Carlisle Barracks, PA: U.S. Army War College.
- U.S. is Ready to Act Alone Against Iraq, Albright Says (1998, January 29). Baltimore Sun, p. 14A.
- U.S. Total Army Personnel Command, Deputy Chief of Staff for Plans, Force Integration and Analysis (1993). FOOTPRINT on decision support system (users' guide). Alexandria, VA: Author.
- Weiss, R.A. (1997). Enhanced expedient hood (escape hood): User requirements and market survey (ARL-TR-1414). Aberdeen Proving Ground, MD: U.S. Army Research Laboratory.
- Windrem, R. (1998). U.N. suspicious of Iraqi experiments. NBC News.

APPENDIX A
PILOT EVALUATION

PILOT EVALUATION

Overview

A pilot evaluation was completed in order to narrow the focus and refine the techniques to be used in the primary evaluation described in this report (pages 5 through 71). Independent variables, test procedures, and strap adjustment conditions were modified as a result of this evaluation.

Procedure

The procedure used for the pilot evaluation has been described previously (Cohen, 1995). Only the major procedural differences between the primary and pilot evaluations are reviewed in this appendix. In the pilot evaluation, the mask was left on the headform over a series of day-long trials in which the head harness straps were gradually tightened. Six series of data were collected. Seven strap adjustment conditions (see Table A-1) were used in each of the first three series, and five strap adjustment conditions were used for the last three series (Conditions 2-6 from Table A-1). Thus, each series consisted of either five or seven trials and an entire series was conducted using a single head harness. The mask was removed from the headform between series but not between trials. The reason for the different number of conditions between the first three and second three series is discussed in *Results and Conclusions: Series 1-3* (p. 83).

In the pilot evaluation, two additional independent variables, seal contact area and number of seal gaps, were evaluated. Seal contact area was calculated by the pressure measurement software as each of the 11 seal pressure measurements was made. The number of seal gaps was determined from each pressure distribution. Each pressure distribution normally exhibited a distinct line of pressure that crossed the sensor and was assumed to be the seal created between face and mask. In some distributions, the line of pressure was not continuous; small gaps or breaks were observed in the line. The number of seal gaps was interpreted as the number of sensing elements on the sensor that spanned a gap or break in the line of seal pressure. A gap or break is indicated by regions where no pressure was measured and appears to be a hole in the pressure distribution, which could allow air to pass from outside to inside the mask.

Table A-1

Head Harness Strap Adjustment Conditions

Condition	Number of trials	Length of strap pulled through buckle (mm)		
		Forehead	Temple	Cheek
1	3	41.0	81.0	81.0
2	6	46.0	86.0	86.0
3	6	51.0	91.0	91.0
4	6	56.0	96.0	96.0
5	6	61.0	101.0	101.0
6	6	66.0	106.0	106.0
7	3	71.0	111.0	111.0

There are two of each (right and left) forehead, temple, and cheek straps. Right and left straps were adjusted identically.

Analysis

Series 1-3

After data for the first three series were collected, preliminary modeling efforts using regression were performed in order to determine which independent variables were most strongly related to FF and to determine if there was a strong relationship between pressure and strap stretch. The following independent variables were evaluated: seal pressure (P_n), seal contact area (E_n), number of seal gaps (G_n), and strap stretch (S_n). The following relationships were modeled:

$$FF = A + \alpha_1 P_1 + \alpha_2 P_2 + \dots + \alpha_{11} P_{11} \quad (\text{A-1})$$

$$FF = D + \beta_1 E_1 + \beta_2 E_2 + \dots + \beta_{11} E_{11} \quad (\text{A-2})$$

$$FF = H + \varepsilon_1 G_1 + \varepsilon_2 G_2 + \dots + \varepsilon_{11} G_{11} \quad (\text{A-3})$$

$$FF = B + \delta_1 S_1 + \delta_2 S_2 + \dots + \delta_6 S_6 \quad (\text{A-4})$$

$$\begin{aligned} P_1 &= C_1 + \eta_{11} S_1 + \eta_{12} S_2 + \dots + \eta_{16} S_6 \\ P_2 &= C_2 + \eta_{21} S_1 + \eta_{22} S_2 + \dots + \eta_{26} S_6 \\ P_3 &= C_3 + \eta_{31} S_1 + \eta_{32} S_2 + \dots + \eta_{36} S_6 \\ &\vdots \\ P_{11} &= C_{11} + \eta_{11,1} S_1 + \eta_{11,2} S_2 + \dots + \eta_{11,6} S_6 \end{aligned} \quad (\text{A-5})$$

in which P_{1-11} are LCS, LC, LTS, LT, LFS, F, RFS, RT, RTS, RC, RCS pressures, respectively; E_{1-11} are LCS, LC, LTS, LT, LFS, F, RFS, RT, RTS, RC, RCS contact areas, respectively; G_{1-11} are LCS, LC, LTS, LT, LFS, F, RFS, RT, RTS, RC, RCS seal gaps, respectively; and S_{1-6} are LCS, LTS, LFS, RFS, RTS, RCS stretch values, respectively. The regression constants are A, B, C, D, H and $\alpha, \beta, \delta, \epsilon, \eta$ are the regression coefficients. Independent variables were selected for further evaluation, based on squared multiple correlations (R^2 close to 1) and their significance ($p < 0.05$), as well as the author's hypotheses about the relative importance of each independent variable and its relationship with FF. These hypotheses were formed, based on years of experience in evaluating protective masks. Estimates of FF produced by the model of FF in terms of pressure (A-1) were graphically compared to the measured FF to determine the predictive capability of the model. If necessary, changes in the procedure or modeling were made to enhance the predictive capability.

Series 1-6

An additional three series of data were collected and modeling was performed using the six series of data. Modeling was based on decisions that were made from the series 1-3 modeling efforts, described in *Results and Conclusions: Series 1-3* (this page). Models (A-1), (A-4), and (A-5) were again developed, using data for Conditions 3, 4, and 5.

Then, 12 validation trials (three in Condition 3, three in Condition 4, and six in Condition 5) were conducted according to the procedure described in the primary evaluation (see *Procedure*, p. 40). The mask and head harness were removed after each trial and a new head harness was used for each trial. The validation data were used to predict FF using models (A-1) and (A-4). Estimated FF was graphically compared to measured FF to determine the predictive capability of each model. Then FF estimates and actual measures were converted to pass or fail scores, based on whether they were below or above the FF criterion of 1667 and compared again. If necessary, changes in the procedure or modeling were made to enhance the predictive capability.

Results and Conclusions

Series 1-3

First, the three measures obtained using the pressure sensor were evaluated: seal pressure, seal contact area, and number of seal gaps. Regression analysis of FF as a function of 11 seal pressures (model (A-1)) revealed potential for a strong relationship ($R^2 = 0.92, p = 0.001$). In addition, based on extensive experience with masks, the researcher theorized that pressure was the

key to defining whether a seal was capable of providing adequate protection. Thus, the independent variable pressure was selected for further evaluation.

Fit factor estimates produced by model (A-1) based on seven strap adjustment conditions are shown in Figure A-1. Model (A-1) predicted FFs greater than 40,000 (A of Figure A-1) better than it predicted FFs less than 20,000 (B of Figure A-1). The primary region of interest for this study is FFs below 10,000 and especially FFs near the criterion of 1667. The large changes and large range (2.6 to 172,000) of FF data over the seven conditions (see Figure A-2) appeared to prevent adequate estimates below an FF of 10,000. Based on these results, the following changes were made in an effort to increase predictive capability of the model: collect additional data (three series), eliminate the extremes (Conditions 1, 2, 6 and 7), and concentrate modeling efforts on Conditions 3, 4, and 5, for which FF data were observed to pass through the criterion of 1667.

Regression analysis of FF as a function of seal contact area (model (A-2)) revealed potential for a strong relationship ($R^2 = 0.87$, $p = 0.008$) but not as strong as the relationship of FF and pressure. In addition, the researcher felt that seal contact area alone would not determine whether a seal was capable of providing adequate protection. Because the pressure sensor was a new technology that had never been applied in a similar manner, the researcher also felt it was desirable to select the single best measure (pressure, area, or seal gaps) provided by the sensor for analysis in the present study. Any other promising measures would be evaluated in subsequent efforts. Thus, the seal contact area independent variable was not selected for further evaluation at this time.

Regression analysis of FF as a function of the number of seal gaps (model (A-3)) revealed a weak, nonsignificant relationship ($R^2 = 0.46$, $p = 0.479$). Thus, the number of seal gaps independent variable was not selected for further evaluation.

Second, relationships of strap stretch to FF and to seal pressure were explored. Regression analysis of FF as a function of six strap stretch measurements (model (A-4)) revealed potential for a strong relationship ($R^2 = 0.85$, $p = 0.000$). Because strap adjustment was the means of controlling the experiment as well as controlling the fit of a mask in general, the researcher felt it was important to continue to evaluate the relationship of strap stretch and FF. In addition, an important objective of this research was to determine proper strap adjustment to produce a protective seal between mask and face. Thus, the strap stretch independent variable was selected for further evaluation.

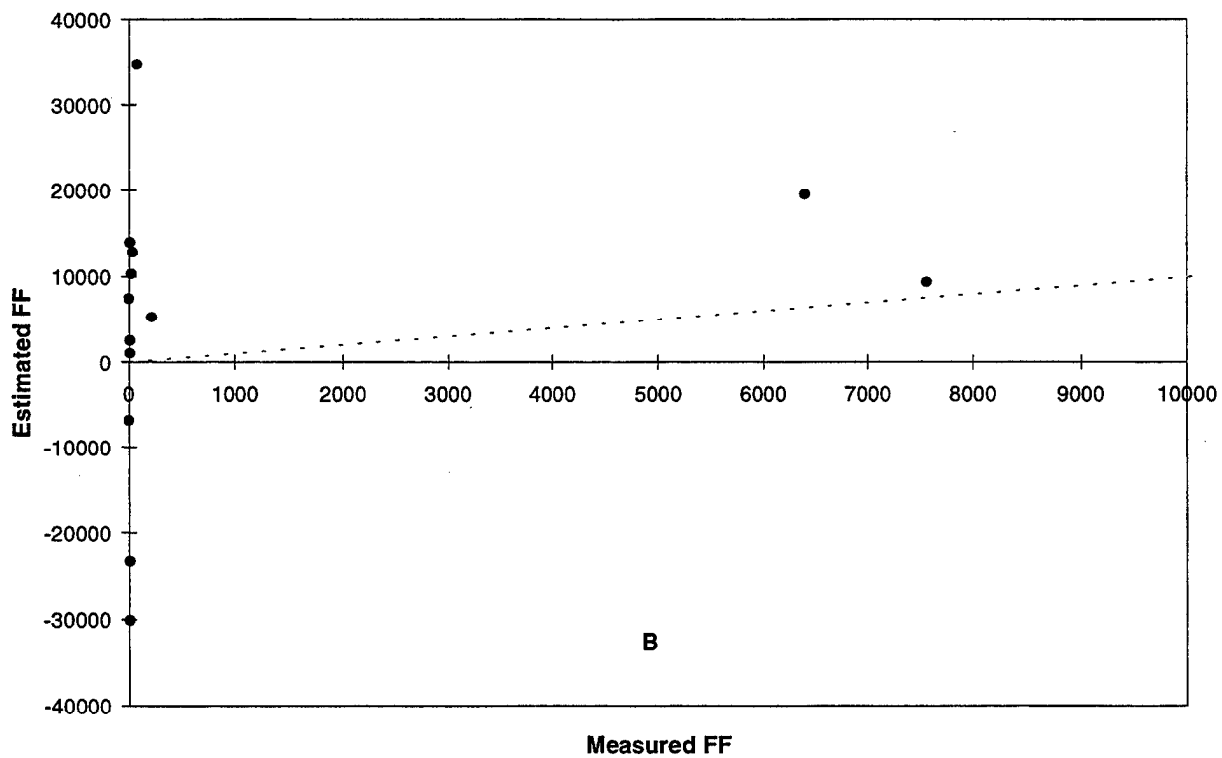
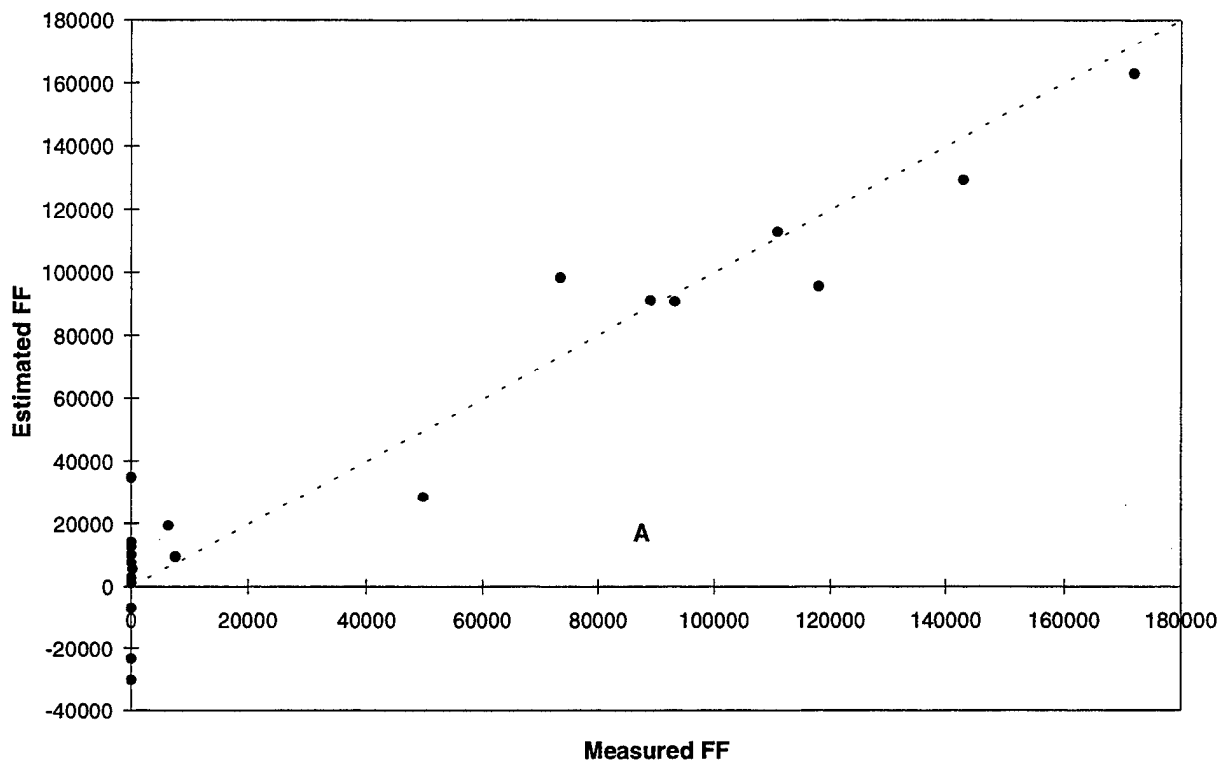


Figure A-1. Estimated FF based on modeling FF as a function of 11 seal pressures. (Plot A represents all estimates; B is focused on estimates below 10,000.)

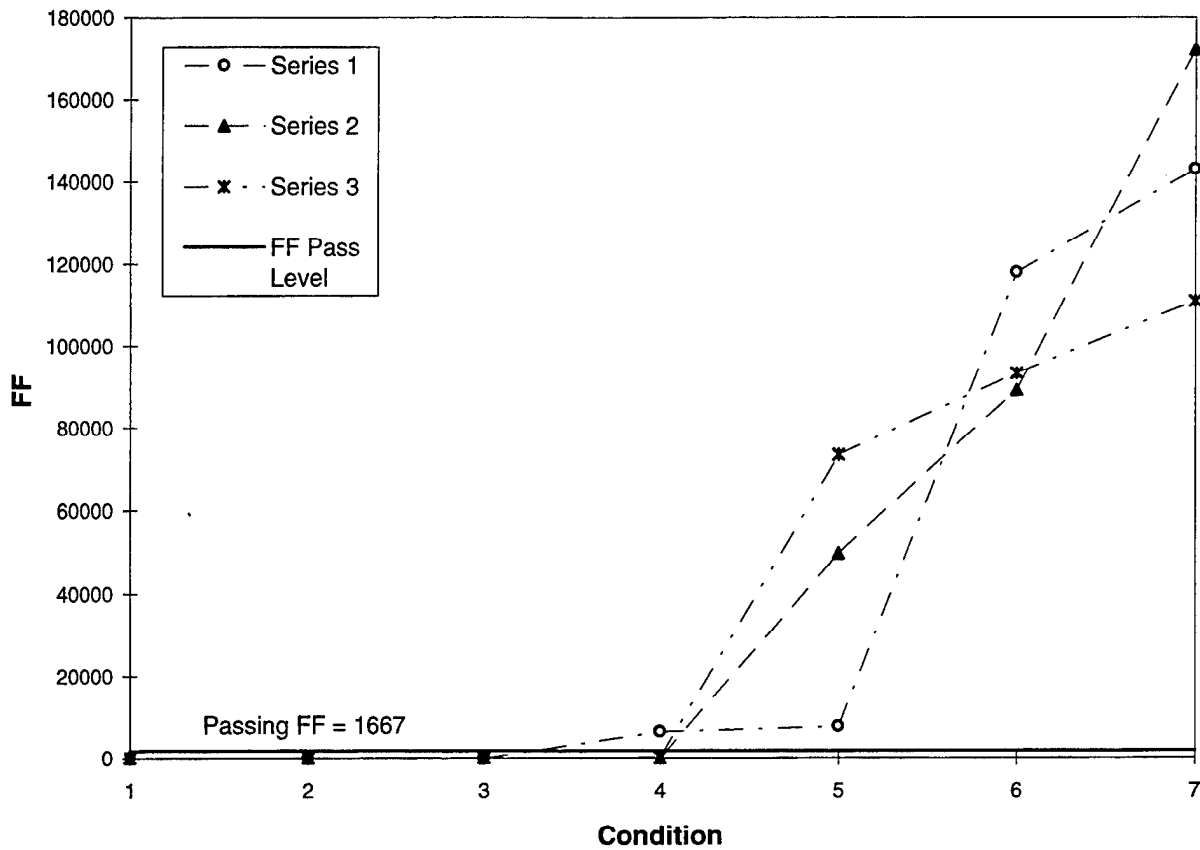


Figure A-2. FF data for first three series in seven strap adjustment conditions as in Table A-1.

Regression analysis of individual seal pressures as functions of the six strap stretch measurements (model (A-5)) revealed potential for strong relationships ($R^2 = 0.84$ to 0.98 , $p = 0.000$). These relationships were selected for further evaluation in order to explore how the independent variables, pressure and stretch, are interrelated. In conclusion, the following model relationships were selected for further evaluation in the primary study: (A-1), (A-4), and (A-5).

Series 1-6

The FF data for the six series, as well as an example of the pressure data for a single series, are presented in Figures A-3 and A-4. The results of modeling are presented in Table A-2.

When estimated to measured FF were compared (see Figure A-5), both models (A-1) and (A-4) provided poor estimates across the entire range of FFs. Fit factor data were converted to pass or fail scores and compared again (see Tables A-3 and A-4). The models predicted 5 to 6 of the 12 FFs correctly and predicted failing and passing equally well. However, the predictive capability is far from adequate. A probable explanation for this is that the data used to construct the model and the validation data were collected via different procedures. In order to eliminate this source of

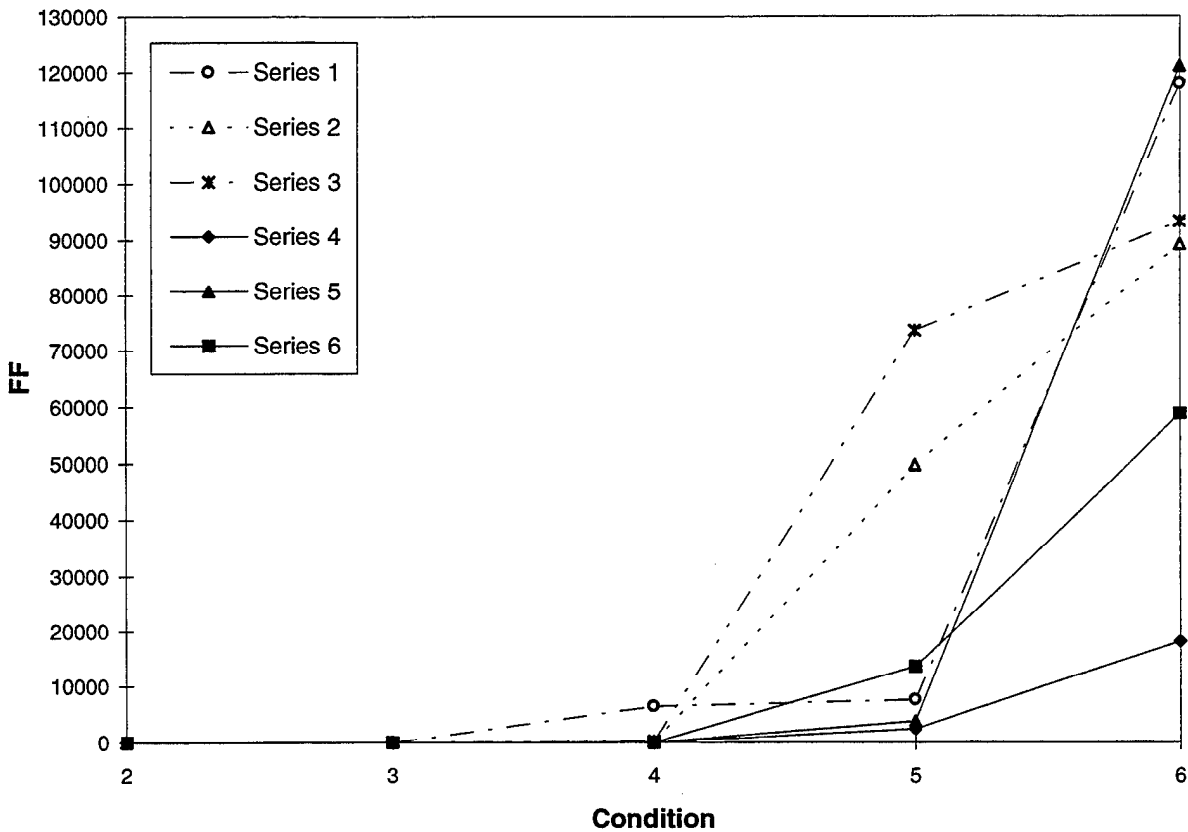


Figure A-2. FF data for first three series in seven strap adjustment conditions as in Table A-1.

Regression analysis of individual seal pressures as functions of the six strap stretch measurements (model (A-5)) revealed potential for strong relationships ($R^2 = 0.84$ to 0.98 , $p = 0.000$). These relationships were selected for further evaluation in order to explore how the independent variables, pressure and stretch, are interrelated. In conclusion, the following model relationships were selected for further evaluation in the primary study: (A-1), (A-4), and (A-5).

Series 1-6

The FF data for the six series, as well as an example of the pressure data for a single series, are presented in Figures A-3 and A-4. The results of modeling are presented in Table A-2.

When estimated to measured FF were compared (see Figure A-5), both models (A-1) and (A-4) provided poor estimates across the entire range of FFs. Fit factor data were converted to pass or fail scores and compared again (see Tables A-3 and A-4). The models predicted 5 to 6 of the 12 FFs correctly and predicted failing and passing equally well. However, the predictive capability is far from adequate. A probable explanation for this is that the data used to construct the model and the validation data were collected via different procedures. In order to eliminate this source of

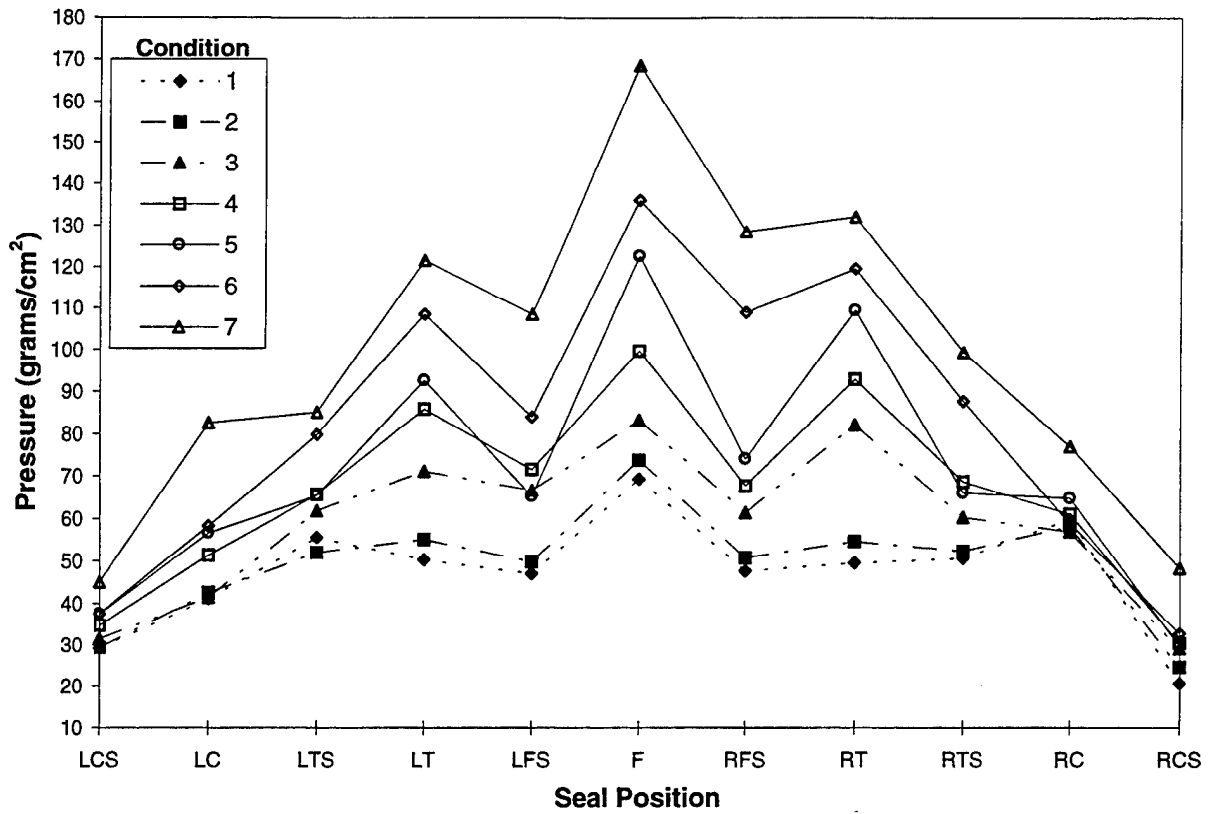


Figure A-4. Seal pressure data for Series 2 in seven strap adjustment conditions as in Table A-1.

Table A-2

Model Results for Six Series of Data for Conditions 3 Through 5

Model	R ²	p
$FF = A + \alpha_1 P_1 + \alpha_2 P_2 + \dots + \alpha_{11} P_{11}$	0.88	0.048
$FF = B + \delta_1 S_1 + \delta_2 S_2 + \dots + \delta_6 S_6$	0.69	0.021
$P_1 = C_1 + \eta_{11} S_1 + \eta_{12} S_2 + \dots + \eta_{16} S_6$	0.71	0.017
$P_2 = C_2 + \eta_{21} S_1 + \eta_{22} S_2 + \dots + \eta_{26} S_6$	0.79	0.003
$P_3 = C_3 + \eta_{31} S_1 + \eta_{32} S_2 + \dots + \eta_{36} S_6$	0.95	0.000
⋮	0.86	0.000
⋮	0.91	0.000
⋮	0.82	0.001
⋮	0.90	0.000
⋮	0.75	0.008
⋮	0.84	0.001
⋮	0.39	0.398
$P_{11} = C_{11} + \eta_{11,1} S_1 + \eta_{11,2} S_2 + \dots + \eta_{11,6} S_6$	0.68	0.026

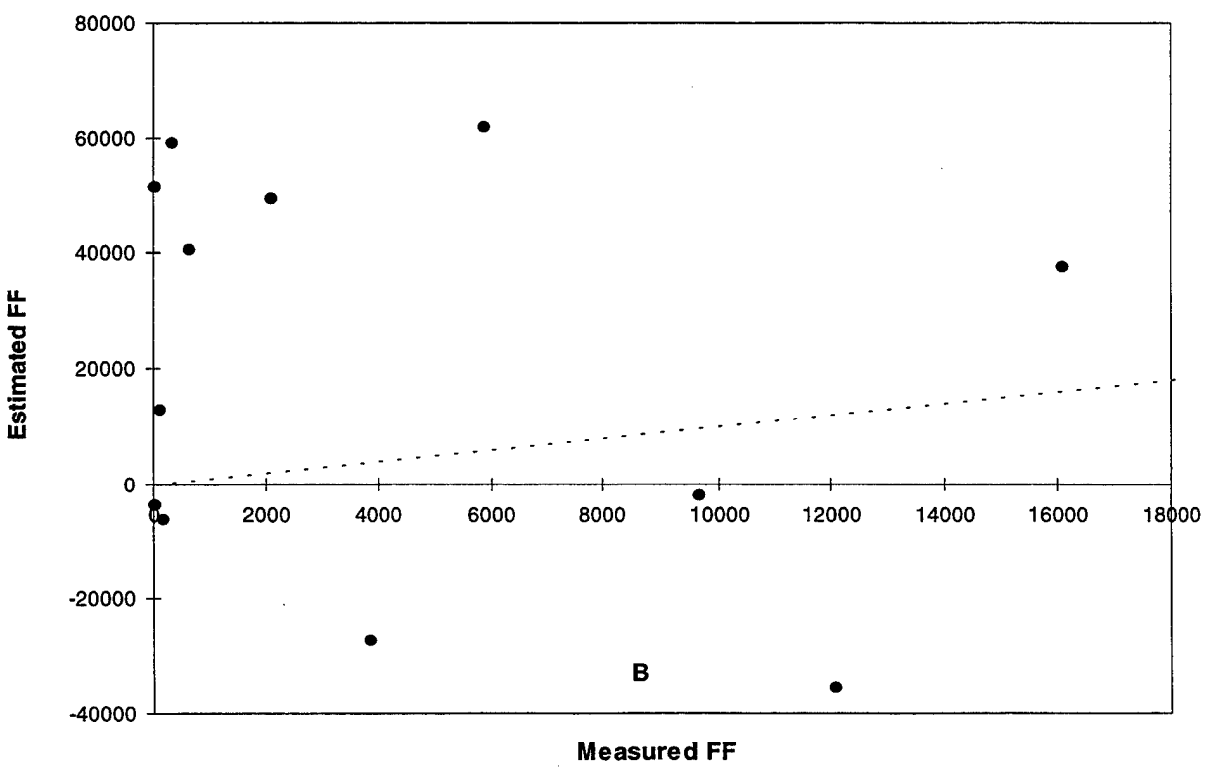
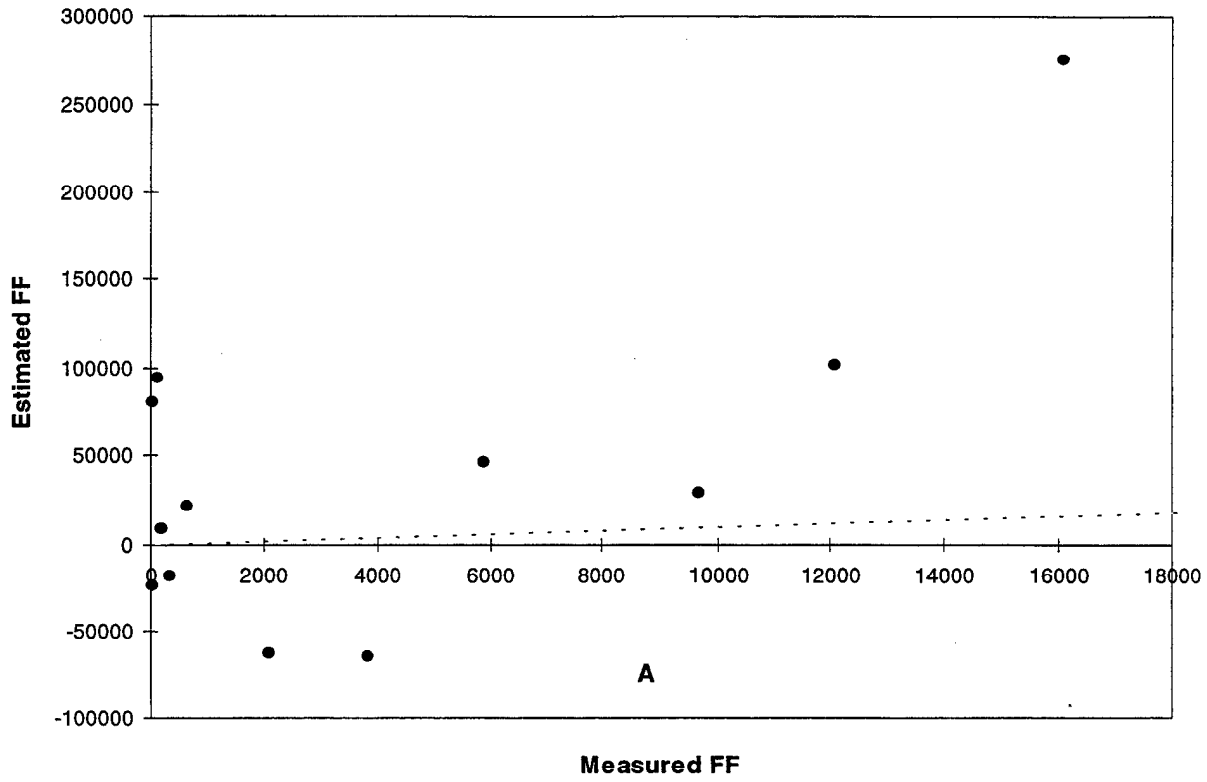


Figure A-5. FF estimates based on (A) seal pressure and (B) strap stretch.

Table A-3

Prediction of Passing or Failing by Model of FF as a Function of 11 Seal Pressures

Validation trial	1	2	3	4	5	6	7	8	9	10	11	12
Measured FF	P	P	F	F	F	F	F	P	P	P	P	F
Estimated FF	F	F	F	F	P	P	P	P	P	P	P	P
Correct prediction			✓	✓				✓	✓	✓	✓	

Model (A-1). P is passing; F is failing based on a criterion of 1667.

Table A-4

Prediction of Passing or Failing by Model of FF as a Function of Six Strap Stretches

Validation trial	1	2	3	4	5	6	7	8	9	10	11	12
Measured FF	P	P	F	F	F	F	F	P	P	P	P	F
Estimated FF	F	P	P	P	P	F	F	F	P	F	P	P
Correct prediction		✓				✓	✓		✓		✓	

Model (A-4). P is passing; F is failing based on a criterion of 1667.

Summary

As a result of the pilot evaluation, the following changes were made in the experimental procedure:

- The number of strap adjustment conditions or trials used to build the model was reduced to three to focus on the primary region of interest, the region in which the FF passes through the criterion of 1667.

- The procedure was modified to that used in the primary evaluation (pp. 5 through 71) because a satisfactory validation procedure could not be designed for the approach reported in this appendix. Also, the procedure of progressively tightening the mask over a series of trials does not reflect the normal procedure for donning and fitting the mask.

- In addition, two independent variables (seal contact area and number of seal gaps) were eliminated from further analysis because they were either not strongly related to FF or the researcher felt that they were not as important as other independent variables such as pressure. Independent variables were eliminated in order to focus the scope of the evaluation on the most important and potentially fruitful relationships.

APPENDIX B
HEAD HARNESS EVALUATION

HEAD HARNESS EVALUATION

Overview

A pilot evaluation was completed in order to develop calibration curves for determining tension in a head harness strap from the measured strap stretch. Wide variations in strap behavior were observed; thus, reliable tension predictions could not be made using these load-stretch curves.

In addition, head harness strap gauge length was measured at a single strap location over the course of a day to determine how this measure may change with time. Changes that were observed were within measurement error. Thus, any viscoelastic effects that occur will not confound the results of this evaluation. A rest period of 2 hours after mask adjustment on the headform was selected to begin testing. This period was convenient for the test scenario but not necessary for settling any viscoelastic effects.

Procedure

Tension tests were performed on head harness straps to determine the load deflection characteristics of the strap material. A single strap was removed from each of eight head harnesses. The strap was fastened between two buckle fixtures mounted on an Instron Universal Testing Instrument. The buckle fixture was fabricated from a mask buckle attached to a threaded shaft for attachment to either the base of the test machine or the load cell. The strap was threaded through the buckle as it is on the mask. At the start of the test, the buckle fixtures were approximately 135 mm apart, with the strap loosely fastened at either end. A 10-mm gauge length was marked at the midpoint of the strap with reflective markers. A 5-lb load cell was used, and a total deflection of 80 mm at 4 mm/sec was applied to the strap by the actuator. Six cycles of loading were used to precondition the straps so that hysteresis effects were minimized (see Figure B-1). Strap deflection data were acquired with a video system and recorded at 25 Hz.

For the gauge length evaluation, the mask was fit on the headform, and repeated gauge length measures were made on a single head harness strap over an 8-hour time period. Gauge length was measured using a digital caliper.

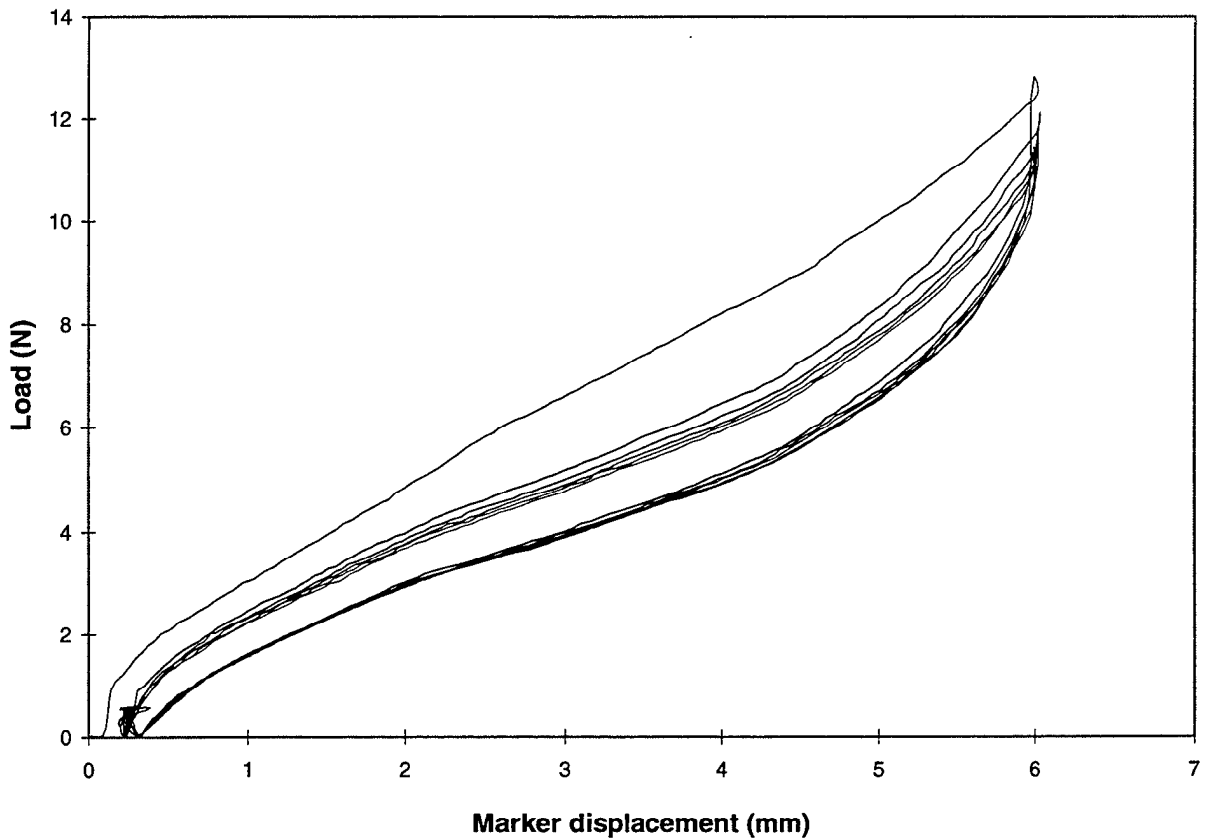


Figure B-1. Load-deflection curve for six cycles of loading on a single strap. (A total deflection of 80 mm at 4 mm/sec was used as input.)

Results and Conclusions

The loading portion of the sixth cycle of each load-deflection curve was extracted and converted to a load-stretch curve (see Figure B-2). Pilot mask fittings were conducted to determine the range of stretch (1.1 to 1.5) of interest for the subject evaluation. At stretches greater than 1.2, the variability in load increases rapidly. Conversion of stretch values to tension based on these curves would have greatly increased the data variability. Thus, raw stretch data were used to develop models. For future evaluations, it will be desirable to develop a means to measure and control strap tension directly.

Gauge length measures varied slightly over the course of 8 hours (see Figure B-3). Because the variations were small and within operator measurement error (0.10 mm), any viscoelastic effects that occur within 8 hours of loading will not confound the results of the present study. All trials were completed in 8 hours or less.

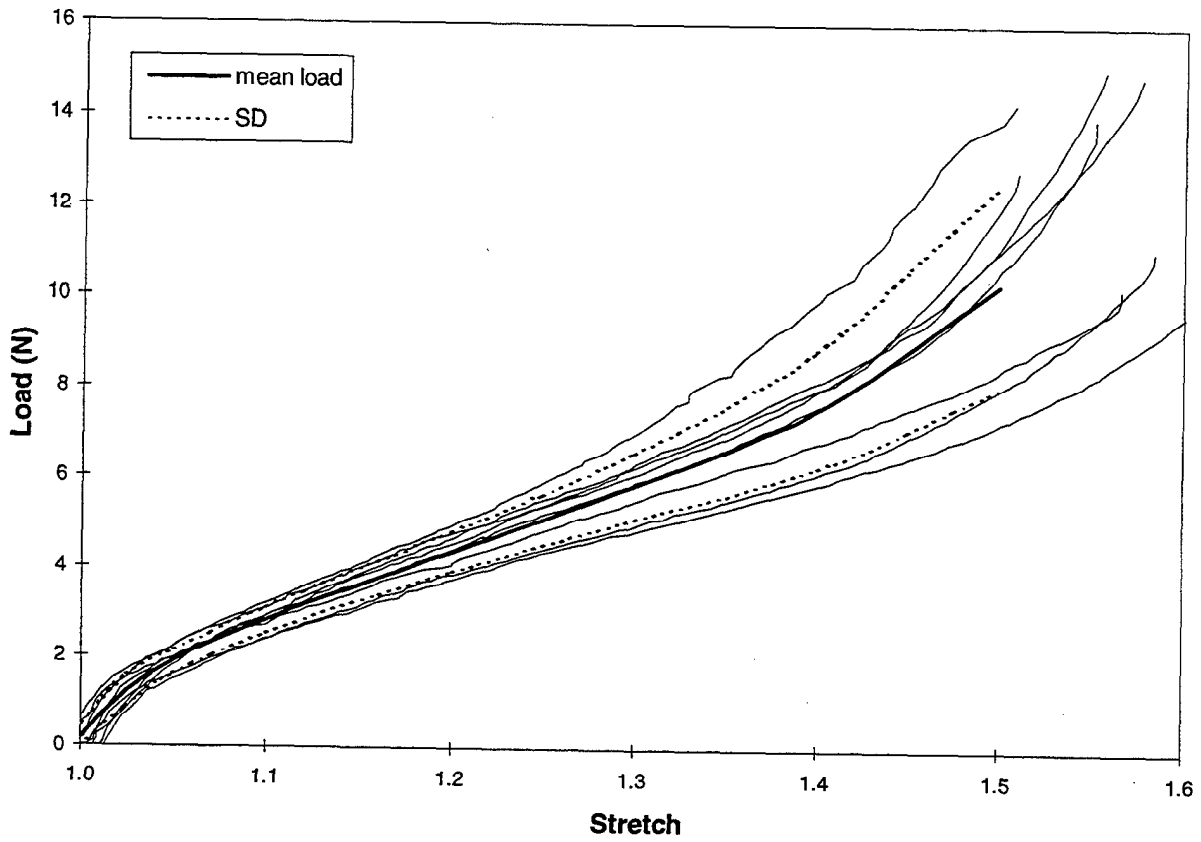


Figure B-2. Load-stretch curves, with mean and one standard deviation, for the sixth loading cycle of each of eight straps. (A total deflection of 80 mm at 4 mm/sec used as input.)

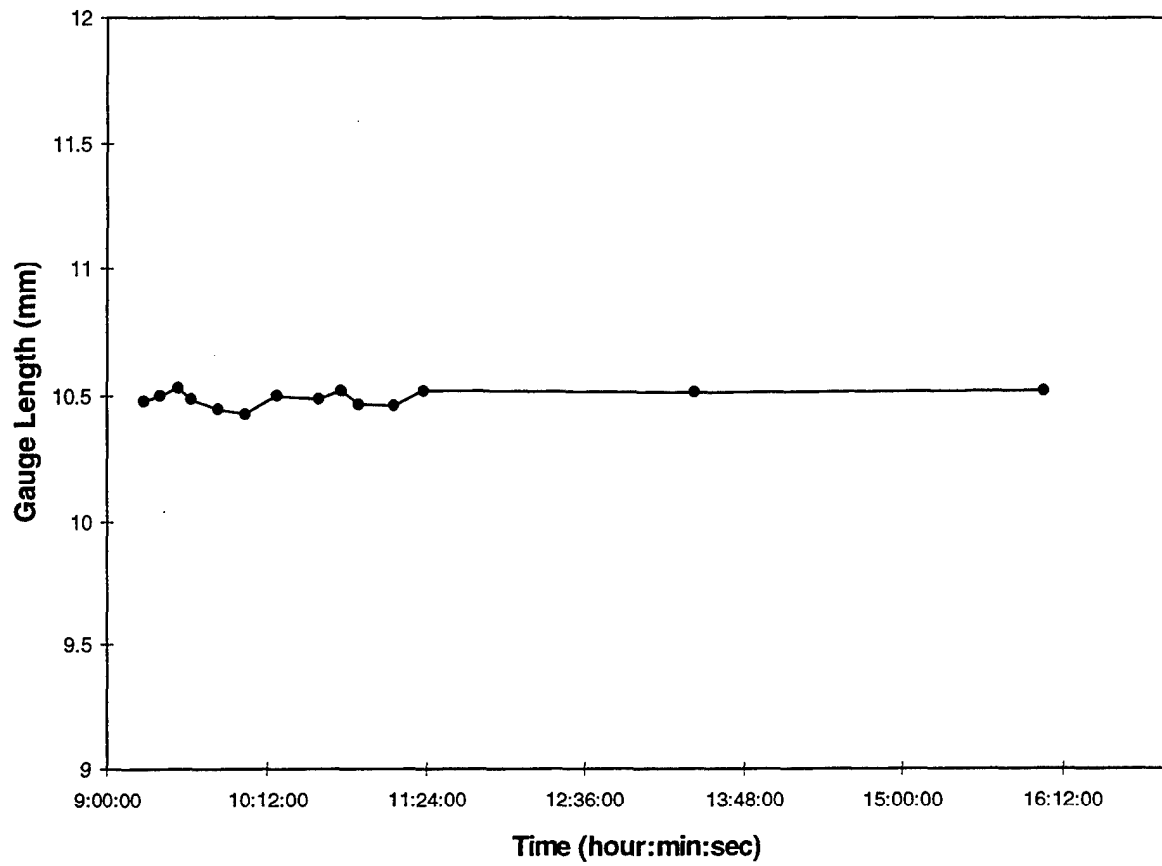


Figure B-3. Gauge length variation in a loaded head harness strap over an 8-hour period.

APPENDIX C
PROTECTIVE MASK CLEARING EVALUATION

PROTECTIVE MASK CLEARING EVALUATION

Overview

A pilot evaluation was completed in order to determine the amount of time necessary to clear particles from inside the mask on the headform in order to perform accurate fit testing.

Procedure

The mask was fit on the headform. The filter canister was removed from the mask, and the breathing simulator was turned on and operated at 20 breaths per minute at a 1.5-liter tidal volume. This allowed the internal mask air to equilibrate with the ambient air. With the filter removed, the particle concentration inside the mask was normally slightly below the ambient concentration. This provided a consistent point at which to start clearing the mask.

Clearing was started by attaching the filter canister to the mask. Particle concentrations were measured at 15-second intervals using the protective mask fit tester. Several trials were conducted in this manner. The mask was removed and refit on the headform for each trial, and both loose and tight fittings were used. In addition, ambient concentrations and initial mask concentrations varied.

Results and Conclusions

After 5 minutes of clearing, steady state particle concentrations were reached (see Figures C-1 and C-2). Steady state was reached at approximately the same time for both tightly (Trial A) and loosely fitted masks (Trial B). Based on starting (ambient) and ending concentrations, Trial A represents a mask that would pass the FF test, while Trial B represents a mask that would fail. To ensure that mask clearing reached steady state before fit testing, a 10-minute clearing period was selected for the evaluation.

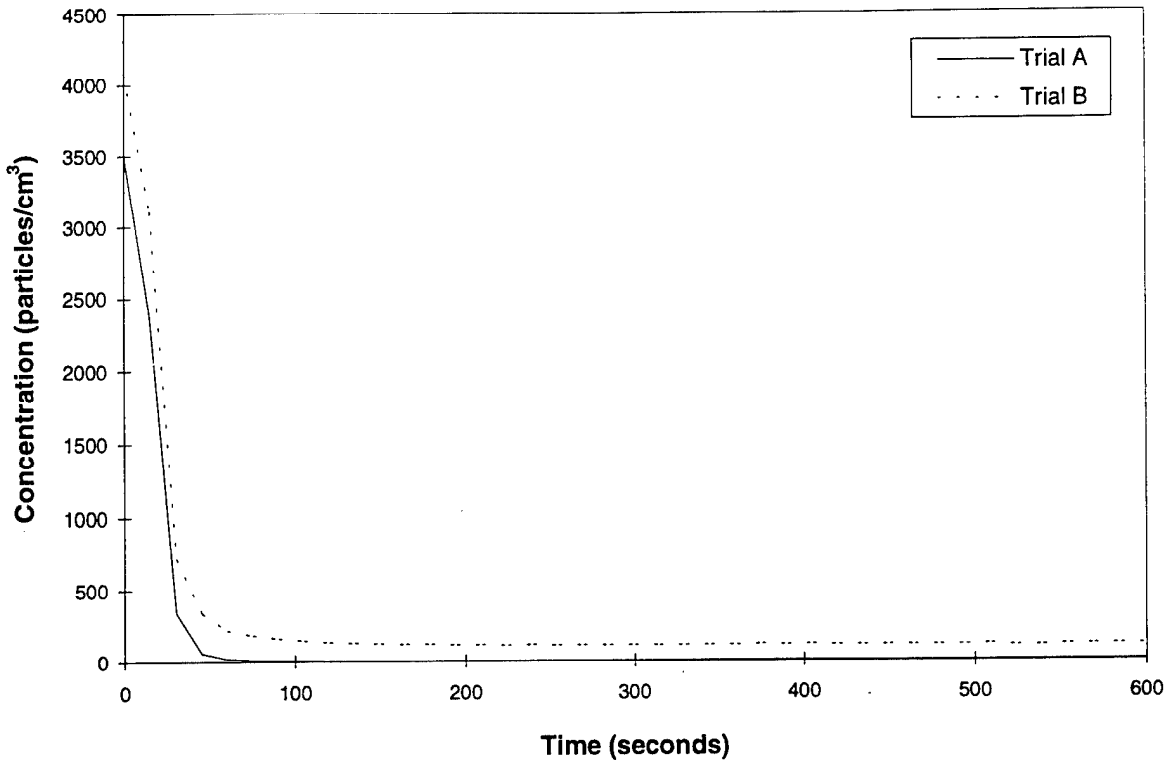


Figure C-1. Inside mask concentrations during the clearing period.

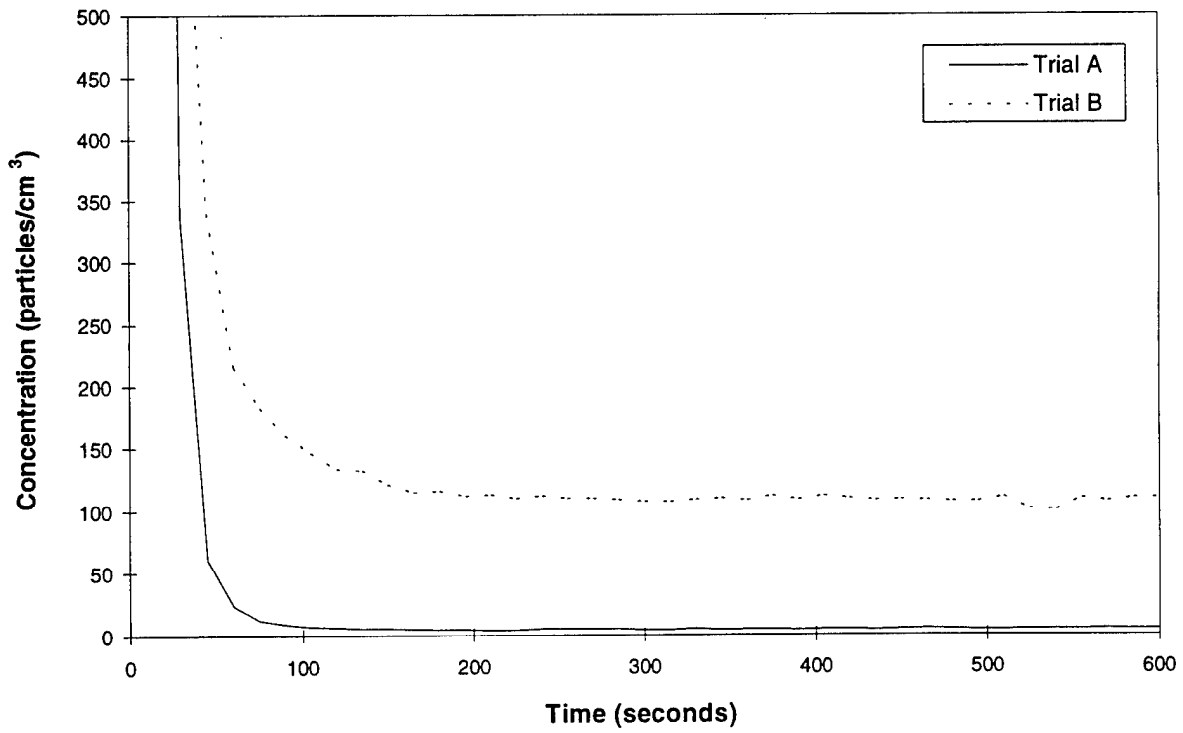


Figure C-2. Figure C-1 data plotted on smaller scale.

APPENDIX D
PRESSURE SENSOR CALIBRATION EVALUATION

PRESSURE SENSOR CALIBRATION EVALUATION

Overview

A pilot evaluation was completed in order to determine effects of sensor performance on calibration. First, drift characteristics were investigated and a time period for load settling before calibration was determined. Second, calibration accuracy was verified over time to ensure that a calibration file would remain valid over the measurement period.

Procedure

In order to investigate drift characteristics of the pressure sensors, a 30-second recording of force was made at one frame per second while a 518-gram load (498-gram weight plus 20-gram platform) was placed on an uncalibrated sensor. Sensor response was plotted and examined in order to determine the period of time necessary to reach minimal drift of values. After the time period for settling was determined, sensors were calibrated using a 518-gram load at the end of the settling time period. Drift characteristics were examined again on calibrated sensors. A 30-second recording of force was made after loading the sensor with a 518-gram load.

In order to check calibration accuracy, sensors were calibrated using two different weights (200 and 498 grams, plus a 20-gram platform). Force exerted on the sensor by the 220- or 518-gram weight was measured at periodic time intervals for 3 to 4 hours after calibration.

Results and Conclusions

With respect to drift characteristics, the sensor response in raw units of force increased greatly in the first 5 seconds after loading (see Figure D-1). At 15 seconds after loading, the increase in force was less than 1% per second (0.93% average, 0.36% standard deviation, $n = 5$). Thus, a 15-second time period for settling of the sensor for both calibration and measurements was selected. Calibrated sensors experienced less than 1% per second increase in force (0.95% average, 0.95% standard deviation, $n=5$) at 15 seconds after loading (see Figure D-2). Also note that the force at 15 seconds is 522 grams, a 0.8% increase over the calibrated weight of 518 grams, and is considered acceptable for the present evaluation because it is well within the criterion of 10% of the load placed on the sensor. The approach of calibrating and making all measurements at 15 seconds after loading will ensure that drift characteristics of the sensors are minimized and do not confound the results of the present study.

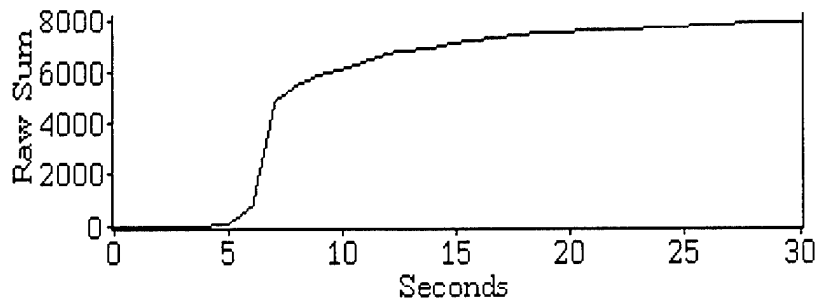


Figure D-1. Sensor response in raw units of force for a 518-gram load placed on the sensor at 5 seconds.

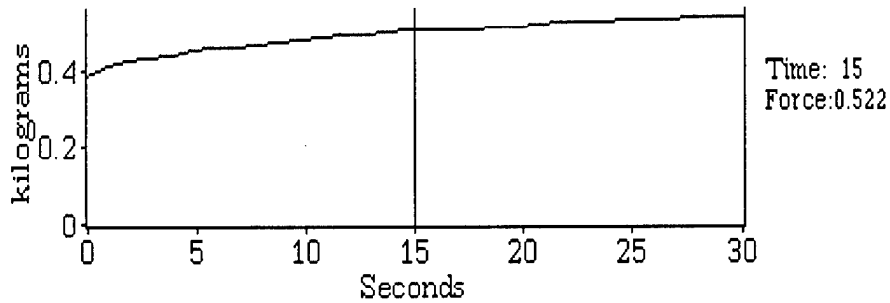


Figure D-2. Calibrated sensor response for a 518-gram load placed on the sensor just before initiation of the force recording at 0 seconds.

With respect to calibration accuracy, sensors measured loads within 10% of the actual load placed on the sensor throughout the 3- to 4-hour time period (see Figures D-3 and D-4). This performance is adequate for the present study in which measurements were made within the hour following calibration.

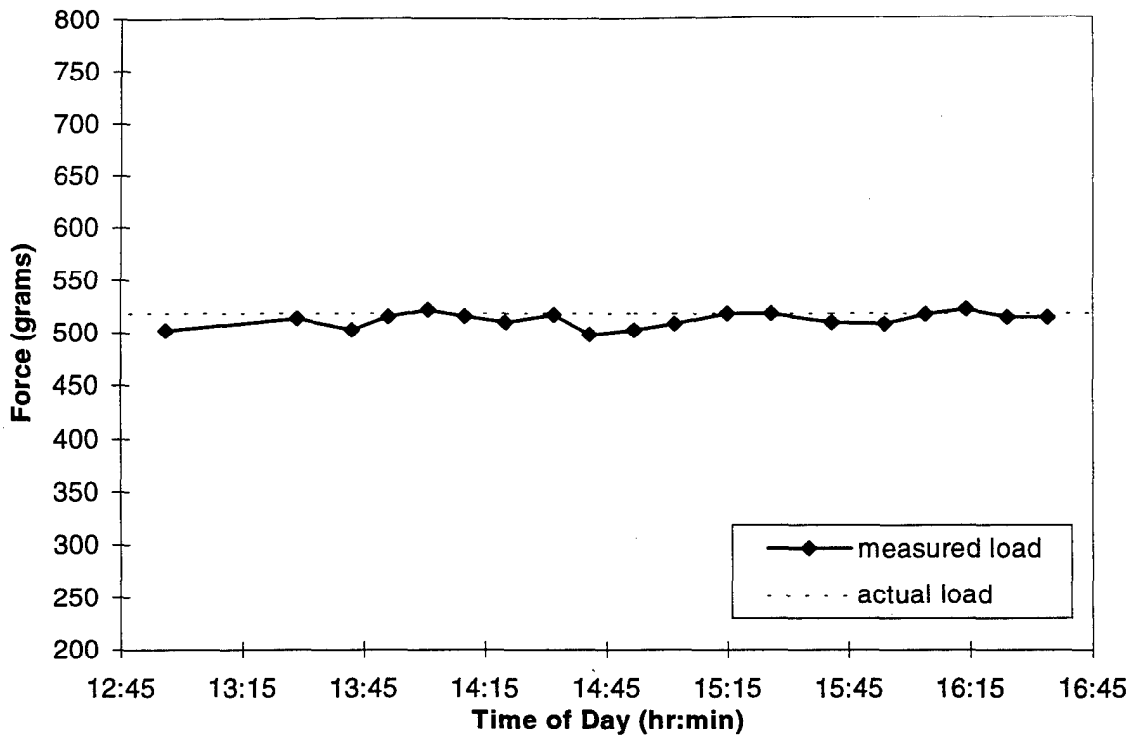


Figure D-3. Example of sensor calibration accuracy at 518 grams.

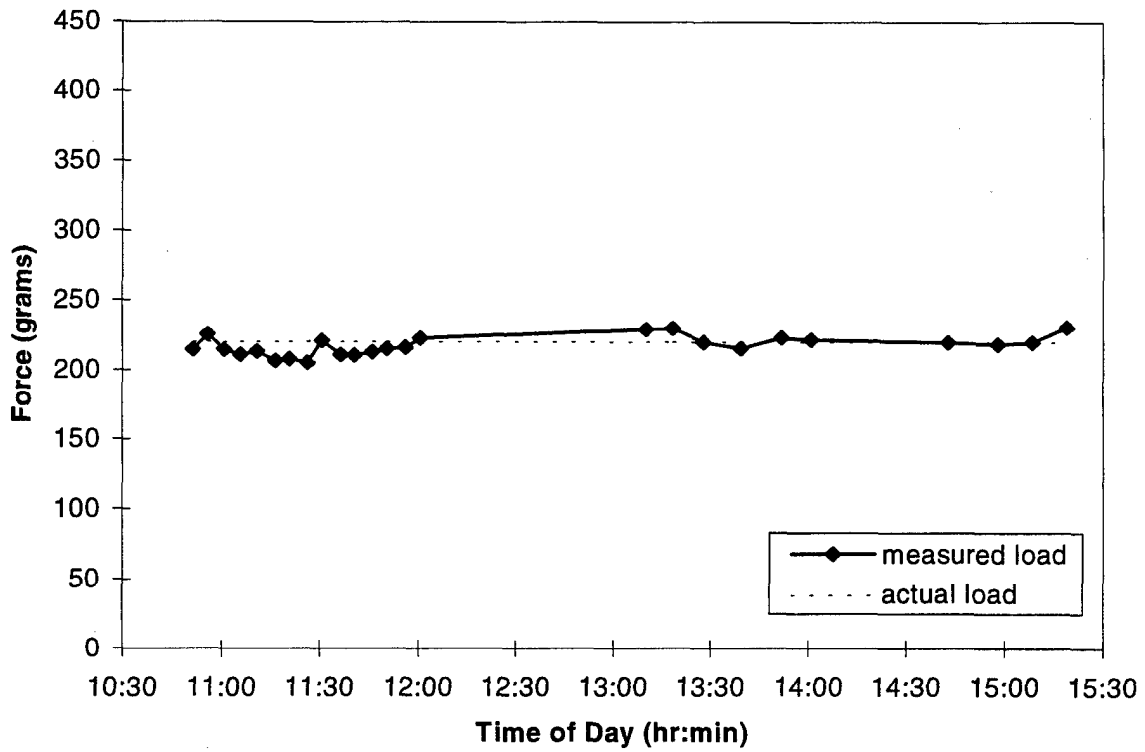


Figure D-4. Example of sensor calibration accuracy at 220 grams.

APPENDIX E
ACRONYMS AND ABBREVIATIONS

LIST OF ACRONYMS AND ABBREVIATIONS

CBDCOM	Chemical and Biological Defense Command
ERDEC	Edgewood Research, Development, & Engineering Center
FF	fit factor
FLSP	forward light-scattering photometry
HEPA	high-efficiency particulate air
HQDA	Headquarters, Department of the Army
PMFVS	Protective Mask Fit Validation System
QA	quality assurance
TRADOC	U.S. Army Training and Doctrine Command
WWI	World War I

<u>NO. OF COPIES</u>	<u>ORGANIZATION</u>	<u>NO. OF COPIES</u>	<u>ORGANIZATION</u>
2	ADMINISTRATOR DEFENSE TECHNICAL INFO CENTER ATTN DTIC OCP 8725 JOHN J KINGMAN RD STE 0944 FT BELVOIR VA 22060-6218	1	COMMANDER USA OPERATIONAL TEST & EVAL AGENCY ATTN CSTE TSM 4501 FORD AVE ALEXANDRIA VA 22302-1458
1	DIRECTOR US ARMY RESEARCH LABORATORY ATTN AMSRL CS AS REC MGMT 2800 POWDER MILL RD ADELPHI MD 20783-1197	1	USA BIOMEDICAL R&D LABORATORY ATTN LIBRARY FORT DETRICK BUILDING 568 FREDERICK MD 21702-5010
1	DIRECTOR US ARMY RESEARCH LABORATORY ATTN AMSRL CI LL TECH LIB 2800 POWDER MILL RD ADELPHI MD 207830-1197	1	HQ USAMRDC ATTN SGRD PLC FORT DETRICK MD 21701
1	DIRECTOR US ARMY RESEARCH LABORATORY ATTN AMSRL DD R ROCCHIO 2800 POWDER MILL RD ADELPHI MD 20783-1197	1	COMMANDER USA AEROMEDICAL RESEARCH LAB ATTN LIBRARY FORT RUCKER AL 36362-5292
1	US ARMY RESEARCH OFC 4300 S MIAMI BLVD RESEARCH TRIANGLE PARK NC 27709	1	US ARMY SAFETY CENTER ATTN CSSC SE FORT RUCKER AL 36362
1	CODE 1142PS OFFICE OF NAVAL RESEARCH 800 N QUINCY STREET ARLINGTON VA 22217-5000	1	CHIEF ARMY RESEARCH INSTITUTE AVIATION R&D ACTIVITY ATTN PERI IR FORT RUCKER AL 36362-5354
1	WALTER REED ARMY INST OF RSCH ATTN SGRD UWI C (COL REDMOND) WASHINGTON DC 20307-5100	1	AIR FORCE FLIGHT DYNAMICS LAB ATTN AFWAL/FIES/SURVIAC WRIGHT PATTERSON AFB OH 45433
1	COMMANDER US ARMY RESEARCH INSTITUTE ATTN PERI ZT (DR E M JOHNSON) 5001 EISENHOWER AVENUE ALEXANDRIA VA 22333-5600	1	US ARMY NATICK RD&E CENTER ATTN STRNC YBA NATICK MA 01760-5020
1	DEPUTY COMMANDING GENERAL ATTN EXS (Q) MARINE CORPS RD&A COMMAND QUANTICO VA 22134	1	US ARMY TROOP SUPPORT CMD NATICK RD&E CENTER ATTN BEHAVIORAL SCI DIV SSD NATICK MA 01760-5020
1	HEADQUARTERS USATRADO ATTN ATCD SP FORT MONROE VA 23651	1	US ARMY TROOP SUPPORT CMD NATICK RD&E CENTER ATTN TECH LIBRARY (STRNC MIL) NATICK MA 01760-5040
		1	DR RICHARD JOHNSON HEALTH & PERFORMANCE DIVISION US ARIEM NATICK MA 01760-5007

<u>NO. OF COPIES</u>	<u>ORGANIZATION</u>	<u>NO. OF COPIES</u>	<u>ORGANIZATION</u>
1	USAF ARMSTRONG LAB/CFTO ATTN DR F WESLEY BAUMGARDNER SUSTAINED OPERATIONS BRANCH BROOKS AFB TX 78235-5000	1	HQ III CORPS & FORT HOOD OFFICE OF THE SCIENCE ADVISER ATTN AFZF CS SA FORT HOOD TX 76544-5056
1	STRICOM 12350 RESEARCH PARKWAY ORLANDO FL 32826-3276	1	COMMANDER HQ XVIII ABN CORPS & FORT BRAGG OFFICE OF THE SCI ADV BLDG 1-1621 ATTN AFZA GD FAST FORT BRAGG NC 28307-5000
1	COMMANDER US ARMY RESEARCH INSTITUTE OF ENVIRONMENTAL MEDICINE NATICK MA 01760-5007	1	SOUTHCOM WASHINGTON FIELD OFC 1919 SOUTH EADS ST SUITE L09 AMC FAST SCIENCE ADVISER ARLINGTON VA 22202
1	COMMANDER USA MEDICAL R&D COMMAND ATTN SGRD PLC (LTC K FRIEDL) FORT DETRICK MD 21701-5012	1	HQ US SPECIAL OPERATIONS CMD AMC FAST SCIENCE ADVISER ATTN SOSD MACDILL AIR FORCE BASE TAMPA FL 33608-0442
1	COMMANDER US ARMY AVIATION CENTER ATTN ATZQ CDM S (MR MCCRACKEN) FT RUCKER AL 36362-5163	1	HQ US ARMY EUROPE AND 7TH ARMY ATTN AEAGX SA OFFICE OF THE SCIENCE ADVISER APO AE 09014
1	DIRECTOR US ARMY AEROFLIGHT DYNAMICS DIR MAIL STOP 239-9 NASA AMES RESEARCH CENTER MOFFETT FIELD CA 94035-1000	1	COMMANDER HQ 21ST THEATER ARMY AREA CMD AMC FAST SCIENCE ADVISER ATTN AERSA APO AE 09263
1	COMMANDER MARINE CORPS SYSTEMS COMMAND ATTN CBGT QUANTICO VA 22134-5080	1	COMMANDER HEADQUARTERS USEUCOM AMC FAST SCIENCE ADVISER UNIT 30400 BOX 138 APO AE 09128
1	DIRECTOR AMC-FIELD ASSIST IN SCIENCE & TECHNOLOGY ATTN AMC-FAST (RICHARD FRANSEEN) FT BELVOIR VA 22060-5606	1	HQ 7TH ARMY TRAINING COMMAND UNIT #28130 AMC FAST SCIENCE ADVISER ATTN AETT SA APO AE 09114
1	COMMANDER US ARMY FORCES COMMAND ATTN FCDJ SA BLDG 600 AMC FAST SCIENCE ADVISER FT MCPHERSON GA 30330-6000	1	COMMANDER HHC SOUTHERN EUROPEAN TASK FORCE ATTN AESE SA BUILDING 98 AMC FAST SCIENCE ADVISER APO AE 09630
1	COMMANDER I CORPS AND FORT LEWIS AMC FAST SCIENCE ADVISER ATTN AFZH CSS FORT LEWIS WA 98433-5000		

<u>NO. OF COPIES</u>	<u>ORGANIZATION</u>	<u>NO. OF COPIES</u>	<u>ORGANIZATION</u>
1	COMMANDER US ARMY PACIFIC AMC FAST SCIENCE ADVISER ATTN APSA FT SHAFTER HI 96858-5L00	1	ARL HRED AMCOM FIELD ELEMENT ATTN AMSRL HR MI (D FRANCIS) BUILDING 5678 ROOM S13 REDSTONE ARSENAL AL 35898-5000
1	COMMANDER US ARMY JAPAN/IX CORPS UNIT 45005 ATTN APAJ SA AMC FAST SCIENCE ADVISERS APO AP 96343-0054	1	ARL HRED AMCOM FIELD ELEMENT ATTN ATTN AMSRL HR MO (T COOK) BLDG 5400 RM C242 REDSTONE ARS AL 35898-7290
1	AMC FAST SCIENCE ADVISERS PCS #303 BOX 45 CS-SO APO AP 96204-0045	1	ARL HRED USAADASCH FLD ELEMENT ATTN AMSRL HR ME (K REYNOLDS) ATTN ATSA CD 5800 CARTER ROAD FORT BLISS TX 79916-3802
1	NAIC/DXLA 4180 WATSON WAY WRIGHT PATTERSON AFB OH 45433-5648	1	ARL HRED ARDEC FIELD ELEMENT ATTN AMSRL HR MG (R SPINE) BUILDING 333 PICATINNY ARSENAL NJ 07806-5000
1	NAWCAD PAX/4.6.3.1 (J D'ANDRADE) BLDG 2187 SUITE 2240 48110 SHAW RD UNIT 5 PATUXENT RIVER MD 20670	1	ARL HRED ARMC FIELD ELEMENT ATTN AMSRL HR MH (C BIRD) BLDG 1002 ROOM 206B FT KNOX KY 40121
1	MS KATHLEEN M ROBINETTE ATTN AFRL HECF 2255 H STREET WRIGHT-PATTERSON AFB OH 45433-7022	1	ARL HRED CECOM FIELD ELEMENT ATTN AMSRL HR ML (J MARTIN) MYER CENTER RM 2D311 FT MONMOUTH NJ 07703-5630
1	CHEMICAL AND BIOLOGICAL DEFENSE INFO ANALYSIS CTR PO BOX 196 GUNPOWDER BRANCH APG MD 21010-0196	1	ARL HRED FT BELVOIR FIELD ELEMENT ATTN AMSRL HR MK (P SCHOOL) 10115 GRIDLEY ROAD SUITE 114 FORT BELVOIR VA 22060-5846
1	US AIR FORCE MATERIEL CMD ATTN HSC YAC DAVID MANCHESTER 8107 13TH STREET BROOKS AFB TX 78235-5218	1	ARL HRED FT HOOD FIELD ELEMENT ATTN AMSRL HR MV HQ TEXCOM (E SMOOTZ) 91012 STATION AVE ROOM 111 FT HOOD TX 76544-5073
1	MANSCEN COMBAT DEVELOPMENT ATTN ATZT CDC (DON VIERS) 320 ENGINEER LOOP SUITE 141 FT LEONARD WOOD MO 65473	1	ARL HRED FT HUACHUCA FLD ELEMENT ATTN AMSRL HR MY (B KNAPP) GREELY HALL (BLDG 61801 RM 2631) FORT HUACHUCA AZ 85613-5000
1	ARL HRED AVNC FIELD ELEMENT ATTN AMSRL HR MJ (R ARMSTRONG) PO BOX 620716 BLDG 514 FT RUCKER AL 36362-0716	1	ARL HRED FLW FIELD ELEMENT ATTN AMSRL HR MZ (A DAVISON)* 3200 ENGINEER LOOP STE 166 FT LEONARD WOOD MO 65473-8929

<u>NO. OF COPIES</u>	<u>ORGANIZATION</u>	<u>NO. OF COPIES</u>	<u>ORGANIZATION</u>
2	ARL HRED NATICK FIELD ELEMENT ATTN AMSRL HR MQ (M FLETCHER) ATTN SSCNC A (D SEARS) USASSCOM NRDEC BLDG 3 RM 140 NATICK MA 01760-5015	1	LIBRARY ARL BLDG 459 APG-AA
1	ARL HRED OPTEC FIELD ELEMENT ATTN AMSRL HR MR (M HOWELL) OPTEC CSTE OM PARK CENTER IV RM 1040 4501 FORD AVENUE ALEXANDRIA VA 22302-1458	1	ARL HRED ECBC FIELD ELEMENT ATTN AMSRL HR MM (R MCMAHON) BLDG 459 APG-AA
1	ARL HRED SC&FG FIELD ELEMENT ATTN AMSRL HR MS (L BUCKALEW) SIGNAL TOWERS RM 303A FORT GORDON GA 30905-5233	1	USATECOM RYAN BUILDING APG-AA
1	ARL HRED STRICOM FIELD ELEMENT ATTN AMSRL HR MT (A GALBAVY) 12350 RESEARCH PARKWAY ORLANDO FL 32826-3276	1	COMMANDER CHEMICAL BIOLOGICAL AND DEFENSE COMMAND ATTN AMSCB CI APG-EA
1	ARL HRED TACOM FIELD ELEMENT ATTN AMSRL HR MU (M SINGAPORE) BLDG 200A 2ND FLOOR WARREN MI 48397-5000	2	ECBC ATTN AMSSB RRT PR (MR CARETTI MR KUHLMAN) BLDG 5604 APG-EA
1	ARL HRED USAFAS FIELD ELEMENT ATTN AMSRL HR MF (L PIERCE) BLDG 3040 RM 220 FORT SILL OK 73503-5600	2	ECBC ATTN AMSSB RRT PR (MR GROVE) BLDG 3514 APG-EA
1	ARL HRED USAIC FIELD ELEMENT ATTN AMSRL HR MW (E REDDEN) BLDG 4 ROOM 332 FT BENNING GA 31905-5400	1	PM NBC DEFENSE SYSTEMS ATTN AMSSB PM RNN M(J) MESSRS DECKER AND FRITCH APG-EA
1	ARL HRED USASOC FIELD ELEMENT ATTN AMSRL HR MN (F MALKIN) HQ USASOC BLDG E2929 FORT BRAGG NC 28310-5000		<u>ABSTRACT ONLY</u>
1	US ARMY RSCH DEV STDZN GP-UK ATTN DR MICHAEL H STRUB PSC 802 BOX 15 FPO AE 09499-1500	1	DIRECTOR US ARMY RESEARCH LABORATORY ATTN AMSRL CS EA TP TECH PUB BR 2800 POWDER MILL RD ADELPHI MD 20783-1197
	<u>ABERDEEN PROVING GROUND</u>		
2	DIRECTOR US ARMY RESEARCH LABORATORY ATTN AMSRL CI LP (TECH LIB) BLDG 305 APG AA		

REPORT DOCUMENTATION

Form Approved
OMB No. 0704-0188

Public reporting burden for this collection of information is estimated to average 1 hour per response, including the time for reviewing instructions, searching existing data sources, gathering and maintaining the data needed, and completing and reviewing the collection of information. Send comments regarding this burden estimate or any other aspect of this collection of information, including suggestions for reducing this burden, to Washington Headquarters Services, Directorate for Information Operations and Reports, 1215 Jefferson Davis Highway, Suite 1204, Arlington, VA 22202-4302, and to the Office of Management and Budget, Paperwork Reduction Project (0704-0188), Washington, DC 20503.

1. AGENCY USE ONLY (Leave blank)		2. REPORT DATE September 1999		3. REPORT TYPE AND DATES COVERED Final	
4. TITLE AND SUBTITLE Relationship of Protective Mask Seal Pressure to Fit Factor and Head Harness Strap Stretch				5. FUNDING NUMBERS AMS Code 611102.74A00011 PR: 1L1611102.74A PE: 6.11.10	
6. AUTHOR(S) Cohen, K.S. (ARL)					
7. PERFORMING ORGANIZATION NAME(S) AND ADDRESS(ES) U.S. Army Research Laboratory Human Research & Engineering Directorate Aberdeen Proving Ground, MD 21005-5425				8. PERFORMING ORGANIZATION REPORT NUMBER	
9. SPONSORING/MONITORING AGENCY NAME(S) AND ADDRESS(ES) U.S. Army Research Laboratory Human Research & Engineering Directorate Aberdeen Proving Ground, MD 21005-5425				10. SPONSORING/MONITORING AGENCY REPORT NUMBER ARL-TR-2070	
11. SUPPLEMENTARY NOTES					
12a. DISTRIBUTION/AVAILABILITY STATEMENT Approved for public release; distribution is unlimited.				12b. DISTRIBUTION CODE	
13. ABSTRACT (Maximum 200 words) Currently, protective mask seals are evaluated indirectly by measuring fit factor (FF), a ratio of the concentration of particles outside versus the concentration of particles inside the mask. This report describes an alternate process for evaluating mask seals by measuring seal pressure distribution. The goal was to develop a relationship between FF and seal pressure for evaluating seal performance, and relationships between FF and strap stretch and between seal pressure and strap stretch for determining proper strap adjustment. Pressure was measured using a thin film flexible sensor placed at 11 locations around the seal of an M40 mask on a headform. Corresponding FF was measured using a protective mask fit tester. Stretch in each of the six head harness straps was measured manually using a caliper and gauge length markers on the strap. Measurements were made for three degrees of strap tightness over a total of 22 trials. Data and model analysis indicated a strong relationship between FF and seal pressure ($R^2 = 0.87$), and weak relationships between FF and strap stretch ($R^2 = 0.2$) and between seal pressures and strap stretch ($R^2 = 0.09-0.27$). Eleven validation trials were conducted to verify predictive capability of the seal pressure and FF relationships. Passing or failing FF was correctly predicted by a single seal pressure in 9 of 11 trials. These findings suggest that seal pressure measurement may be a promising new tool for design and evaluation of protective mask seals. In contrast, strap stretch measurements could not be used to determine proper adjustment of the head harness for achieving a passing FF and adequate seal pressure.					
14. SUBJECT TERMS fit factor M40 protective mask strap stretch head harness seal pressure				15. NUMBER OF PAGES 120	
				16. PRICE CODE	
17. SECURITY CLASSIFICATION OF REPORT Unclassified		18. SECURITY CLASSIFICATION OF THIS PAGE Unclassified		19. SECURITY CLASSIFICATION OF ABSTRACT Unclassified	
20. LIMITATION OF ABSTRACT					